ABSTRACT

Title of Dissertation: ENGINEERED MULTIVALENCY FOR ENHANCED AFFIBODY-BASED HER3 CANCER THERAPY

John Samuel Schardt
Doctor of Philosophy, 2018

Dissertation directed by: Steven M. Jay
Assistant Professor
Fischell Department of Bioengineering

The receptor tyrosine kinase HER3 is well established as a compelling therapeutic target in numerous cancers, including ovarian cancer. HER3 potently activates the PI3K/Akt pro-survival pathway, mediates drug resistance, and is implicated in cancer progression and poor clinical outcomes. Yet, conventional small molecule- and monoclonal antibody-based approaches have so far failed to yield a widely used therapeutic that directly targets HER3. Here, we investigated a novel approach involving specific, multivalent engagement of HER3 with affibody molecules as an alternative to existing therapeutics. We established that multivalent HER3-targeted affibodies more effectively inhibit neuregulin 1β-mediated HER3 activation compared to monovalent affibodies; these multivalent ligands induced rapid and prolonged HER3 downregulation, indicating a potentially valuable mechanism of action to limit HER3-mediated pro-mitogenic signaling and acquired resistance.

HER3-targeted affibodies also proved highly amenable to molecular engineering approaches, as modulation of linker length, valency, and albumin binding domain (ABD) fusion placement allowed for robust retention of ligand bioactivity. We further report significant mechanistic evidence supporting HER3 downregulation as a highly specific phenomenon prompted by HER3 sequestration by multivalent ligands. Most importantly, we show that both monovalent and bivalent HER3-targeted affibody-ABD fusion proteins significantly reduce tumor burden in an adriamycin-resistant ovarian cancer model in mice. Overall, these data serve as compelling evidence for HER3 multivalent ligands as promising experimental therapeutics for the treatment of ovarian cancer as single agents as well as in combination with other drugs. Further, HER3 affibodies represent a promising template for development of targeted therapies or drug conjugates for more powerful ovarian cancer therapy in the future.

ENGINEERED MULTIVALENCY FOR ENHANCED AFFIBODY-BASED HER3 CANCER THERAPY

by

John Samuel Schardt

Dissertation submitted to the Faculty of the Graduate School of the
University of Maryland, College Park, in partial fulfillment
of the requirements for the degree of
Doctor of Philosophy
2018

Advisory Committee:
Assistant Professor Steven M. Jay, Chair
Chief of Women's Malignancies Branch, NCI, Stanley Lipkowitz
Assistant Professor Amy J. Karlsson
Associate Professor Christopher M. Jewell
Professor David Fushman, Dean's Representative

Acknowledgements

I am tremendously grateful for the unwavering support that has enabled the completion of this dissertation project. First, I acknowledge my mentor Dr. Steven Jay, whom I cannot thank enough for the exceptional mentorship and wisdom that he provided on a daily basis. It's been a pleasure learning from him and developing as a researcher and professional under his direction. Second, I acknowledge my co-mentor Dr. Lipkowitz, who has provided invaluable support and insights toward advancing this research and my professional career. I recognize the National Cancer Institute-University of Maryland Partnership and American Association of Pharmaceutical Scientists for generous financial support and incredible professional development opportunities. To my labmates Anjana Jeyaram, Divya Patel, and Eli Pottash: thank you for being supportive, fun, and generous colleagues and friends; I have thoroughly enjoyed journeying with you toward our Ph.Ds. To my undergraduate research team Jinan Oubaid, Sonya Williams, Madeleine Noonan-Shueh, and Riyadh Ali: thank you for the countless hours you have devoted to advancing this research, and for the incredible mentorship opportunity you provided. To my friends: thank you for fun, adventures, and memories along the way. To my family Tim, Kim, Mary, Alex, and Tobi: thank you for your continuous love and support!

Table of Contents

List of Figures

List of Abbreviations

Albumin binding domain	ABD
Neuregulin-1β	NRG
Intraperitoneal	i.p.
Epidermal growth factor	EGF
Wild type	WT
high-grade serous ovarian cancer	HGSOC
Green fluorescent protein	GFP

Chapter 1: Introduction

1.1 Cancer: a general overview

Cancer, defined as the uncontrolled growth of abnormal cells, is the 2nd leading cause of death in the United States, accounting for 1 in 4 deaths [1]. Over 1.6 million Americans are expected to be diagnosed with cancer in 2016, which will account for 600,000 deaths this year and over 1,600 deaths per day in the United States [1]. Notwithstanding these statistics, the 5 year survival rates for patient's diagnosed with certain cancers continue to increase as improved and more informed treatment options are developed [2].

Cancer can be caused by external factors such as diet, smoking and exposure to carcinogenic material as well as from internal factors such as inherited genetic mutations [1]. Treatment decisions are largely dictated by the tissue involved, the stage of progression, the cancer's biological features and whether or not the cancer has recurred [3]. Common treatment options include surgery, chemotherapy, radiation therapy, hormone therapy, immune therapy, and targeted therapy [4,5].

Cancer stage is a predictor of clinical outcome [3] and can most generally be classified as *in situ*, local, regional or distal with respect to increased invasion [3]. More specifically, clinicians use the TNM staging system, which designates primary tumor (T), lymph node involvement (N), and distant metastases (M) [3]. The most common treatment for *in situ* and local tumors is surgical removal, which can also be

combined with adjuvant radiation or chemotherapy in an effort to combat cancer cells that were potentially missed during the surgical resection [3]. For more advanced stage tumors, chemotherapy and radiation therapy are also common, however these therapies have limited efficacy, and cause side effects that limit treatment regimens [5]. Early detection is crucial for survival chances; for example, breast cancer patients with local stage tumors have a 5-year survival of nearly 99%, which drops to 85% for patients with regional tumors, and plummets to 25% for those with distant tumors [3].

Based on these statistics, more effective treatment for distant and refractory tumors is a clear unmet clinical need. One clinically available solution is the systemic delivery of targeted therapeutics that bind to and inhibit biological features that are unique or overexpressed on cancer cells. Targeted therapies allow for improved selectivity for cancer cells and reduced side effects compared to chemotherapeutic agents [5].

Clinical screening of a patient's cancer for biomarkers is useful toward informing treatment decisions. As an example, breast cancer screening will typically include identification of the presence or absence of estrogen receptor (ER), progesterone receptor (PR), and human epidermal growth factor receptor 2 (HER2), with HER2 amplification and overexpression indicative of negative clinical outcome and an increased chance of recurrence [6]. Further, identification of HER2- positive cancer commonly indicates that a patient would be more likely to benefit from HER2-targeted therapy, such as Herceptin [6].

Similarities in genetic mutations in cancer often exist across tissues, which has led to the emergence of more personalized medicine-based approaches emphasizing a cancer's particular biomarkers to inform treatment decisions [7]. Yet, careful consideration of both the tissue of origin and cancer biomarkers is important toward identification of an appropriate therapy option [7].

1.2 ErbB receptor biology

1.2.1 ErbB family overview

Amongst potential targets for specific cancer therapies, the ErbB receptor family has attracted significant attention due to its ubiquity and prevalent role in mediating progression of numerous cancers.

The ErbB family of transmembrane tyrosine kinase receptors (**Figure 1.1**) is composed of four members: the founding receptor epidermal growth factor receptor EGFR (HER1 - Human Epidermal Growth Factor Receptor 1), ErbB2 (HER2), ErbB3 (HER3), and ErbB4 (HER4). Each ErbB member has unique biological function; In mice, loss of any of the ErbB members results in lethality and based on the specific receptor loss, defects were found in tissues including brain, gastrointestinal tract, heart, lung, and skin [8]. The ErbB family is involved in complex signaling networks and is responsible for regulating cellular proliferation in both embryonic and adult tissues, and these receptors are often deregulated in cancer [8].

Structurally, each ErbB receptor contains an extracellular domain, a single transmembrane spanning region, a cytoplasmic tyrosine kinase domain, and a C-terminal phosphorylation tail [8,9]. ErbB2 is unique in that it has no known ligand and is constitutively available for heterodimerization with other receptors for activation [10]. ErbB3 is also unique in that it has a weak receptor tyrosine kinase (RTK) domain necessitating its partnership with other receptors for signal transduction [9,10].

Generally, ErbB receptor signal transduction occurs at three levels of molecular interactions: first an activating ligand binds an ErbB receptor extracellular domain, second the active receptor undergoes a conformational change and dimerizes (or oligomerizes) with other active receptors, and third the intracellular tyrosine kinase domain of a dimerized receptor phosphorylates *in trans* the cytoplasmic tail of its dimerization partner leading to interaction with downstream effector proteins and signal transduction [11]. There are 12 known ligands that interact with the ErbB family members, some of which interact exclusively with one ErbB member, and others with specificity for multiple ErbB members [10,12]. Neuregulin-1β (NRG) is the native ligand for ErbB3 and ErbB4 [10]. Upon ErbB receptor activation, dimerization generally occurs amongst ErbB family members (**Figure 1.1**), although higher order oligomeric interactions and interactions with non-ErbB members have also been identified [10,13]. ErbB2 is the preferred heterodimerization partner for all other ErbB family members [14]. Generally heterodimerization, especially with ErbB2, leads to more potent mitogenic signaling compared to homodimerization [10].

Further, each ErbB receptor heterodimer pairing can achieve unique downstream signaling effects [10]. After complex signal processing events, ErbB-mediated signal transduction ultimately controls cellular responses such as apoptosis, migration, growth, adhesion, and differentiation [10].

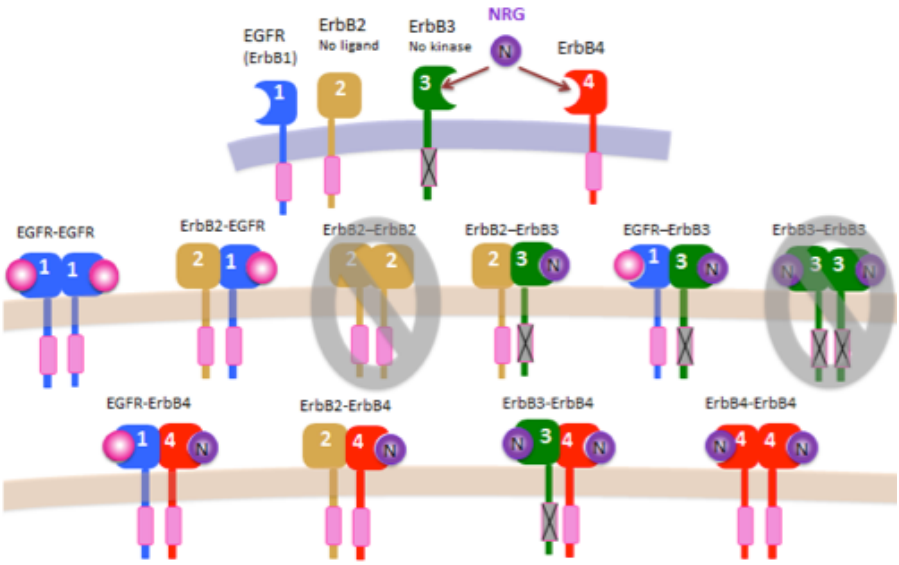

Figure 1.1: The ErbB receptor family This receptor family is composed of 4 members: EGFR (HER1), ErbB2 (HER2), ErbB3 (HER3), and ErbB4 (HER4) [10]. ErbB2 has no known ligand and is constitutively active for dimerization [10]. ErbB3 has a weak RTK domain necessitating its partnership with other receptors for signal transduction [10]. NRG is the native ligand for ErbB3 and ErbB4 [10]. Upon activation, the ErbB family members interact via dimerization for signal transduction [10]. Each ErbB receptor pairing can achieve unique downstream signaling effects [10]. ErbB2 homodimers and ErbB3 homodimers are not known to have physiological signaling significance [10].

1.2.2 ErbB3 receptor biology

ErbB3 receptors tend to exist as inactive oligomeric complexes in the absence of ligand, which become disrupted upon NRG binding [15]. ErbB3's weak tyrosine kinase domain necessitates partnership of ErbB3 with other receptors for signal transduction [10]. After ligand-mediated activation, ErbB3 is readily available for heterodimerization with other ErbB family members such as ErbB2 [10]. Notably, the

ErbB2/ErbB3 heterodimer is the most potent oncogenic unit of the entire ErbB family [12]. Despite its weak tyrosine kinase domain, ErbB3 uniquely contains six consensus phosphotyrosine sites on its C-terminal tail that when phosphorylated *in trans* allow for signal transduction through docking of the p85 subunit of the effector molecule phosphatidylinositide 3-kinase (PI3K), which then leads to downstream activation of protein kinase B (Akt) [9]. The PI3K/Akt axis leads to downstream activation of the following effector molecules: NF-KB, P27, BAD, GSK3B, and mTOR, which ultimate allows for regulation of apoptosis, cell cycle, survival, and proliferation [9].

ErbB3 (HER3)-mediated signaling through the PI3K/Akt axis is implicated in a variety of cancers including breast, ovarian, lung, and prostate [9], and HER3 signaling can be classified as either ligand-dependent or ligand-independent. Following the aforementioned signaling cascade, ligand-dependent signaling is initiated by NRG binding to HER3, which activates the receptor for dimerization. Ligand-dependent HER3 signaling is a key driver of cancer proliferation in some cancers [16]. In subsets of advanced-staged ovarian cancers, the presence of a NRG/HER3 autocrine loop has been documented to drive cancer proliferation, and treatment with HER3-targeted antibodies or knockdown with HER3-targeted siRNA reduced cancer cell proliferation *in vivo* [16] suggesting potential oncogenic addition to this autocrine loop. In this study by Sheng et al., 4 of 7 tumor samples from patients with advanced-stage ovarian cancers revealed activated HER3 that coimmunoprecipitated with the p85 subunit of PI3K [16].

Beyond NRG-mediated activation, ligand-independent HER3 activation has been reported especially in cases with HER2 overexpression. As addressed in more detail in section *2.3*, inactive HER3 is in equilibrium between a locked and open conformation, whereby the open conformation facilitates dimerization; NRG binding to HER3 is thought to stabilize this open conformation [8]. Thus, overexpression of HER2 can reasonably increase the likelihood of heterodimerization with an openly conformed HER3 that has not been activated by NRG. In cancers with HER2 amplification, HER2/HER3 heterodimerization still readily occurs, and HER2 overexpression can drive ligand-independent HER3-mediated mitogenic signaling [17].

1.2.3 HER3 extracellular domain structure

The 620 amino acid extracellular region of HER3 is composed of four domains (**Figure 1.2**), organized as a tandem repeat of a two domain unit [8]. Domains I and III are beta helical and are involved with ligand binding specificity; Domains II and IV are cysteine rich [8,9]. In its locked conformation, HER3 contains an interdomain tether between domains II and IV, which results in a large pore circumscribed by domains II, III, and IV (**Figure 1.2**) [8]. This tether is formed by a main-chain/main-chain hydrogen bond and three side-chain/side-chain interactions [8]. The inter-domain tether is conserved among HER3 and HER4, both of which are activated by the native ligand NRG, but this feature is not present in HER2, the constitutively active receptor that has no known ligand [8].

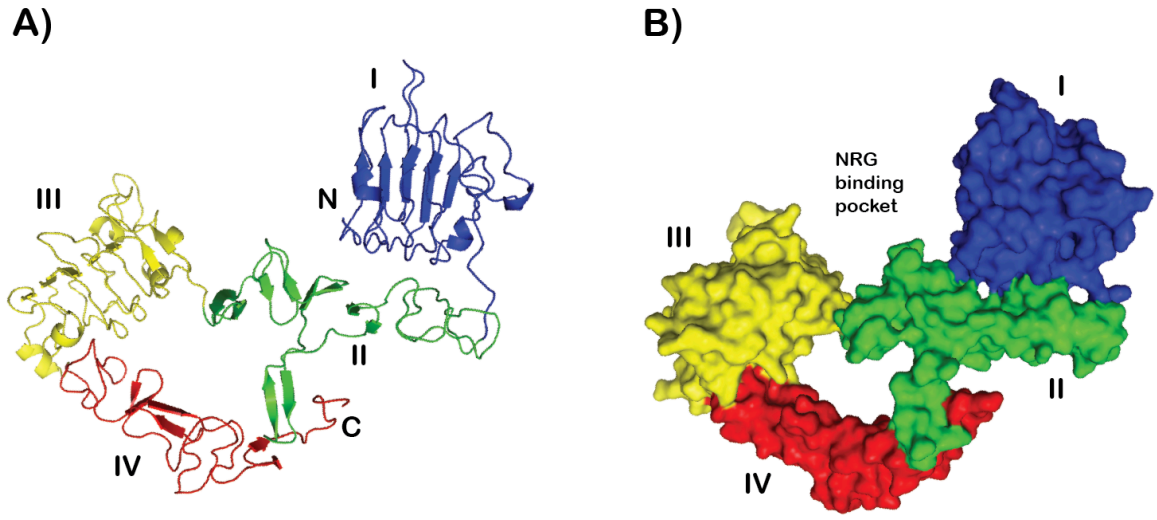

Figure 1.2: HER3 extracellular region structure: A. HER3 cartoon schematic **B.** HER3 surface schematic. The HER3 extracellular region is composed of four domains: I (blue), II (green), III (yellow), and IV (red); N- and C-termini are labeled in **A** and are respectively located in Domains I and IV. The HER3 extracellular region is depicted in a locked conformation with inter-domain tether contacts between domains II and IV causing the large pore encircled by domains II, III, and IV. NRG binding at the NRG binding pocket depicted in **B** stabilizes an open conformation of HER3 (not depicted); in its open conformation, the interdomain tether contacts between domains II and IV are released, thus making HER3 available for dimerization. In its open form, dimerization contacts exist on domains II. In its full transmembrane form, the C-terminus depicted in domain IV is connected to the transmembrane domain followed by the intracellular domain. This schematic was adapted from protein data bank file 1M6B and figures from Cho et al [8].

HER3 is known to adapt a variety of conformations, as a result of flexibility between extracellular domains II and III [8]. In its inactive state prior to ligand binding, HER3 receptors are in equilibrium between a locked and open conformation, whereby the locked conformation typically exists on the cell surface as a monomer and the open conformation allows for the formation of inactive dimers and oligomers [18]. In its closed conformation, the NRG binding site is located within the pocket surrounded by domains I, II, and III (**Figure 1.2B**) [8]. Domain I was validated to have a binding site for HER3 via proteolytic cleavage analysis, and a truncated HER3 extracellular region composed of domains I and II binds NRG but with 30-fold lower affinity than the complete four domain extracellular region [8]. Binding of NRG to HER3 stabilizes the open conformation of the receptor and promotes dimerization with other

ErbB family members [18]. In HER3's open conformation, the interdomain tether between domains II and IV is released, making HER3 available for dimerization via contacts exist on domain II [19,20].

1.2.4 HER3-mediated resistance

HER3 activation and overexpression is a key mediator of cancer cell resistance to targeted therapies via compensatory survival signaling [21–27]. HER3-mediated resistance has been found to compensate for inhibition of both "horizontal" and "vertical" signaling pathways, which respectively refer to signaling lateral to HER3 by receptors such as HER2 or Axl, and signaling immediately downstream of HER3 via effectors such PI3K/Akt [23,26–28] as will be elaborated on in section *5.4*.

1.3 Multivalency principles for molecular design

1.3.1 Multivalency in the clinic

Multivalency, the phenomenon by which a single molecule can be involved in multiple simultaneous molecular recognition events, is a promising concept toward the design of pharmaceuticals with enhanced efficacy by means of improved avidity, residence time, selectivity, and differential receptor trafficking [29–33]. The typical engineered multivalent molecule includes multiple binding moieties connected by a spacer domain (**Figure 1.3**). Both the binding domains and spacer domain can influence the efficacy of the molecule, and each should be considered carefully in engineering design.

Naturally, multivalency has been effective in biological systems; take for example the immune defense molecule the antibody; the typical IgG is inherently bivalent. Surprisingly, the translation of multivalent engineering principles to the clinic is limited and has only recently emerged. The microbicidal dendrimer VivaGel, targeting bacterial and viral surfaces, is currently in stage III clinical trial [34], and the tetravalent bi-specific antibody MM-141, targeting IGF1R and HER3 has been designated as an orphan drug [35].

1.3.2 Avidity effects and multivalent binding kinetics

Engineered multivalency has profound implications in drug discovery, whereby low affinity binding domains can be engineered into high avidity multivalent ligands, abating the need for time-intensive processes of iterative molecular screening and redesign to enhance monovalent ligand affinity [30]. The expected enhancement in efficacy for multivalent ligands as compared to their monovalent counterparts is fundamentally explained by an increase in apparent affinity by means of increased effective concentration, a phenomenon known as avidity [30]. In a multivalent system, the monovalent affinities can synergize to promote the probability of subsequent binding following an initial event (**Figure 1.3**) [30]. Furthermore, the dissociation rate for a multivalent ligand is decreased compared to a monovalent analog [29,30,33]. A bivalent ligand in a monovalently bound state has the propensity to re-establish a bivalent interaction as opposed to complete molecular dissociation, which is illustrated in **Figure 1.3B** by a shift from State 2 to State 3 as opposed to a shift to State 1. Notably, Vauquelin et al. show through mathematical simulations that the kinetics for multivalent ligands compared to monovalent ones are different,

whereby multivalent ligands show increased residence time at the target, and a longer lasting therapeutic effect [33]. With regard to limitations and design considerations, the authors caution that multivalent therapeutics may take longer to reach equilibrium, and may not have sufficient time to equilibrate *in vivo*, thus the expected efficacy of multivalent ligands might not scale directly to experimental values [33].

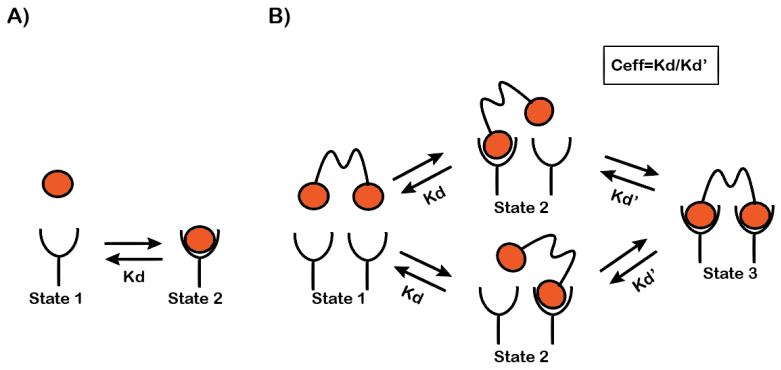

Figure 1.3: Increased valency enhances residence time and effective concentration. A. Monovalent ligand binding rate can be described by dissociation constant Kd. **B.** A bivalent ligand with two identical binding domains linked by a flexible spacer molecule exhibits differential kinetics compared to **A**. Upon monovalent binding of a bivalent ligand to a target receptor (State 2), the unbound ligand is brought effectively close to its target assuming adequate overexpression of the target receptor [30]. Bivalent binding events (State 3) accumulate and effective concentration is enhanced if Kd' < Kd [30]. This schematic was based on drawings from Liu et al. [30]

1.3.3 Linker domain considerations

Although the linker domain in a multivalent molecule theoretically does not bind or interact with the therapeutic target, it is a key aspect of multivalent ligand design based on thermodynamic considerations [30]. Specifically, the parameters of linker stiffness, length, and geometry may impact therapeutic function and should be considered in molecular engineering design [30]. The optimal choice for these parameters depends greatly on the specific application, and the knowledge available regarding the target of interest. If the distance between two binding sites is known

and fixed, a rigid spacer that geometrically allows for unconstrained multivalent binding might be advantageous; rigid linkers are more entropically favorable for binding events [29,30]. However, flexible linkers have also proven effective in a variety of multivalent ligand designs [36]. A flexible spacer has the advantage of sampling a greater space, increasing the probability of multivalent binding [30]. However, ligand binding impairs the rotational and conformational freedom of the flexible linker, and therefore has a higher entropic cost compared to rigid linkers [30]. Yet, the enthalpic benefit of multivalent ligand binding will often offset this entropic penalty, thus allowing an avidity affect [30]. Linker domain length is another important parameter in multivalent ligand design. Various computational and experimental models have been developed to explore the influence of linker length and flexibility [36,37]. Theoretically, the longer and more flexible the linker, the greater the entropic cost for multivalent binding events [30]. Interestingly, Krishnamurthy et al. find that the theoretical penalty for these entropy losses is much lower than previously hypothesized based on their model system of a ligand tethered to the surface of a protein by a poly (ethylene glycol) linker [36]. The authors argue that a flexible spacer much longer than the necessary length to simultaneously bind multiple target sites is advantageous for multivalent ligand design given their unexpected finding that effective molarity is only weakly dependent on linker length [36].

1.3.4 Selectivity in multivalent engineering design

Beyond improved apparent affinity for target cells, increased ligand valency is expected to enhance target specificity (**Figure 1.4**), quantified as the percentage of

ligand bound to a target cell versus ligand bound to a non-target cell [30]. Selectivity is especially important for systemic delivery applications, whereby a drug with improved selectivity will likely have enhanced efficacy and reduced off-target effects. Considering ligand binding to a surface receptor overexpressed on cancers cells and expressed at low levels on healthy cells, a monovalent ligand will theoretically show no preference for the receptors on the cancer cell, and thus if the receptors are overexpressed on the cancer cells by two-fold, the monovalent ligands will bind the cancer cells twice as frequently. A multivalent ligand, however, is expected to exhibit a higher degree of specificity compared its monovalent counterparts. Assuming the first binding event between a ligand and a target will be kinetically similar across valencies, then when a target is expressed at low levels, monovalent interactions will dominate, even when multivalent ligands are employed [30]. But when the target is overexpressed, subsequent binding events after the docking of multivalent ligands will exhibit an enhanced avidity effect based on the aforementioned differential binding kinetics (**Figure 1.3**), and therefore show greater selectivity for a target cancer cell (**Figure 1.4**) [30].

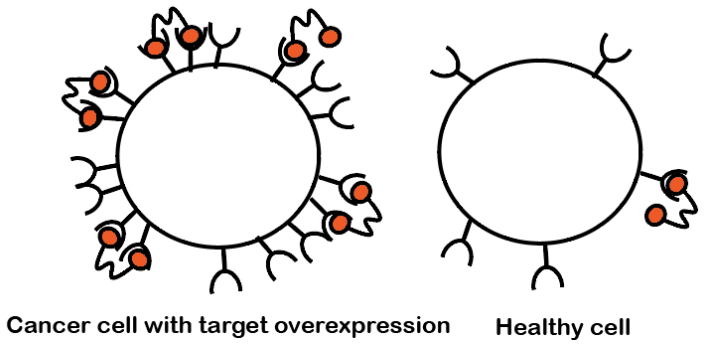

Figure 1.4: Multivalent ligands enhance selectivity. When bivalent ligands are deployed against a cancer cell with target overexpression, bivalent binding events dominate leading to enhanced residence time and avidity effects [30]. The bivalent ligands show preference for the receptors on the cancer cell as opposed to a healthy cell with low target expression because monovalent binding events dominate in

on the healthy cell due to an inadequate level of surface receptors [30]. Schematic based on drawings from Liu et al. [30]

1.3.5 Cautionary multivalent design considerations

Notably, maximum binding moiety affinity is not always optimal in multivalent ligand engineering especially when considering selectivity; instead optimal selectivity is dictated by a careful balance between low monovalent constituent affinity, and high avidity of the multivalent molecule as a whole [30]. Likewise, extreme ligand affinity might not be ideal for trafficking through tumor vasculature. In the phenomenon of the "binding site barrier", antibodies with very high affinity bind strongly to the first tumor antigens located and accumulate heterogeneously throughout the tumor, primarily in the peri-vasculature region which leads to suboptimal efficacy [33,38]. Thus, optimal monovalent affinity and multivalent apparent affinity should be carefully considered and can be modulated by valency and appropriate binding moiety selection. Overall engineered multivalency provides a powerful tool for enhanced therapeutic efficacy in pharmaceutical design.

1.4 ErbB-family targeted therapeutics

1.4.1 FDA approved ErbB family-targeted therapies

Targeting the ErbB family of receptor tyrosine kinases, which includes EGFR, HER2, HER3, and HER4, has been of clinical interest for more than two decades with an initial focus on targeting HER2 and EGFR. Generally, the HER family of transmembrane receptors contain an extracellular ligand binding domain targetable by antibody-based approaches, and an intracellular RTK domain targetable by small molecule therapeutics. Several monoclonal antibody based approaches have received FDA approval including the blockbuster drug herceptin (trastuzumab), a HER2-

targeted monoclonal antibody, and cetuximab and panitumumab, two EGFR-targeted monoclonals [39]. Several small molecules drugs that interact with the intracellular ATP binding pocket thus inhibiting RTK function have also gained FDA approval including EGFR targeted gefitinib and erlotinib, dual EGFR and HER2 targeted small molecule lapatinib, and more recently HER2 targeted neratinib (approved in 2017) [40].

1.4.2 Antibody-based approaches against HER3

HER3 has emerged as a therapeutic target in a variety of cancers including ovarian, prostate, breast, and lung [41], with HER3 expression occurring in 36-90% of breast cancers, and HER3 overexpression occurring in 16% of ovarian cancers [19].

Despite the significant clinical need to combat HER3-related mitogenic effects, no current HER3-targeted therapeutics have been FDA approved [42] and only the bispecific anti-HER3 anti-insulin like growth factor receptor 1 (IGF-IR) antibody MM-141 has been designated with orphan drug status (treatment of pancreatic cancer) [35]. HER3 structurally has a weak RTK domain, thus small molecule inhibitors disrupting RTK function are not considered an appropriate targeting strategies. Despite this weak RTK domain, HER3 is a key node in the ErbB signaling network forming potent mitogenic heterodimers with HER2 [12], activating survival signaling through the Akt/PI3K pathway [43,44], and serving as a mechanism of cancer resistance to targeted therapies through its overexpression and alternative activation [21–25,45]. Targeting HER3 is of significant clinical interest with several HER3-targeted antibodies in clinical development including both monospecific and

bispecific approaches [19], and various peptide and protein-based targeting strategies under investigation [46–50].

The fully humanized HER3-targeted monoclonal MM-121 is currently in phase 2 clinical trial in combination with the anti-mitotic chemotherapeutic docetaxel or replication and transcription inhibitor pemetrexed for the treatment of non-small cell lung cancer in which patients are selected for treatment based on NRG expression profile [51]. In previous work, Merrimack Pharmaceuticals demonstrated high heregulin-1β expression is positively correlated with cancer susceptibility to MM-121 therapy, whereas other biomarkers including HER3, HER2, and EGFR expression have limited predictive value [43]. Mechanistically, the efficacy of MM-121 is at least in part due to inhibition of NRG-mediated HER3 activation, presumably by steric blockade of the HER3's NRG-binding site. Interestingly, MM-121 treatment led to HER3 receptor downregulation in some cell lines (e.g. MALME 3M) but not others (e.g. DU145) and the specific mechanism of downregulation was unknown [43]. MM-121 showed limited efficacy and minimal pHER3 inhibition in cell lines with ligand-independent HER3 activation such as the HER2 amplified BT474 breast cancer cell line [43].

Mechanistically, the design of antibodies to target HER3 is not limited to inhibition of NRG-mediated activation. Design of the fully human HER3-targeted antibody LJM716, currently in phase 1 clinical trials in HER2 positive tumors, was informed by the ability of HER3 to be activated in both ligand-dependent and ligand-

independent manners with the latter occurring predominantly by HER3 activation *in trans* in cancers with HER2 overexpression [17,34]. LJM716 does not does not prevent NRG binding to HER3, but instead locks HER3 into an inactive conformation that prevents HER3 interaction with its preferred dimerization partner HER2 [17]. LJM716 showed efficacy in various tumor models and also reduced proliferation in combination with the HER2-targeted monoclonal trastuzumab [17].

Optimized immune effector function is another strategy to improve the therapeutic efficacy of HER3 targeted therapies. The humanized anti-HER3 monoclonal antibody RG7116, currently in Phase I clinical trial in combination with various ErbB-targeted therapeutics for the treatment of breast, non-small-cell lung cancer, and various solid tumors, has a glycoengineered FC domain that enhances antibody-dependent cell-mediated cytotoxicity (ADCC) [34,52,53]. Like LJM716, RG7116 locks HER3 into an inactive conformation preventing both NRG-mediated HER3 activation, and heterodimer formation [52].

Bispecific antibody-based approaches are also being exploited to treat HER3-mediated malignancies by inhibiting specific dimerization partnerships. MM-111, a bispecific antibody for HER2 and HER3, failed clinical trials for the treatment of several HER2 positive cancers in combination with trastuzumab and paclitaxel [54]. Despite the aforementioned clinical trial results, MM-111 showed potent anti-tumor activity *in vivo* in several xenograft models, and mechanistically has advantages for HER2/HER3 dimerization blockade over HER3 monoclonal antibody approaches in

that HER2 is commonly overexpressed to a much greater degree than HER3 and thus antibody docking to HER2 receptors on the cancer cell surface can subsequently increase the effective concentration of MM-111's HER3-binding domain for enhanced HER3 blockade [55]. HER3 dimerization and oligomerization partners are not limited to ErbB family members. The design of MM-141, a tetravalent antibody with bispecificity for HER3 and IGF-IR, is informed by reports of a HER2/HER3/IGF-IR trimeric interactions responsible for trastuzumab resistance in some breast cancer cell lines [56]. Orphan drug MM-141, currently in phase II clinical trials in combination with chemotherapeutics nab-paclitaxel and gemcitabine for the treatment of metastatic pancreatic cancer in patients with the identified biomarker of high IGF-1 [51], strategically blocks the PI3K/AKT/mTOR signaling axis that is redundantly and compensatorily activated by HER3 and the structurally similar IGF-IR [56].

1.4.3 Non-antibody scaffolds and next-generation antibody therapeutics

Antibody approaches are limited by size, stability, and the ability to effectively penetrate tissues [57] as these molecules are high molecular weight, rely on multiple domains, disulfide bonds, and complex glycosylation patterns [58]. Further, antibody-based therapies have shown limited efficacy, for example, HER2-targeted therapies typically show efficacy in ~24%-64% of patients with HER2-overexpressing tumors [59], and thus new approaches with improved efficacy and novel mechanisms of action are of clinical interest. Peptide and antibody fragment-based approaches provide an alternative therapeutic approach with enhanced tissue penetration and

easier manufacturability [57]. By employing low molecular weight binding moieties or antibody fragments, tethered multivalent ligands can be engineered for the design of custom therapeutics with control over half-life, tissue penetration, specificity, valency, affinity, and avidity [60]. Pharmaceutical companies such as Boehringer Ingelheim have engaged in blockbuster deals toward research and development on these next generation multivalent binding-fragment based approaches [61].

Similar to antibody fragments, affibody molecules provide an alternative scaffold for the development of high-affinity binding proteins. The affibody refers to a 58 amino acid, cysteine-free, three-helix bundle motif derived from the B-domain of staphylococcal protein A [58]. The B-domain was mutated for enhanced stability and this derivative is known as the Z-domain [58]. Affibodies have high stability and solubility as well as good tissue penetration, marking them as emerging scaffolds for therapeutic and imaging applications [46,58]. The affibody scaffold is highly amenable to phage display for the generation of high affinity binding molecules, and has demonstrated advantages over antibody fragments with regard to ease of molecular display [46,58]. Both monospecific and bispecific affibodies have been engineered for high-affinity to ErbB family receptors including ABY-025, a radiolabeled HER2 specific affibody currently in Phase II clinical trials for positron emission tomography imaging of breast cancer [46,49,50,57,58,62]. Therapeutic HER3 specific affibodies that block ligand-mediated HER3 activation and reduce cancer cell survival *in vitro* have been engineered with sub-nanomolar affinity through combined phage and staphylococcal display technology [46,50], and were

further matured to low picomolar affinity through alanine scanning-based approaches [49]. Additional HER3 binding proteins include a bispecific albumin binding domain designed for improved half-life [48], and a HER3-specific surrobody, derived from a pre-B-cell receptor complex that inhibited both ligand-independent and ligand-dependent HER3 signaling and proliferation, and showed efficacy *in vitro* and *in vivo* [47].

Antibody fragments and low molecule weight proteins also have limitations compared to full-length monoclonal antibodies in that these scaffolds often have shorter half-lives, increased clearance due to reduced size and they inherently lack immune effector function [63]. To overcome these limitations, fusion with albumin-binding proteins or PEGylation can enhance half-life [48,64]. Beyond protein-based strategies to target HER3, aptamer-based approaches against HER3 have also been developed [65]. With their low molecular weight, aptamers achieve many of the same advantages of fragment-based approaches including improved tissue penetration, but unmodified aptamers are limited by rapid clearance and degradation in the serum, and have received less developmental focus due to intellectual property restrictions [66].

1.5 Opportunities and novel mechanism-based approaches against HER3

While it is probable that some of aforementioned HER3-targeted approaches will emerge as effective therapeutics, either alone or in combination with other drugs, these approaches are still likely to be ineffective on a significant proportion of patients as indicated by past history; for example, HER2-targeted therapies typically

show efficacy in ~24%-64% of patients with HER2-overexpressing tumors [59], thus highlighting the need for novel therapeutic approaches to target HER3.

1.5.1 HER3 sequestration-based approaches

HER3 sequestration by engineered multivalent ligands is an innovative approach whereby HER3 is locked into non-signaling homotypic interactions (**Figure 1.5**) promoted by the tendency of HER3 to exist predominantly in clusters of pre-formed homotypic dimers or oligomers on the cell surface prior to ligand stimulation [67]. Proof-of-concept for HER3 sequestration was demonstrated by Jay et al. using an engineered bivalent Neuregulin-1β (NRG) molecule, which led to reduced proliferation and chemokinesis, and increased apoptosis in multiple cancer cell lines [68,69]. Treatment with bivalent Neuregulin-1β (NRG) reduced HER3, Akt, and HER2 phosphorylation, presumably by sequestering HER3 to homotypic interactions and thereby limiting interactions with its preferred dimerization partner HER2; these phenomena were in direct opposition to treatment with native monovalent NRG, which activates HER3 and promotes HER2/HER3 dimerization [68].

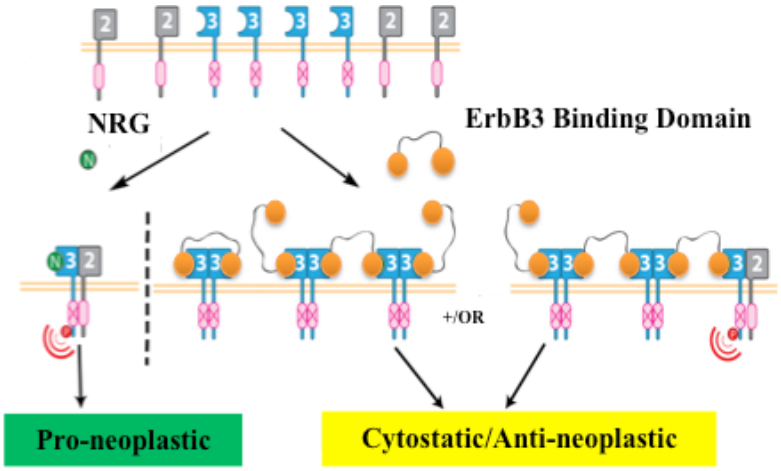

Figure 1.5: ErbB3 sequestration by bivalent ligands: Multiple ErbB3 binding domains linked by a flexible spacer domain can sequester ErbB3 into non-signaling homotypic clusters, which occur at a cost to natural NRG-activated ErbB2/ErbB3 mitogenic heterodimer formation [68,69]. HER3 sequestration was demonstrated to reduce cancer cell proliferation and chemokinesis [68]. Schematic adapted from Jay et al. [68].

1.5.2 Induced HER3 degradation and differential trafficking

Upon ligand binding, EGFR is traditionally endocytosed and degraded [10]. On the contrary, the other ErbB members are more commonly recycled [10]. HER3 is constitutively recycled back to the cell surface, and heterodimerization with HER2 reduces the HER3 internalization rate and increases the HER3 recycling rate [10], thus HER3 degradation represents a mechanistic strategy to inhibit HER3-mediated mitogenic signaling [19,30,43]. Multivalent ligands have been documented to promote receptor degradation via induced receptor clustering and differential trafficking [30]. This phenomenon of HER3 degradation has been induced by antibody-based HER3-targeting strategies [19,43], which could be explained mechanistically by bivalent binding of a HER3-targeted IgG antibody to two HER3 receptors as an initiator of the process [19]. In traditional receptor degradation processes, the receptor is first ubiquitin-tagged and then traffics to either the lysosome or the proteasome for degradation [70].

1.5.3 Targeting the ErbB family with multiple binding epitopes

Targeting the ErbB family members with multiple antibody epitopes has demonstrated enhanced therapeutic efficacy compared to monoclonal antibody treatment in a variety of cancer models [13,71,72]. MM-151, an oligoclonal antibody that binds multiple regions of the EGFR extracellular domain, is designed to overcome EGFR mutation-mediated resistance, and has proved beneficial especially where monoclonal approaches have failed [13]. MM-151 is currently in clinical trials for the treatment of a variety of solid tumors including colorectal cancer [34]. Two monoclonal antibodies specific against HER3 enhanced therapeutic efficacy in combination with BRAF/MEK inhibitors and prevented BRAF inhibition resistance for the treatment of melanoma [72]. Likewise dual treatment with HER3 monoclonal antibodies specific for domain I and domain III of the ECD of HER3 enhanced efficacy *in vitro* and *in vivo* in NCI-N87 gastric carcinoma compared to either monoclonal treatment alone; dual treatment with these antibodies led to inhibition led to potent blockade of ligand-dependent and ligand-independent HER3 signaling [71]. Overall, targeting an ErbB receptor with multiple antibodies specific for unique epitopes of the extracellular domain has shown enhanced therapeutic efficacy in cancers with and without documented ErbB mutations and thus this strategy could show broad utility and be especially beneficially in cancers with ErbB oncoprotein mutations [71,72]. EGFR mutations in cancer are common, occurring in 20% of colorectal cancers [13]. Likewise, Jaiswal et al. identified protein altering HER3 mutations in 12% of gastric (11/92), 11% of colon (11/100), 1% of non-small cell

lung cancer (NSCLC) (adeno; 1/71), and 1% of NSCLC (squamous; 1/67) cancers [41].

1.5.4 HER3-targeting for combination therapies

HER3 compensatory signaling is a critical mediator of cancer cell resistance to targeted therapies and thus "vertical" and "horizontal" combination approaches involving HER3-targeted therapeutics are a clinical need for improved cancer therapies [21–27].

Tumors previously susceptible to "horizontal" EGFR and HER2 tyrosine kinase inhibitors have been reported to grow refractory to such therapies via HER3 overexpression and an equilibrium shift in HER3 phosphorylation [23]. Likewise, cancer therapies targeting the Axl receptor tyrosine kinase, an aggressive driver of cancer growth through activation of the PI3K/Akt, ERK, and NF-κβ, are limited by acquired resistance and compensatory alternative HER3 activation [28]. Torka *et al.* demonstrated that treatment of OvCAR8 and MDA-MB-231 cells with small molecule Axl/Met-related tyrosine kinase inhibitor BMS-777607 leads to increased HER3 expression and NRG-dependent HER3 phosphorylation [28].

The "vertical" PI3K/Akt axis has been regarded as a redundant and promiscuous signaling pathways involving a variety of escape routes and positive feedback mechanisms to evade targeted therapy [26,27]. The use of small molecules to target the PI3K/Akt pathway is of clinical interest for the treatment of a variety of cancers

including ovarian, breast, and prostate [26,27]; for example the Akt inhibitor MK2206 and the PI3K I inhibitor BMK120 are in clinical trials for the treatment of ovarian cancer [21,26]. However, these small molecule drugs have limited efficacy due to compensatory signaling and alternative activation of other RTKs [21,26,27]. Likewise, prostate cancers with acquired resistance to PI3K inhibitors are often characterized by elevated NRG expression, and antibodies against HER2/HER3 have further been demonstrated to improve efficacy in prostate cancers refractory to PI3K inhibition [21].

Chapter 2: Affibody Design, Characterization, and Purification

Acknowledgements:

Figures 2.1-2.12 were adapted from:
Schardt JS; Oubaid JM, Williams SC; Howard JL; Aloimonos CM; Bookstaver ML; Lamichhane TN; Sokic S; Liyasova MS; O'Neill M; Andresson T; Hussain A; Lipkowitz S; Jay SM (2017) Engineered Multivalency Enhances Affibody-Based HER3 Inhibition for Cancer Therapy. Molecular Pharmaceutics. 14(4), 1047-1056.

Figures 2.13-2.19 were adapted from:
Schardt JS; Williams SC; Oubaid JM, Pottash AE, Noonan-Shueh MM, Ali RT, Goodman CA, Hussain A, Rena Lapidus RG, Lipkowitz S, Jay SM (2018). HER3-Targeted Affibodies with Optimized Formats Reduce Tumor Progression In Vivo in an Ovarian Cancer Model. In Review.

Mass spectrometry studies (Figures 2.3-2.5) were conducted by Dr. Yan Wang at University of Maryland Proteomics Core Facility.

Surface plasmon resonance studies (Figure 2.6) were conducted by Dr. Maura O'Neill and Dr. Thorkell Andresson at Protein Characterization Laboratory, Frederick National Laboratory for Cancer Research.

2.1 Introduction

HER3, a member of the ErbB receptor tyrosine kinase (RTK) family, which also includes epidermal growth factor receptor (EGFR), HER2, and HER4 [10], has

emerged as a therapeutic target in ovarian, prostate, breast, lung and other cancer subtypes [41]. HER3 is unique in the ErbB family in that it has a weak tyrosine kinase domain [10,73], necessitating its partnership with other ErbB members for downstream signal transduction. Despite this, HER3 is a key node in the ErbB network, characteristically dimerizing with HER2 or other partner receptors (e.g. c-MET, EGFR) to mediate cancer progression and/or metastasis [44]. Structurally, HER3 contains six phosphotyrosine sites in its C-terminal tail [9,74,75], allowing for potent mitogenic signaling through the PI3K/Akt pathway. Further, HER3 activation can enable acquired resistance to cancer therapeutics, including ErbB-targeted drugs [21–25,45].

Numerous monoclonal antibody (mAb) approaches directed at HER3 are in development [19], and it is probable that some of these will continue to emerge as effective therapeutics, either alone or in combination with other drugs. However, these approaches are still likely to be ineffective in a significant proportion of patients; for example, FDA-approved HER2-targeted therapies have been reported to show efficacy in ~24%-64% of patients with HER2-overexpressing tumors [59]. Thus, development of alternative therapeutic approaches against HER3 as part of anti-tumor targeting strategies, particularly where HER3 acts as a facilitator and modulator of oncogenic signaling cascades, would fill a critical clinical need.

Towards meeting this need, one promising concept for improved design of pharmaceuticals is engineered multivalency, which can be achieved through chemical

biology and protein engineering approaches. Multivalency refers to the phenomenon by which a single molecule can be involved in multiple simultaneous molecular recognition events, which is hypothesized to enhance therapeutic efficacy by means of improved avidity, residence time, selectivity, and differential receptor trafficking [29–33]. The therapeutic potential of multivalent ligands against HER3 specifically is supported by the possibility of inducing HER3 sequestration by engaging HER3 into non-signaling homotypic interactions. This phenomenon may be promoted by the tendency of HER3 to exist predominantly in homotypic clusters on the cell surface prior to ligand stimulation [67]. Our previous work demonstrated the therapeutic potential of multivalent HER3 engagement by using an engineered bivalent Neuregulin-1β (NRG) molecule, which induced decreased proliferation and chemokinesis and increased apoptosis in multiple cancer cell lines [68,69]. However, employing NRG as a HER3-binding domain is problematic from a translational perspective, as it could activate HER3 to induce pro-neoplastic signaling [16,76,77]. The therapeutic potential of bivalent NRG is further limited by potential off-target effects on HER4 as well as challenges in protein production due to aggregation caused by sequence repetition and improper formation of multiple disulfide bonds.

Thus, in this work, we sought to extend the concept of multivalent HER3 engagement by employing HER3-binding domains with greater translational potential and lower risk of pro-neoplastic side effects. Utilizing the Z_{05413} affibody – a 58 amino acid blocking peptide with sub-nanomolar affinity to HER3 developed by Lofblom and colleagues [46] – as the HER3 binding domain, we developed novel multivalent

HER3 ligands and evaluated their functional efficacy in multiple cancer cell lines in comparison to monovalent molecules. We further investigated the relevance of the specific molecular conformation employed as well as the mechanisms contributing to the efficacy of the multivalent ligands. Our results indicate that multivalency enhances HER3 signaling inhibition and induces rapid downregulation of the receptor by affibody molecules, further establishing multivalent engagement of HER3 as a promising therapeutic strategy.

2.2 Methods

2.2.1 Protein production and purification

Coding DNA sequences for affibody constructs were inserted into the pET45b vector (Merck Millipore) and Q5 Directed mutagenesis (New England Biolabs) was used to generate bivalent affibodies with varying domain size. pET45b-affibody constructs were transformed into *Escherichia coli (E. coli)* strain BL21 (DE3) (New England Biolabs). For protein expression, 500 mL LB broth with 100 μg/mL ampicillin was inoculated from a 3 mL overnight starter culture, incubated at 37° C, shaken at 220 rpm, grown to an OD_{600} of 0.6-0.8, induced with 0.4 μM IPTG, and grown for 4 hours at 30°C. The cell pellet was isolated by centrifugation at 6000 rpm for 15 minutes and frozen at -20°C. Soluble protein lysates were generated using B-PER complete protein extraction reagent (Thermo Fisher Scientific) following manufacturer's protocol and purified by immobilized metal affinity chromatography using TALON metal affinity resin (Clontech), and refined/buffer exchanged in PBS using ENrich SEC 650 size exclusion (Bio-Rad) high performance liquid chromatography NGC Quest 10 Plus system (Bio-Rad).

2.2.2 Protein molecular weight and sequence identity determination by mass spectrometry

For molecular weight determination, monovalent, bivalent, and trivalent affibodies were mixed, and then separated with a ProSwift RP-4H monolithic column. Trivalent affibody spectrum was further analyzed with poroshell C3 microbore column. Mass spectra were acquired with a Thermo Scientific Orbitrap Fusion Lumos mass spectrometer at R=120,000 (m/z 200). Protein molecular weight was calculated using XTract. For sequence identity determination, monovalent, bivalent, and trivalent affibodies were diluted with 0.1 M triethylaminebicarbonate (TEAB) and digested with Trypsin/LysC Mix (Promega V5073) at 35°C overnight. Digest was acidified with glacial acetic acid and analyzed by NanoLC-MS/MS using a trap column (Thermo Scientific Acclaim PepMap™ 100, 5 μm, 100 Å, 300 μm × 5 mm) and an analytical column (Thermo Scientific Acclaim PepMap™ 100, 3 μm, 100 Å, 75 μm × 250 mm). Data were processed using Proteome Discoverer (v 2.1) and Sequest HT.

2.2.3 HER3 binding affinity determination by surface plasmon resonance

Interactions between the affibodies and HER3 were analyzed by surface plasmon resonance using a Biacore T200 system (GE Healthcare). HER3 (Human, His-tagged; Sino Biological) at 50 μg/mL in Acetate 4.5 was covalently immobilized on a CM5 chip via amine coupling to a final response of 1600 RU in 25 mM HEPES pH 7.3 at 25°C. Affibody samples were prepared in degassed, filtered HBS-P+ buffer (GE Healthcare). Single cycle kinetic experiments were carried out using five injections

(30 μL/min) of increasing concentration of affibodies (0.1-10 nM) passed over the sensor chip for 120 s association followed by 420 s dissociation. Following buffer and reference subtraction, kinetic constants and binding affinities were determined utilizing the Biacore T200 evaluation software (GE Healthcare).

2.2.4 Cell lines and reagents

The OvCAR8 cell line was obtained from Dr. Christina Annunziata (National Cancer Institute). Du145, BT474 and H1975 cell lines were purchased from ATCC. OvCAR8, Du145, and H1975 were maintained in RPMI 1640 (ATCC), BT474 cells were maintained in Hybri-Care Medium (ATCC).

2.2.5 Cell signaling studies

Cells were serum starved for 4 hours, treated with the indicated concentrations of affibody or the small molecule pan-HER kinase inhibitor N-(4-((3-Chloro-4-fluorophenyl)amino)pyrido[3,4-d]pyrimidin-6-yl)2-butynamide (Millipore 324840) (Total Inhibitor) for 30 minutes, stimulated with 10 nM human heregulin-1β (NRG) (Peprotech) for 10 minutes, lysed, and probed by immunoblot for pHER3, pHER2, pAkt, and pERK1/2. For immunoblotting, membranes were probed with primary antibodies (21D3 pHER3, tyr877 pHER2, D9E pAkt, pERK1/2 #9101, 13E5 β-actin, D65A4 β−tubulin) all from Cell Signaling, and secondary antibody IRDye 800 CW (Licor), and scanned using an Odyssey CLx image system (Licor).

2.2.6 HER3 downregulation assays

To examine HER3 levels, cells were treated with the indicated concentrations of affibody, pan-HER kinase inhibitor (Millipore 324840) or no treatment (media alone)

control, lysed at the indicated time points, and probed by immunoblot for HER3 as previously described using primary antibodies (D22C5 HER3, and 13E5 β−actin).

2.3 Results

2.3.1 Engineered multivalency enhances affibody-induced pHER3 inhibition

The general hypothesis motivating these studies is that engineered multivalency can enhance HER3-targeted therapeutic efficacy by means of enhanced avidity and HER3 sequestration into non-productive homotypic interactions, given that hetero-dimerization is requisite for HER3-mediated signal transduction. Thus, employing the Z_{05413} affibody [46] as the HER3 binding domain and a flexible protease resistant peptide spacer [68] as a linker domain, bivalent and trivalent HER3 affibodies were designed (**Figure 2.1A**). Multivalent affibodies were expressed as recombinant proteins in BL21 (DE3) *E. coli* and purified by immobilized metal ion chromatography and size exclusion chromatography (**Figure 2.1B**). All HER3 affibodies consistently displayed molecular weights higher than their predicted values by SDS-PAGE, which could be a result of electrophoretic interference caused by their helix-

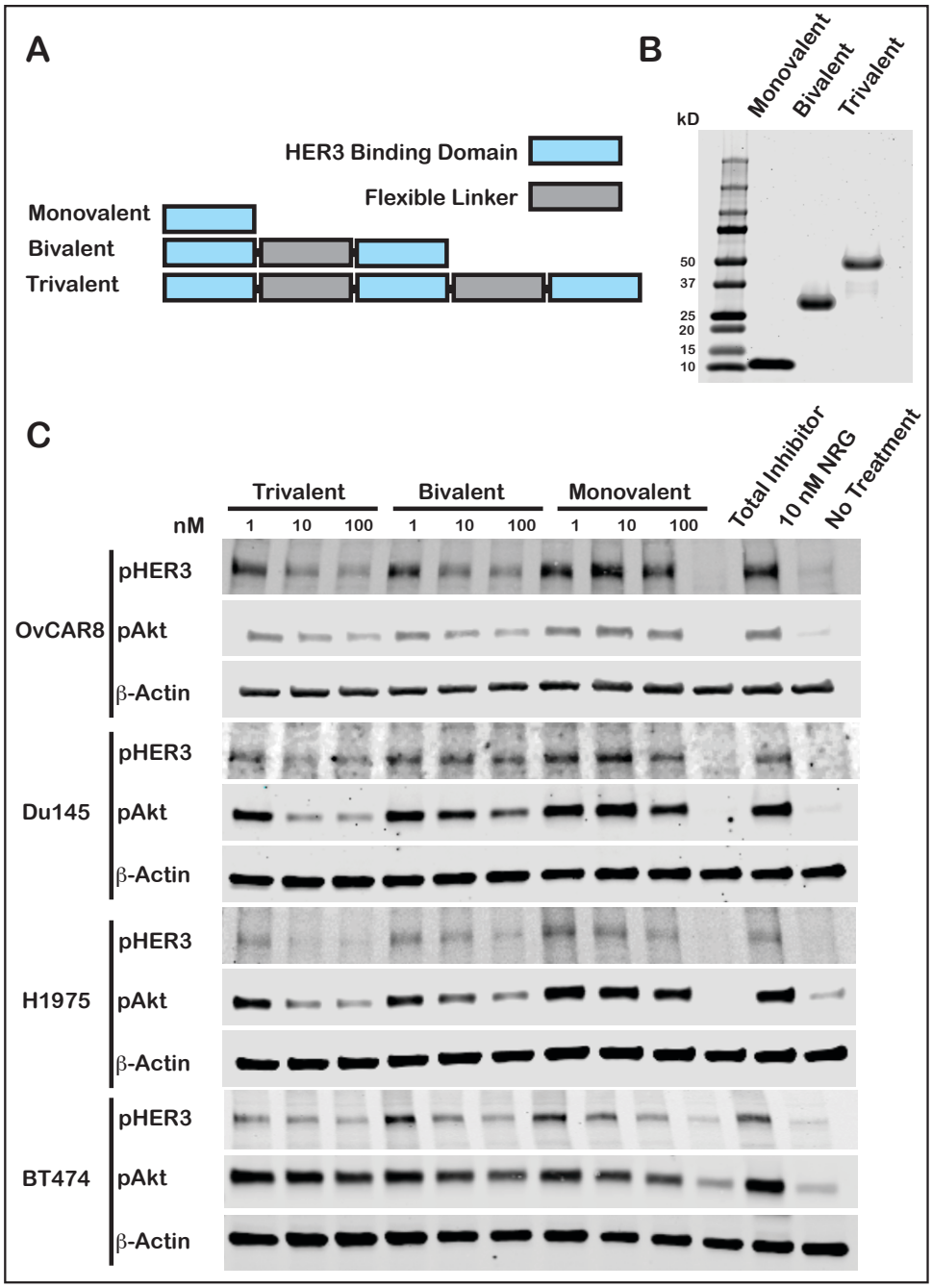

Figure 2.1: Multivalency enhances affibody-mediated pHER3 and pAkt inhibition. A. Schematic representing monovalent, bivalent and trivalent affibody constructs. **B**. Purified protein products are displayed on a Coomassie stained gel loaded at 7.3 mg/lane. Monovalent, bivalent, and trivalent ligands have respective theoretical molecular weights of 7.6, 19.1, 30.5 kDa. **C.** OvCAR8, Du145, H1975 and BT474 cells were treated with the indicated concentrations of trivalent, bivalent or monovalent ligand, or 100 nM pan HER kinase inhibitor (total inhibitor), or media alone (no treatment) for 30 minutes, then stimulated with 10 nM NRG for 10 minutes, lysed, and probed for pHER3, pAkt and b-actin by immunoblot. All multivalent ligand concentrations refer to the concentration of individual affibody domain. Results shown are representative of three independent experiments. All blots were cropped.

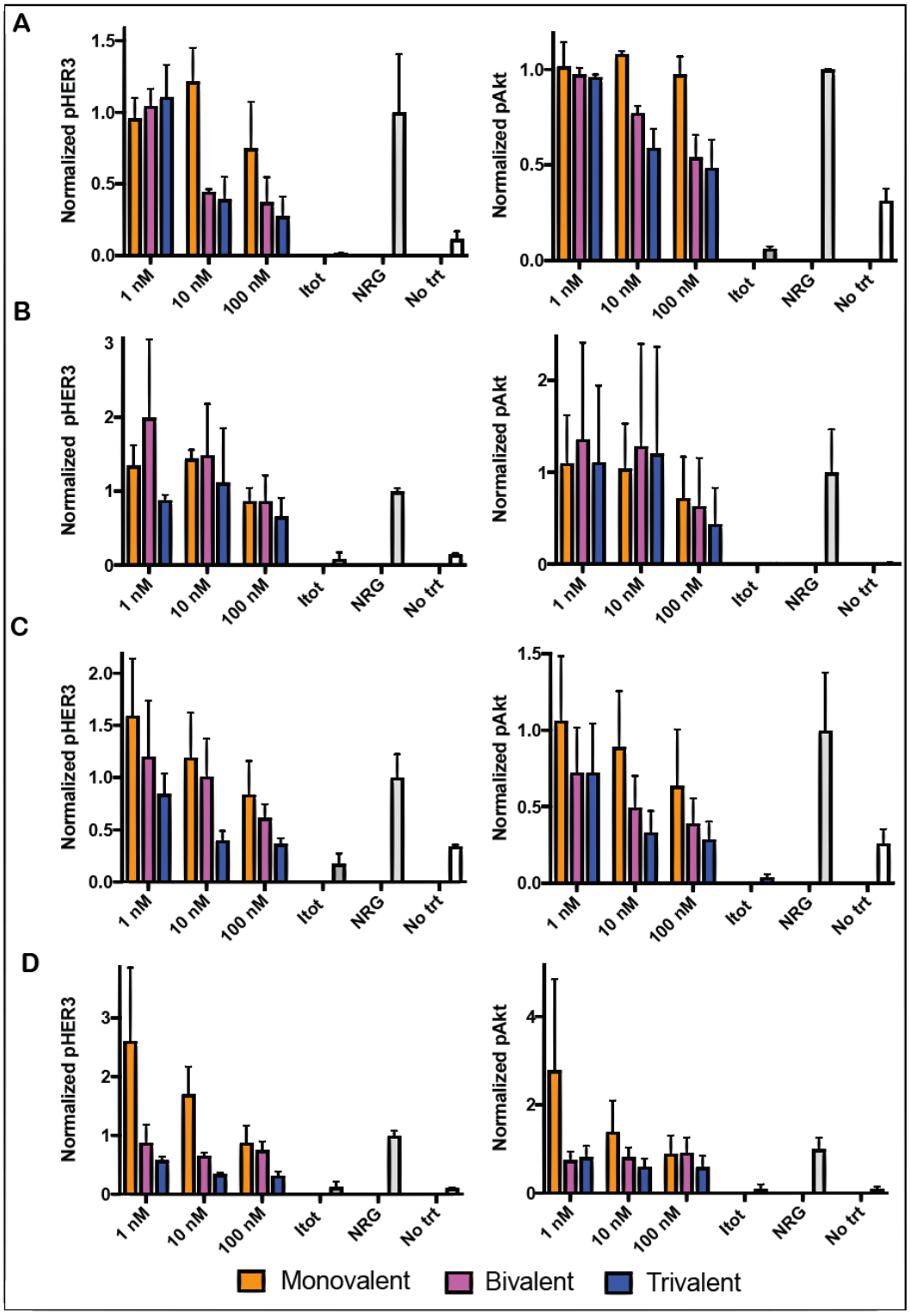

Figure 2.2: Immunoblot quantification of Figure 2.1: Multivalency enhances affibody-mediated pHER3 and pAkt inhibition. Quantified pHER3 (left) and pAkt (right) values are displayed for **A.** OvCAR8 **B.** Du145 **C.** H1975 and **D.** BT474 cells. Blots were quantified using Odyssey CLx image system (Licor) Analysis Tool and normalized to β-actin. Results shown are averages of three independent experiments.

loop-helix motifs [46]. However, mass spectrometry analysis indicated that all affibodies showed molecular weight and amino acid composition consistent with predicted values (**Figures 2.3-2.5**). Binding affinities for HER3 were characterized for all affibodies by surface plasmon resonance. Monovalent and bivalent affibodies had similar affinities to HER3 (monovalent K_D = 316 pM, bivalent K_D = 327 pM, mean values), whereas trivalent affibodies displayed substantially lower affinity (trivalent K_D = 2340 pM) (**Figure 2.6**). These data suggest that any impact of multivalency on the cellular effects of HER3 affibodies is not due to enhanced HER3 binding.

The Z_{05413} affibody is reported to disrupt NRG-mediated HER3 signaling [46]. To assess the effect of multivalency on this phenomenon, cells were treated with the indicated equivalent concentrations of affibody domains (100 nM of monovalent affibody molecule has an equivalent affibody domain concentration to 50 nM of bivalent and 33 nM of trivalent affibody molecules), stimulated with NRG, and then probed for phosphorylated HER3 (pHER3) by immunoblot. The results indicate that multivalency enhanced affibody-mediated pHER3 signal inhibition in a variety of cancer cell lines – OvCAR8 (ovarian), Du145 (prostate), BT474 (breast) and H1975 (lung) – which were selected based on the reported role of HER3 signaling in proliferative and/or metastatic phenotypes as well as in promoting drug resistance [16,22,43,78]. The most significant differential effects were seen between multivalent versus monovalent treatment groups (**Figures 2.1C, 2.2**); differences between the multivalent affibody groups (bivalent versus trivalent) were less pronounced (**Figures**

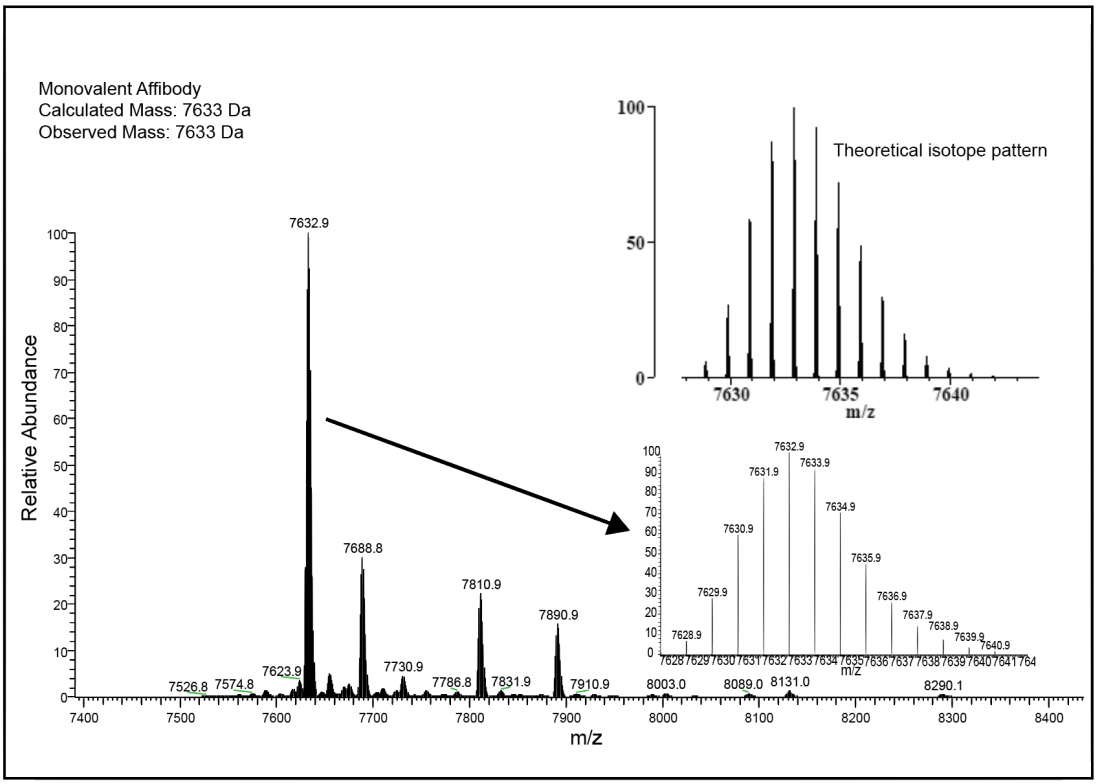

Figure 2.3: Mass spectrum of purified monovalent affibody confirms predicted molecular weight. Monovalent, bivalent, and trivalent affibodies were mixed, and then separated with a ProSwift RP-4H monolithic column. Mass spectra were acquired with a Thermo Scientific Orbitrap Fusion Lumos mass spectrometer at R=120,000 (m/z 200). Protein molecular weight was calculated using XTract.

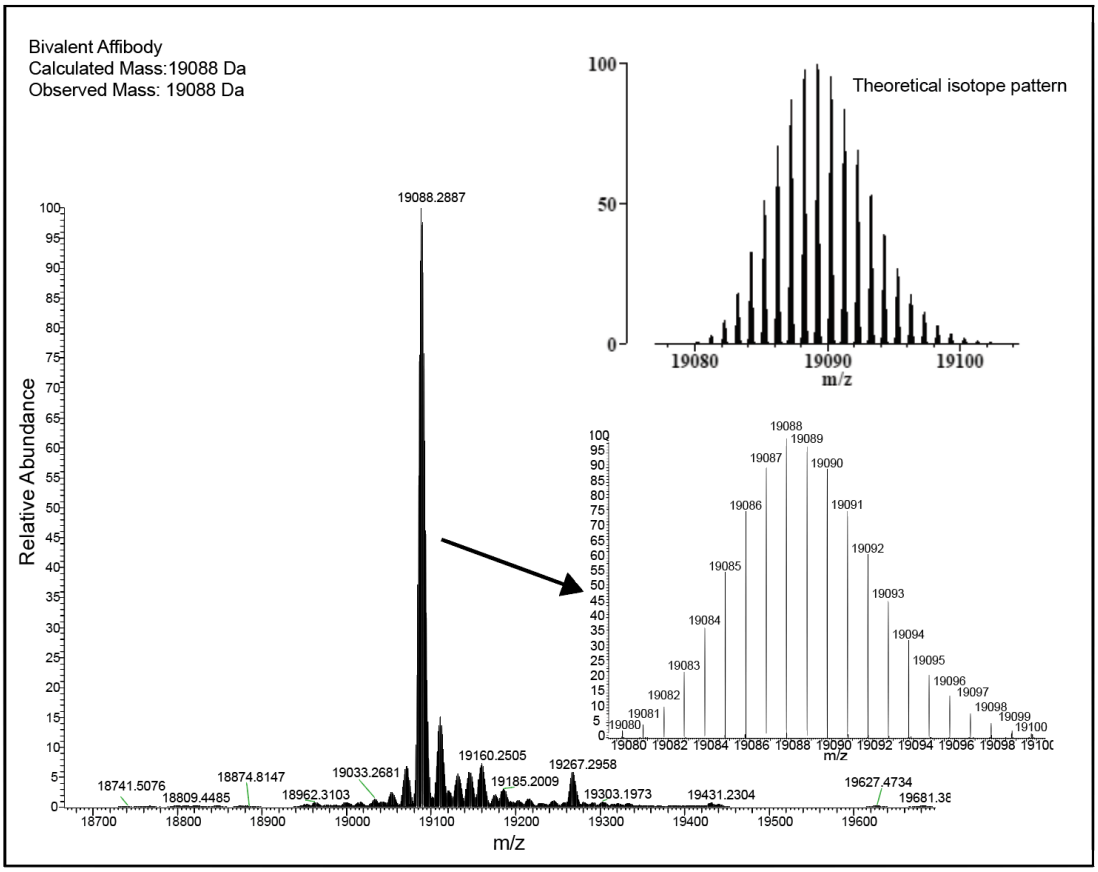

Figure 2.4: Mass spectrum of purified bivalent affibody confirms predicted molecular weight. Monovalent, bivalent, and trivalent affibodies were mixed, and then separated with a ProSwift RP-4H monolithic column. Mass spectra were acquired with a Thermo Scientific Orbitrap Fusion Lumos mass spectrometer at R=120,000 (m/z 200). Protein molecular weight was calculated using XTract.

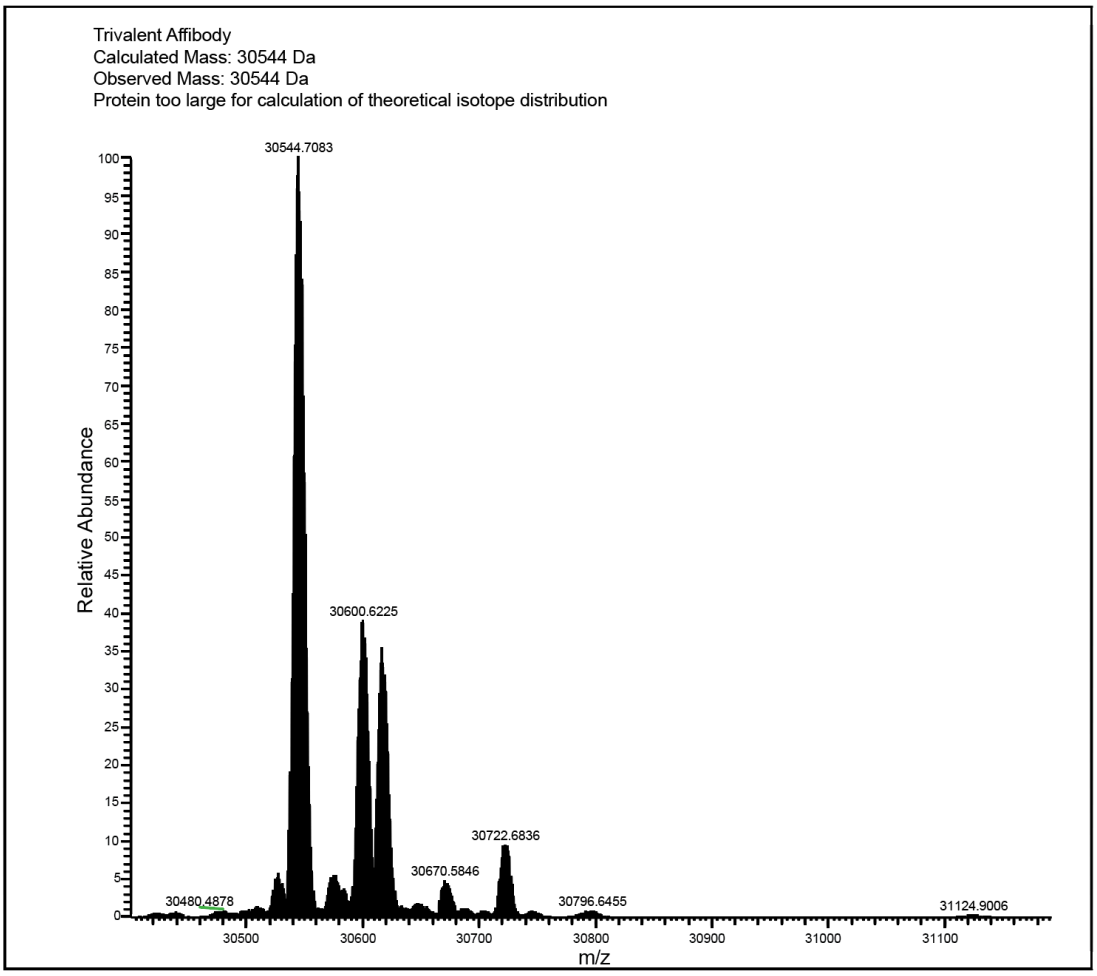

Figure 2.5: Mass spectrum of purified trivalent affibody matches predicted value. Monovalent, bivalent, and trivalent affibodies were mixed, and then separated with a ProSwift RP-4H monolithic column. Trivalent affibody spectrum was further analyzed with poroshell C3 microbore column. Mass spectra were acquired with a Thermo Scientific Orbitrap Fusion Lumos mass spectrometer at R=120,000 (m/z 200). Protein molecular weight was calculated using XTract. Trivalent affibody is too large for calculation of theoretical isotope distribution.

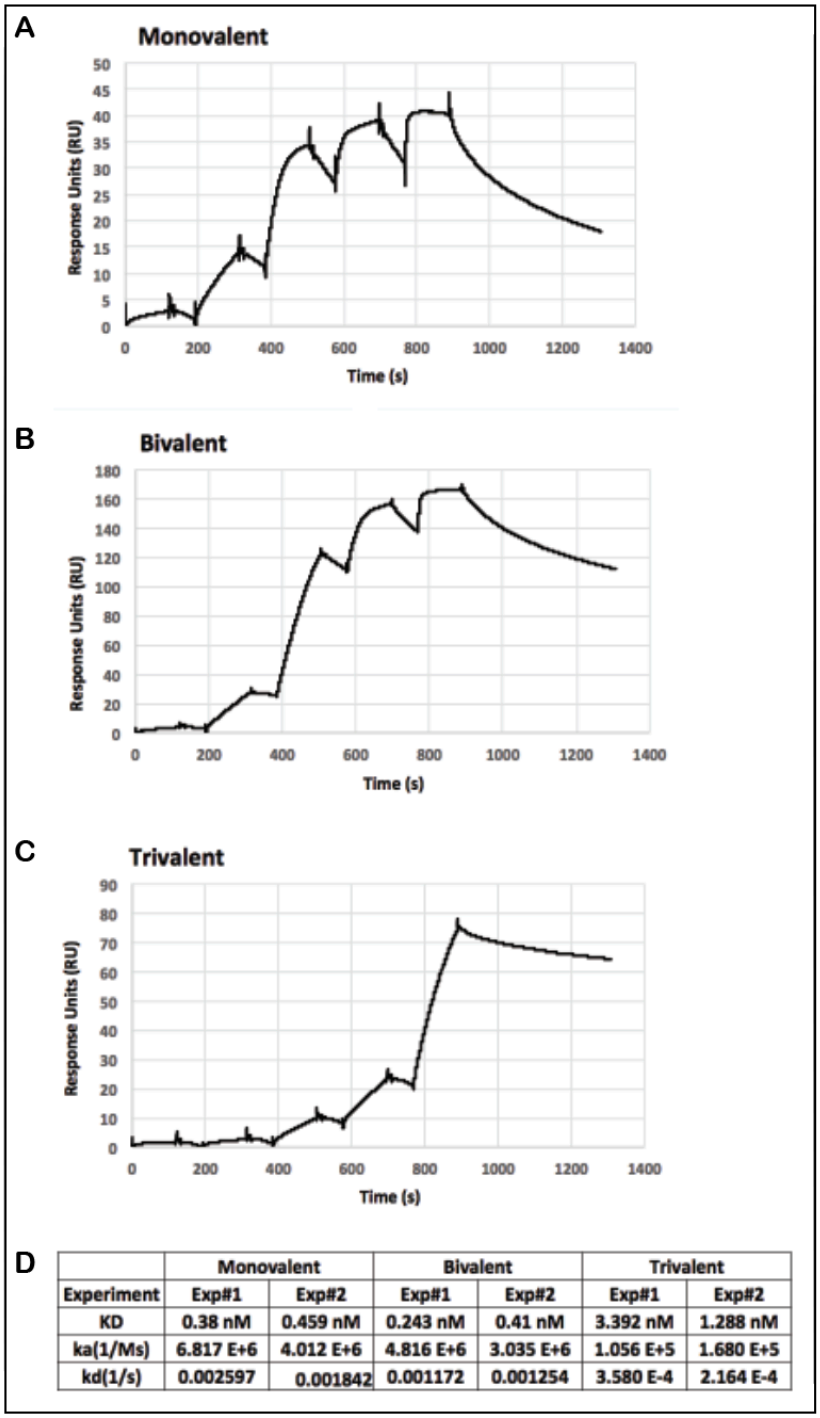

D

	Monovalent		Bivalent		Trivalent	
Experiment	Exp#1	Exp#2	Exp#1	Exp#2	Exp#1	Exp#2
KD	0.38 nM	0.459 nM	0.243 nM	0.41 nM	3.392 nM	1.288 nM
ka(1/Ms)	6.817 E+6	4.012 E+6	4.816 E+6	3.035 E+6	1.056 E+5	1.680 E+5
kd(1/s)	0.002597	0.001842	0.001172	0.001254	3.580 E-4	2.164 E-4

Figure 2.6: Surface plasmon resonance analysis of affibody-ErbB3 interaction. Sensorgrams of **A.** Monovalent **B.** Bivalent and **C.** Trivalent affibody interactions with immobilized ErbB3. **D.** Summary of binding constants (KD, Kd, Ka). Briefly, ErbB3 (50 µg/mL) was covalently immobilized on a CM5 chip via amine coupling to a final response of 1600 RU. Single cycle kinetic experiments were carried out using five injections (30 µL/min) of increasing concentration of affibodies (0.1-10 nM) passed over the sensor chip for 120 second association followed by a 420 second dissociation. Following buffer and reference subtraction, kinetic constants and binding affinities were determined utilizing the Biacore T200 evaluation software (GE Healthcare).

2.1C, 2.2). Additionally, assessment of downstream signaling revealed that, in all cell lines tested, increased valency resulted in enhanced pAkt inhibition, with the most differential effects again seen between multivalent compared to monovalent treatment groups (**Figures 2.1C, 2.2**).

One potential outcome of HER3 engagement by multivalent ligands is deprivation of productive dimerization with HER2, as observed for bivalent NRG in our previous work [68]. Thus, immunoblots for phosphorylated HER2 (pHER2) were performed, with the results indicating that pHER2 levels were not consistently affected by affibody treatments in the BT474 cell line relative to control (10 nM NRG) levels (**Figures 2.7, 2.8A**). Downstream pERK1/2 in this cell line was similarly not significantly affected by affibody treatments (**Figures 2.7, 2.8B**). Notably, pHER2 was not detected by immunoblot in the OvCAR8, Du145, and H1975 cell lines after NRG stimulation (these cell lines are reported to have substantially less HER2 expression compared to the BT474 cell line; Broad-Novartis Cancer Cell Line Encyclopedia). Previous reports indicate that monovalent HER3 affibodies inhibit NRG-induced pHER2 in MCF-7 and SKBR-3 cells [50,62]; the MCF-7 data match our own observations. Taken together, pHER2 inhibition by HER3 affibodies may be cell line specific and does not appear to be a requirement for HER3 signaling inhibition.

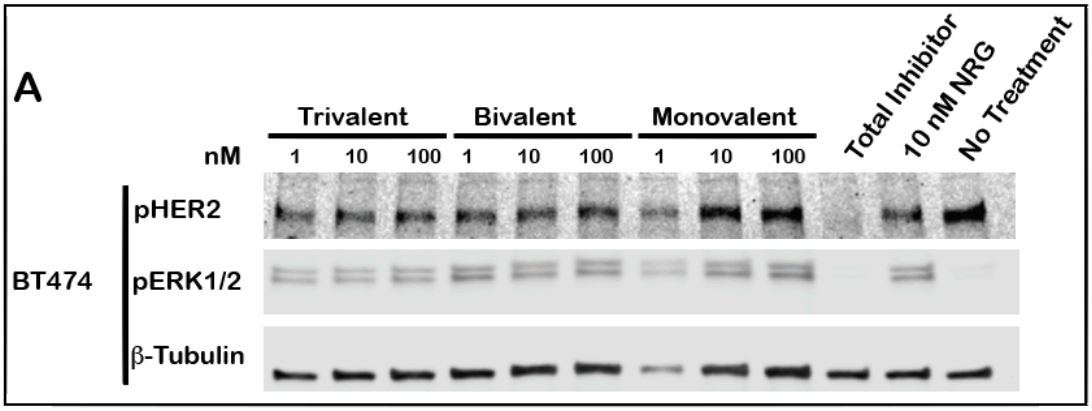

Figure 2.7: HER3 affibodies do not influence pHER2 levels regardless of valency in BT474 cells A. BT474 cells were treated with the indicated concentrations of trivalent, bivalent or monovalent affibodies, or 100 nM pan HER kinase inhibitor (total inhibitor), or media alone (no treatment) for 30 minutes, then stimulated with 10 nM NRG for 10 minutes, lysed, and probed by immunoblot for pHER2, or pERK1/2. β-Tubulin levels were assessed for normalization purposes. Results shown are representative of two independent experiments. All blots were cropped.

2.3.2 Multivalency induces increased affibody-mediated HER3 downregulation

It has been reported that multivalent binding events can induce differential receptor trafficking [30]. Thus, the impact of multivalent affibodies on HER3 expression was investigated as a potential mechanism of their increased HER3 signaling inhibition compared to monovalent analogs. The results of these studies indicate that, in comparison to monovalent affibodies, both bivalent and trivalent affibodies more potently downregulate HER3 protein levels in all cell lines tested. Specifically, substantial HER3 downregulation was observed 3 hours after application of 10 nM equivalent doses of trivalent and bivalent affibodies compared to monovalent affibody-treated cells and untreated controls, and this effect persisted over 72 hours (**Figures 2.9, 2.10**).

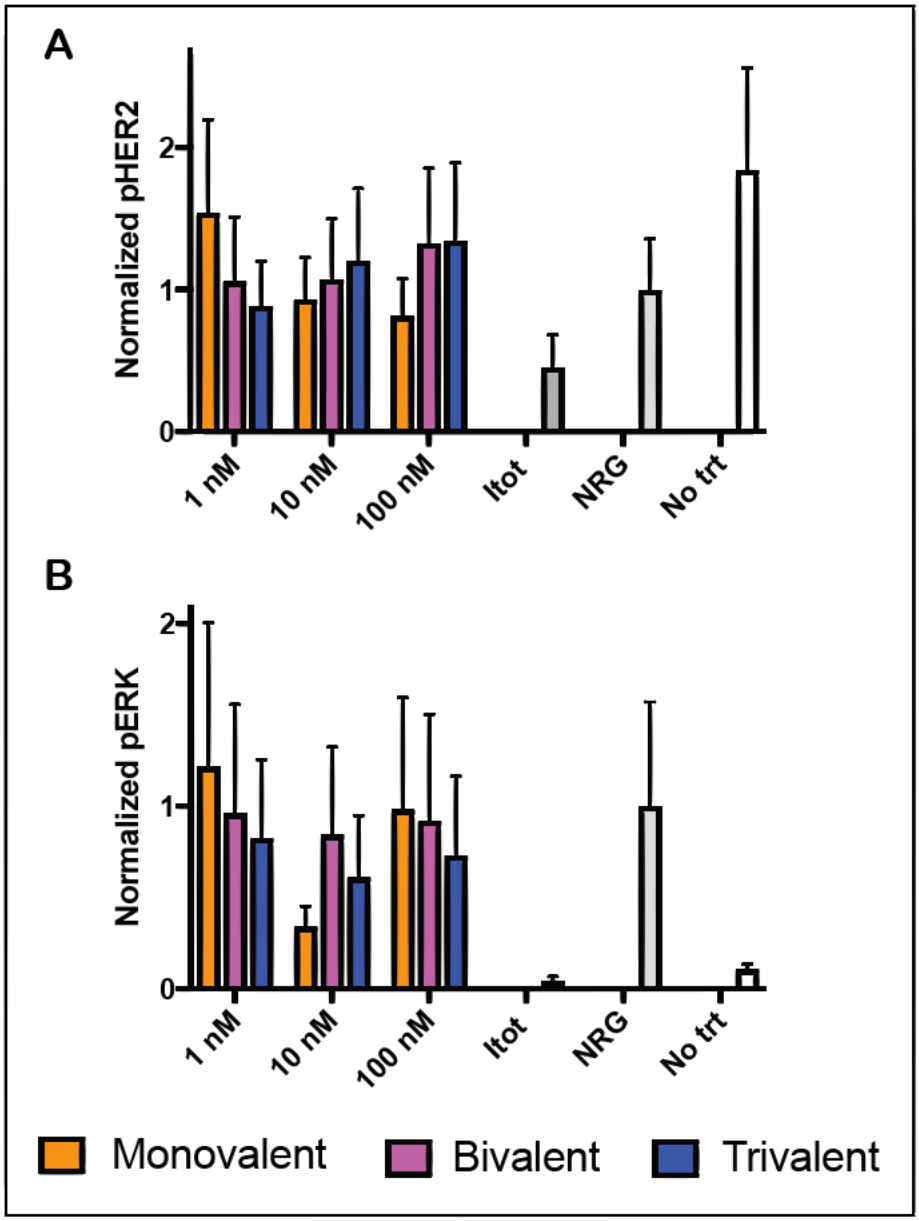

Figure 2.8: Immunoblot quantification of Figure 2.7: HER3 affibodies do not influence pHER2 levels regardless of valency in BT474 cells. Quantified **A.** pHER2 and **B.** pERK1/2 values. Blots were quantified using Odyssey CLx image system (Licor) Analysis Tool and normalized to β-Tubulin. Results shown are averages of three independent experiments with error bars displayed as +- standard error.

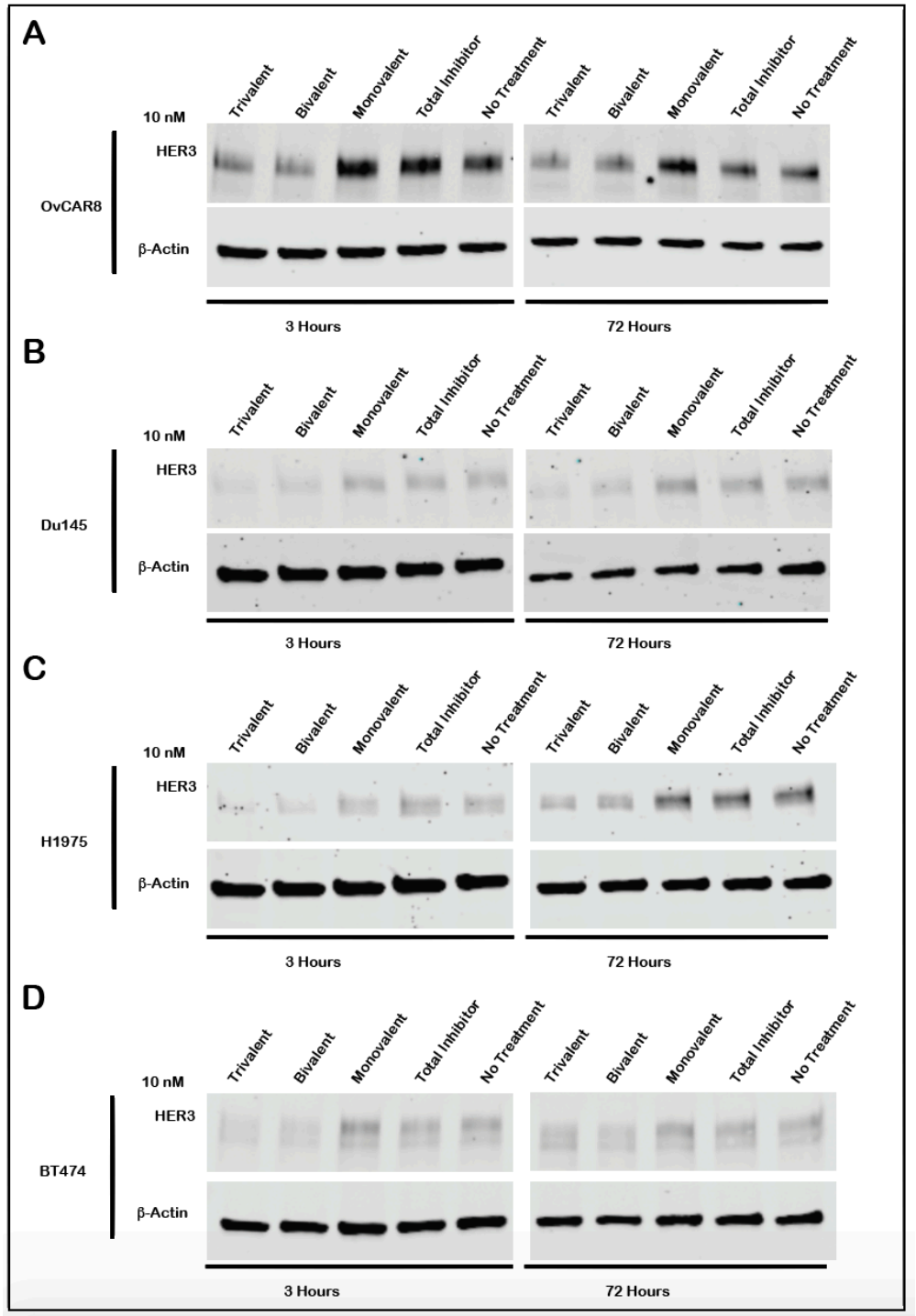

FIGURE 2.9: Multivalency induces affibody-mediated HER3 downregulation. A. OvCAR8 **B.** Du145 **C.** H1975 **D.** BT474 cells were treated with 10 nM trivalent, bivalent or monovalent affibody, pan HER kinase inhibitor (total inhibitor), or media alone (no treatment), lysed at the indicated time points, and probed by immunoblot for HER3. β-actin levels were assessed for normalization. Results shown are representative of three independent experiments. All blots were cropped.

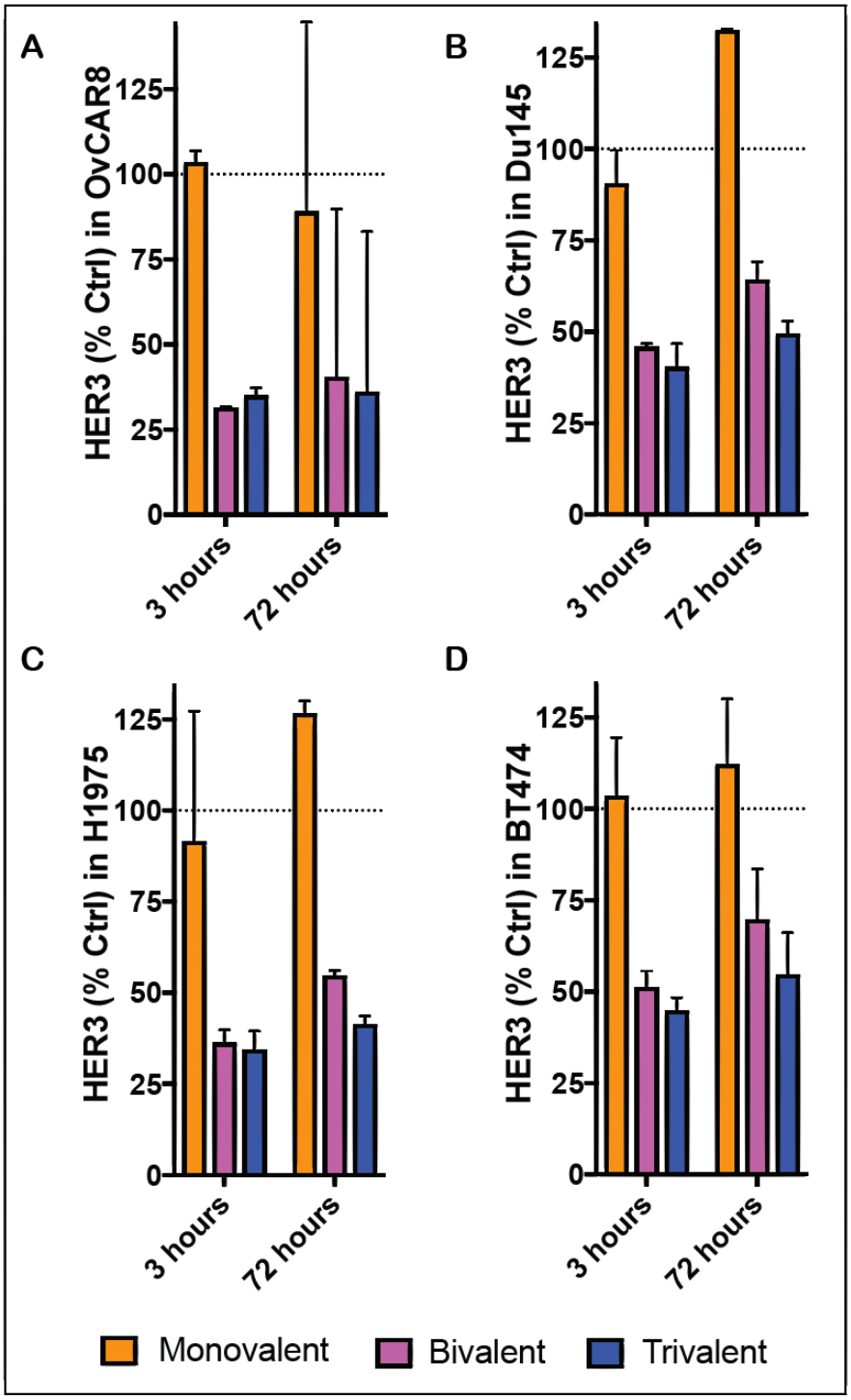

Figure 2.10: Immunoblot quantification of Figure 5: Multivalency enhances affibody-mediated HER3 downregulation. Quantified HER3 values relative to normalized HER3 of no treatment control are displayed for **A.** OvCAR8 **B.** Du145 **C.** H1975 and **D.** BT474 cells. Blots were quantified using Odyssey CLx image system (Licor) Analysis Tool and normalized to b-actin. Results shown are averages of two independent experiments with error bars displayed as +- standard error.

2.3.3 Linker domain size has limited impact on bivalent affibody efficacy

Linker domain size is reported to be an important parameter in multivalent ligand design [30]. The flexible, glycine rich, protease resistant spacer domain employed for the bivalent and trivalent affibodies described in **Figure 2.11** contains 3 repeat units and has a predicted length of approximately 20 nanometers (nm), long enough to traverse the theoretical 10 nm distance required to sequester a cross-facing HER3 homodimer [68]. To systematically investigate the role of linker domain size on efficacy, a panel of bivalent affibodies was engineered by varying the number of repeat units in the spacer peptide from 1 to 4 (each unit having a predicted length of ~7 nm) (**Figures 2.11A, B**). Inhibitory efficacy against HER3 and Akt phosphorylation across multiple cell types with bivalent affibodies of various linker domain sizes was observed to be similar, with no consistent trends relating spacer domain length to inhibitory efficacy (**Figures 2.11C, 2.12**). Interestingly, the increased pHER3 inhibition associated with multivalency was still observed for the smallest linker size tested, suggesting that even lower MW multivalent HER3 affibodies have enhanced therapeutic potential.

2.3.4 Functional effects of bivalency can be achieved with a minimal 3-glycine linker

Interestingly, we find that reducing the linker domain size to approximately 1 nm in length (three glycine residues) did not impair affibody-mediated pHER3/pAkt inhibition or HER3 downregulation (**Figures 2.13, 2.14**) as evaluated in OvCAR8 ovarian cancer cells previously identified to be highly responsive to HER3 affibody therapeutics [79]. These results demonstrate that linker length (and by extension, the potential for cross-facing homodimer sequestration) has limited impact on multivalent

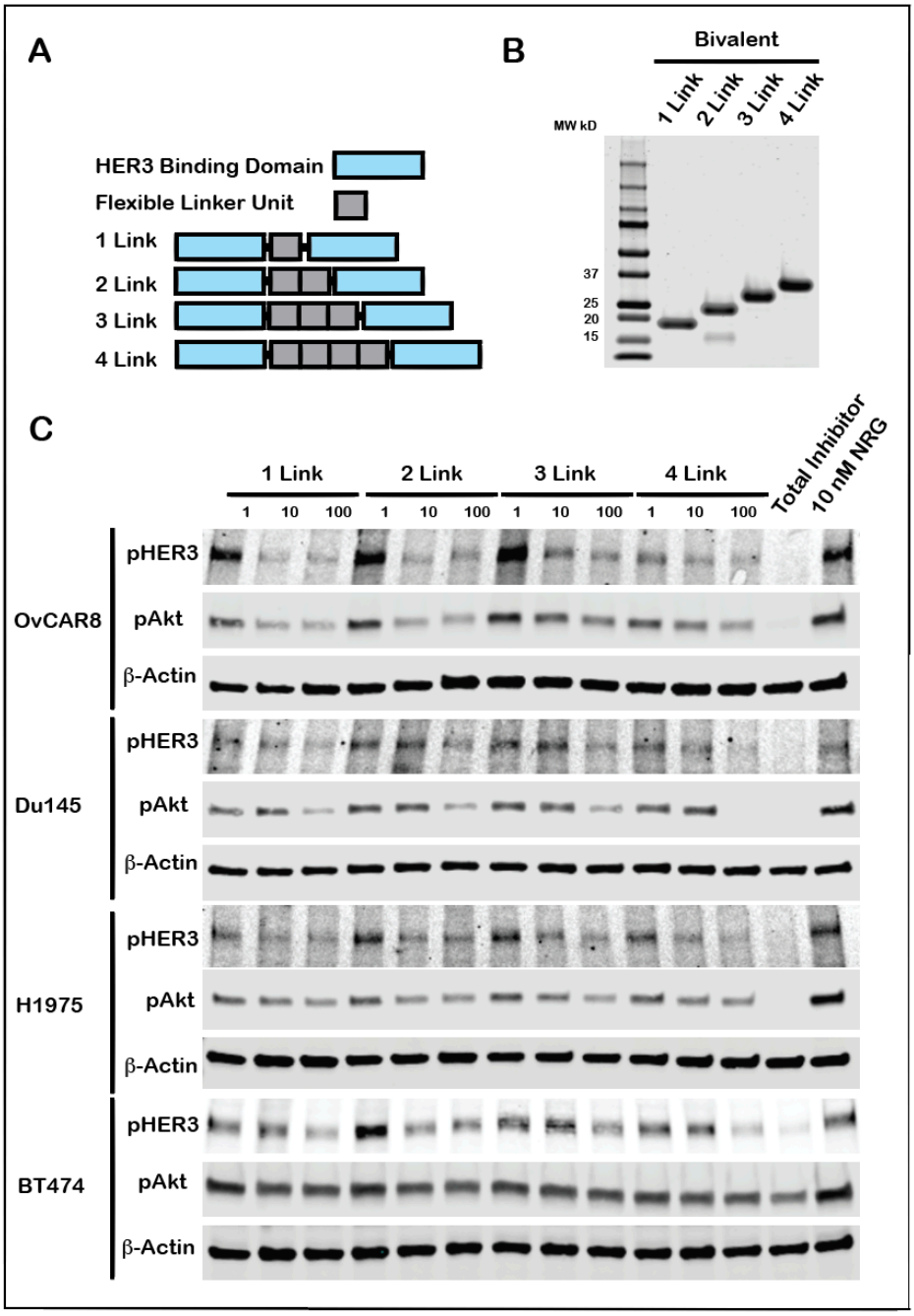

Figure 2.11: Linker domain size has limited impact on bivalent affibody activity. A. Schematic representing bivalent affibodies of varying linker domain size: 1 link (1 repeat unit), 2 link, 3 link, and 4 link. B. Purified protein products of bivalent affibodies with the indicated linker domain size are displayed on a Coomassie stained gel loaded at 7.3 μg/lane. 1 link, 2 link, 3 link, and 4 link bivalent affibodies have respective theoretical molecular weights of 16.0, 17.5, 19.1, 20.6 kDa. C. OvCAR8, Du145, H1975, and BT474 cells were serum starved for 4 hours, treated with the indicated concentrations of trivalent, bivalent or monovalent affibody, pan HER kinase inhibitor (total inhibitor), or media alone for 30 minutes, then stimulated with 10 nM NRG for 10 minutes, lysed, and probed by immunoblot. Results are representative of two independent experiments. All blots were cropped.

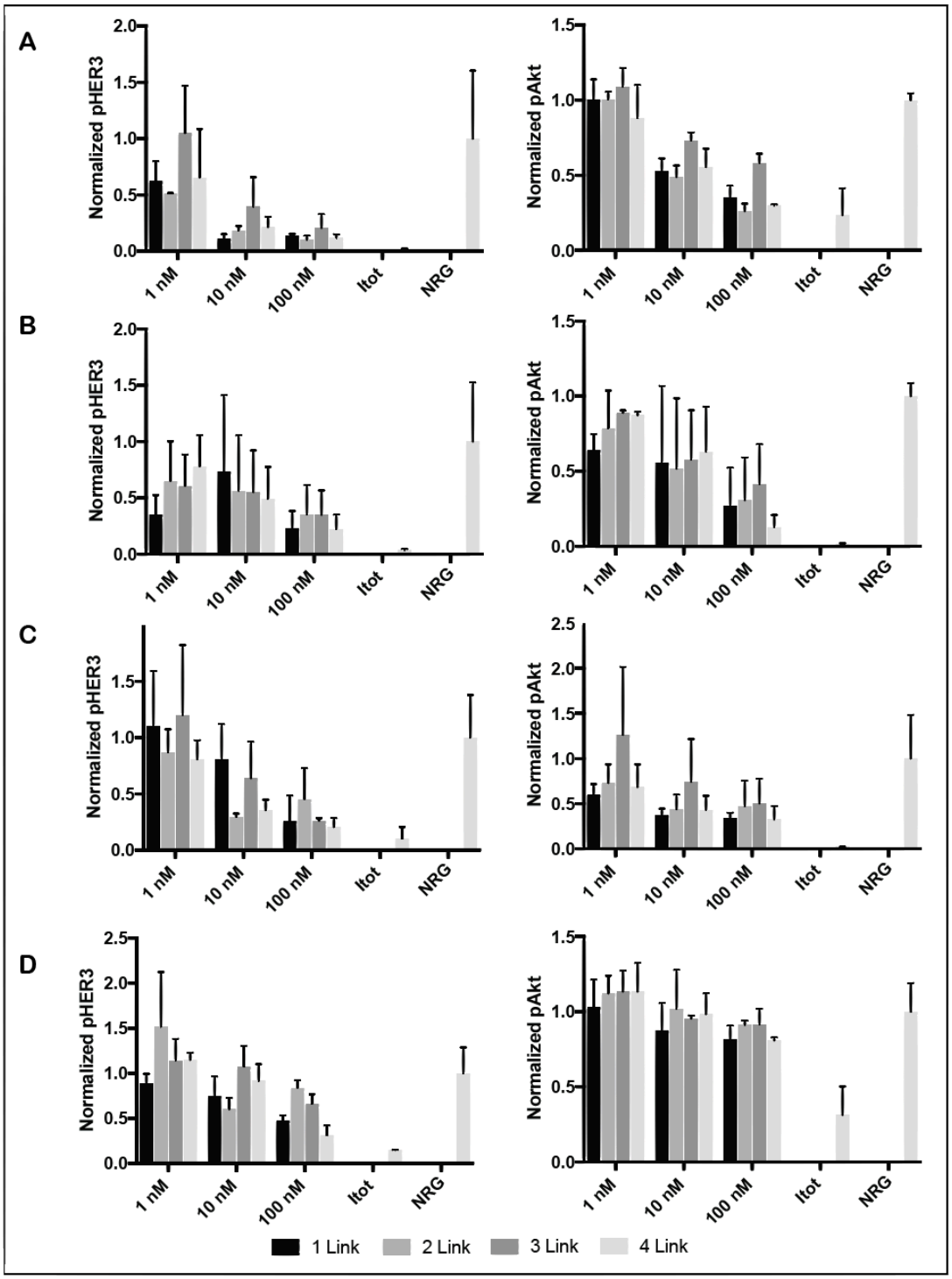

Figure 2.12: Immunoblot quantification of Figure 2.11: Linker domain size has limited impact on bivalent affibody activity. Quantified pHER3 (left) and pAkt (right) values are displayed for **A.** OvCAR8 **B.** Du145 **C.** H1975 and **D.** BT474 cells. Blots were quantified using Odyssey CLx image system (Licor) Analysis Tool and normalized to b-actin. Results shown are averages of two independent experiments with error bars displayed as +- standard error.

HER3 ligand efficacy. A potential advantage of multivalent ligands utilizing a minimalistic linker may be their lower immunogenicity and higher translational potential compared to our first-generation bivalent affibodies, and therefore we moved forward with multivalent ligands incorporating a three-glycine linker for subsequent studies.

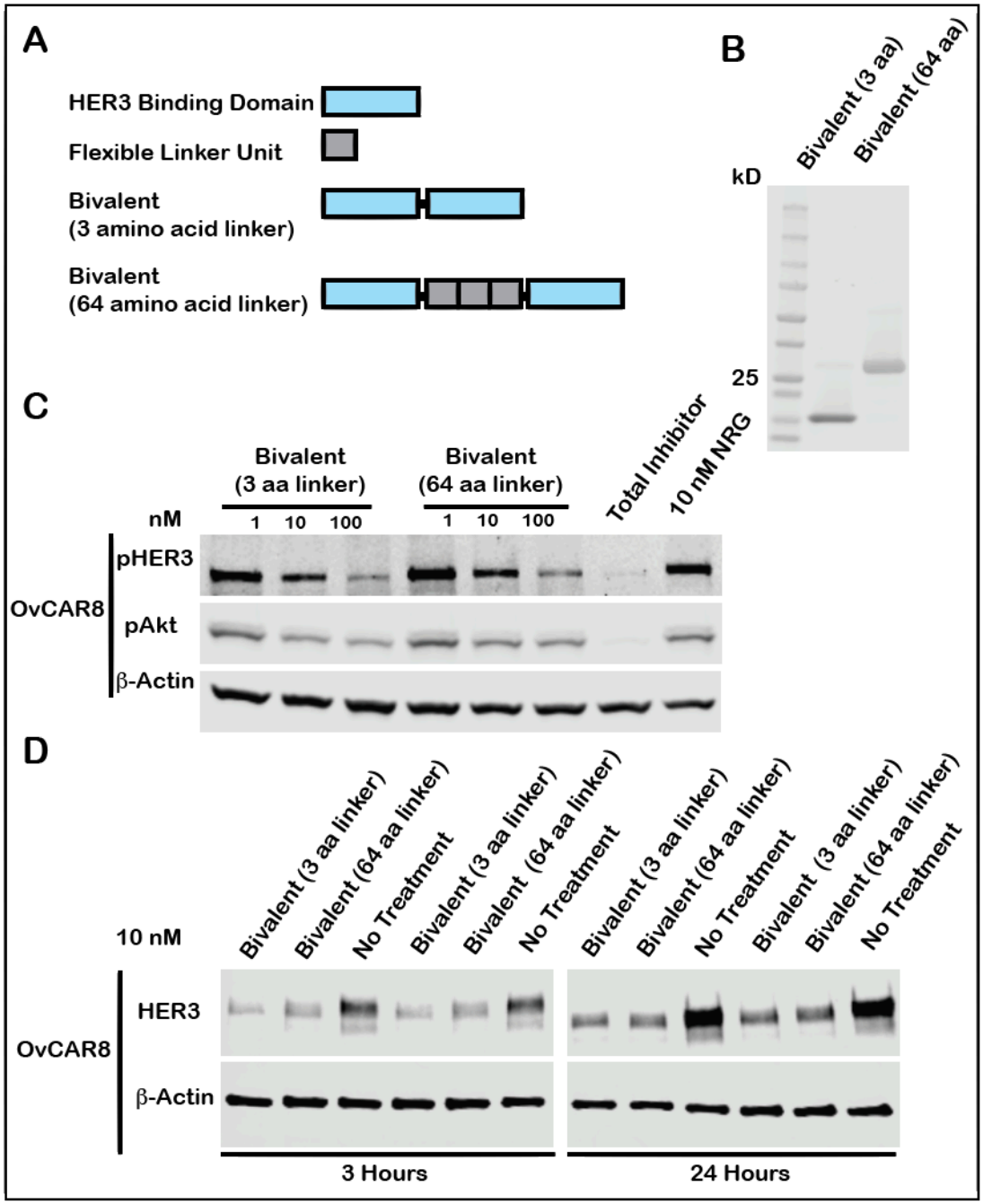

Figure 2.13: Linker length has limited impact on bivalent affibody-mediated pHER3 inhibition and HER3 downregulation. A. Schematic representing multivalent affibody constructs with 3 or 64 amino acid (aa) linker size. **B.** Purified protein products are displayed on a Coomassie stained gel loaded at 10 mg/lane. Bivalent affibody with 3 aa linker and 64 aa linker ligands have respective theoretical molecular weights of 14.4 and 19.1 kDa. **C.** OvCAR8 cells were treated with the indicated concentrations of bivalent affibody 3 or 64 aa linker, or 100 nM pan HER kinase inhibitor (total inhibitor), for 30 minutes, then stimulated with 10 nM NRG for 10 minutes, lysed, and probed for pHER3, pAkt and b-actin by immunoblot. **D.** OvCAR8 cells were treated with 10 nM bivalent affibody with 3 and 64 aa linker, lysed at the indicated time points, and probed by immunoblot for HER3 and b-actin. All multivalent ligand concentrations refer to the concentration of individual affibody domain. Results shown are representative of three independent experiments. All blots were cropped.

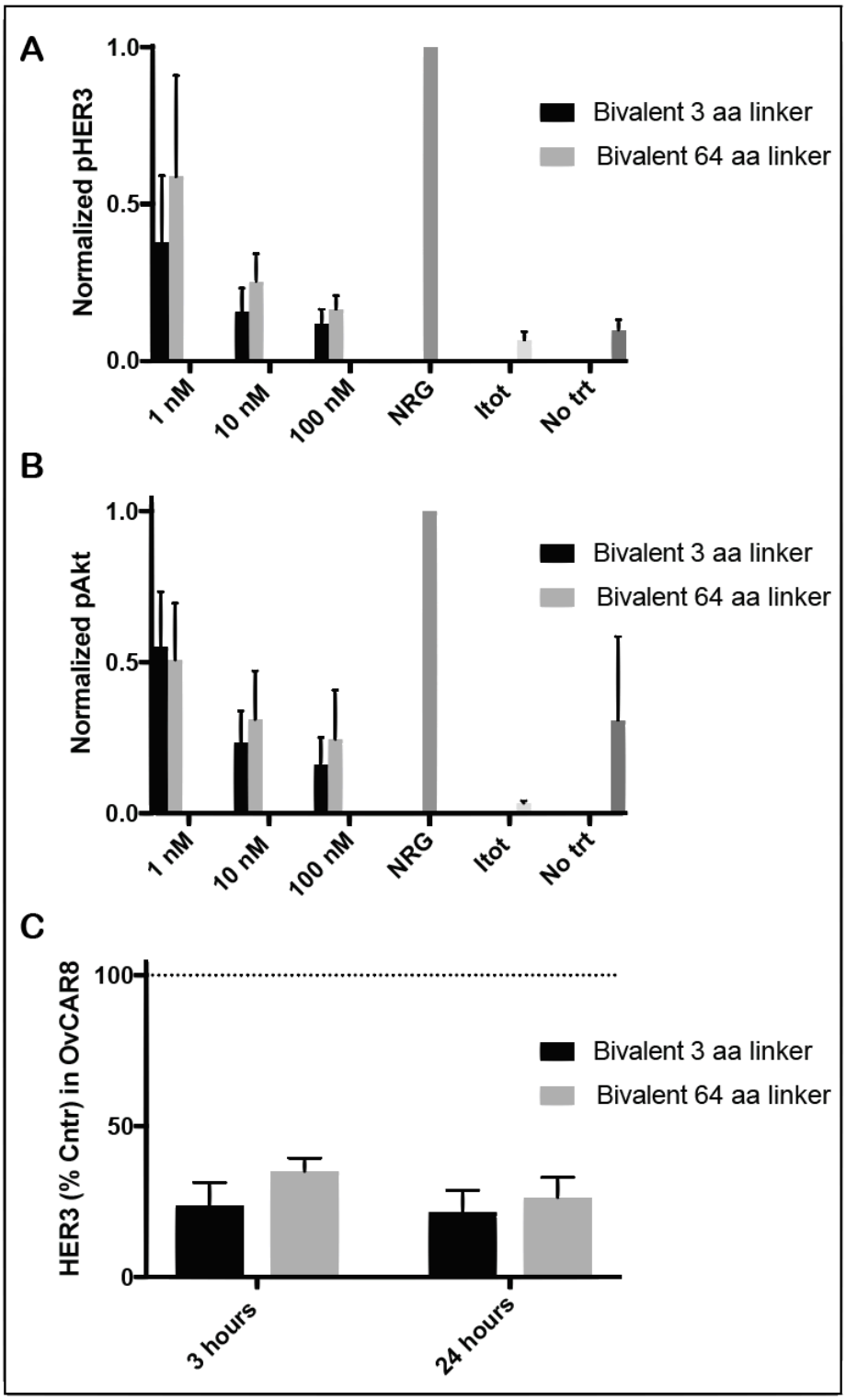

Figure 2.14: Immunoblot quantification of Figure 2.13. Quantified A. pHER3 B. pAkt and C. HER3 values are displayed for Figure 1. Blots were quantified using Odyssey CLx image system (Licor) Analysis Tool and normalized to β-actin. Results shown are mean +/- SEM of three independent experiments with error bars displayed as +- standard error.

2.3.5 Hexavalent and bivalent HER3 affibodies show similar activity.

We hypothesized that engineered multivalency could improve HER3 ligand bioactivity through enhanced avidity effects and HER3 sequestration. Previously, we compared the bioactivity of monovalent, bivalent, and trivalent affibody formats and observed that bivalent and trivalent ligands had comparable bioactivity with regard to pHER3/pAkt inhibition, and HER3 downregulation [79]. To more conclusively assess the impact of valency on affibody bioactivity, we examined the utility of hexavalent ligands in comparison to our bivalent ligands with three-glycine linkers (**Figure 2.15 A, B**). We likewise observed that valency above two had limited impact on pHER3 inhibition and HER3 downregulation (**Figure 2.15C, D, 2.16**). Thus, we focused further investigation on our bivalent affibody with three-glycine linkers.

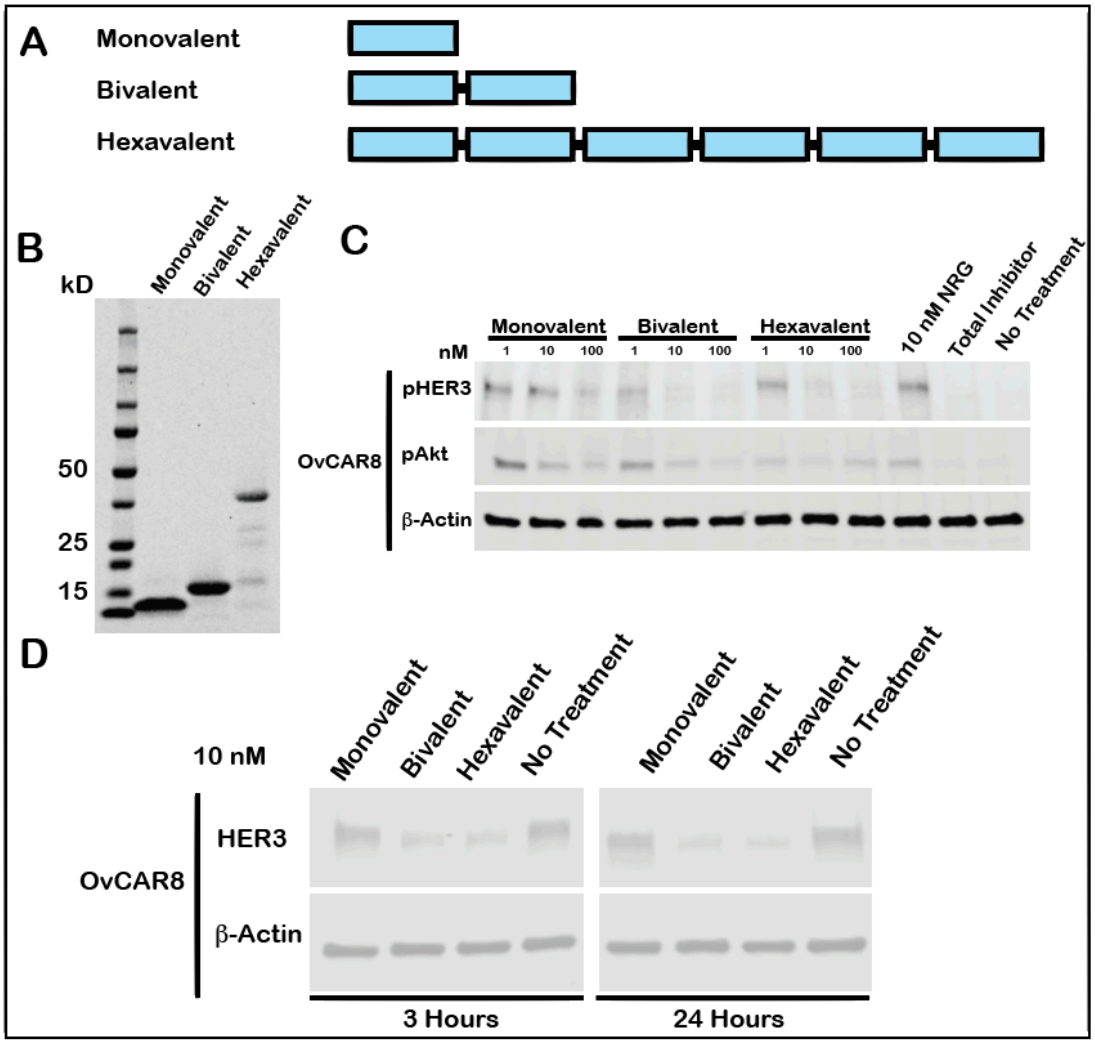

Figure 2.15: Hexavalent and bivalent HER3 affibodies show similar activity.
A. Schematic representing monovalent, bivalent, and hexavalent affibody constructs. **B.** Purified protein products are displayed on a Coomassie stained gel loaded at 10 mg/lane. Monovalent, bivalent, and hexavalent affibody constructs have respective theoretical molecular weights of 7.6, 14.4, and 41.6 kDa. **C.** OvCAR8 cells were treated with the indicated concentrations of monovalent, bivalent, or hexavalent affibodies, or 100 nM pan HER kinase inhibitor (total inhibitor), or media alone (no treatment) for 30 minutes, then stimulated with 10 nM NRG for 10 minutes (except for no treatment negative control), lysed, and probed for pHER3, pAkt and b-actin by immunoblot. **D.** OvCAR8 cells were treated with 10 nM monovalent, bivalent, hexavalent linker, pan HER kinase inhibitor or media alone, lysed at the indicated time points, and probed by immunoblot for HER3 and b-actin. All multivalent ligand concentrations refer to the concentration of individual affibody domains. Results shown are representative of three independent experiments. All blots were cropped.

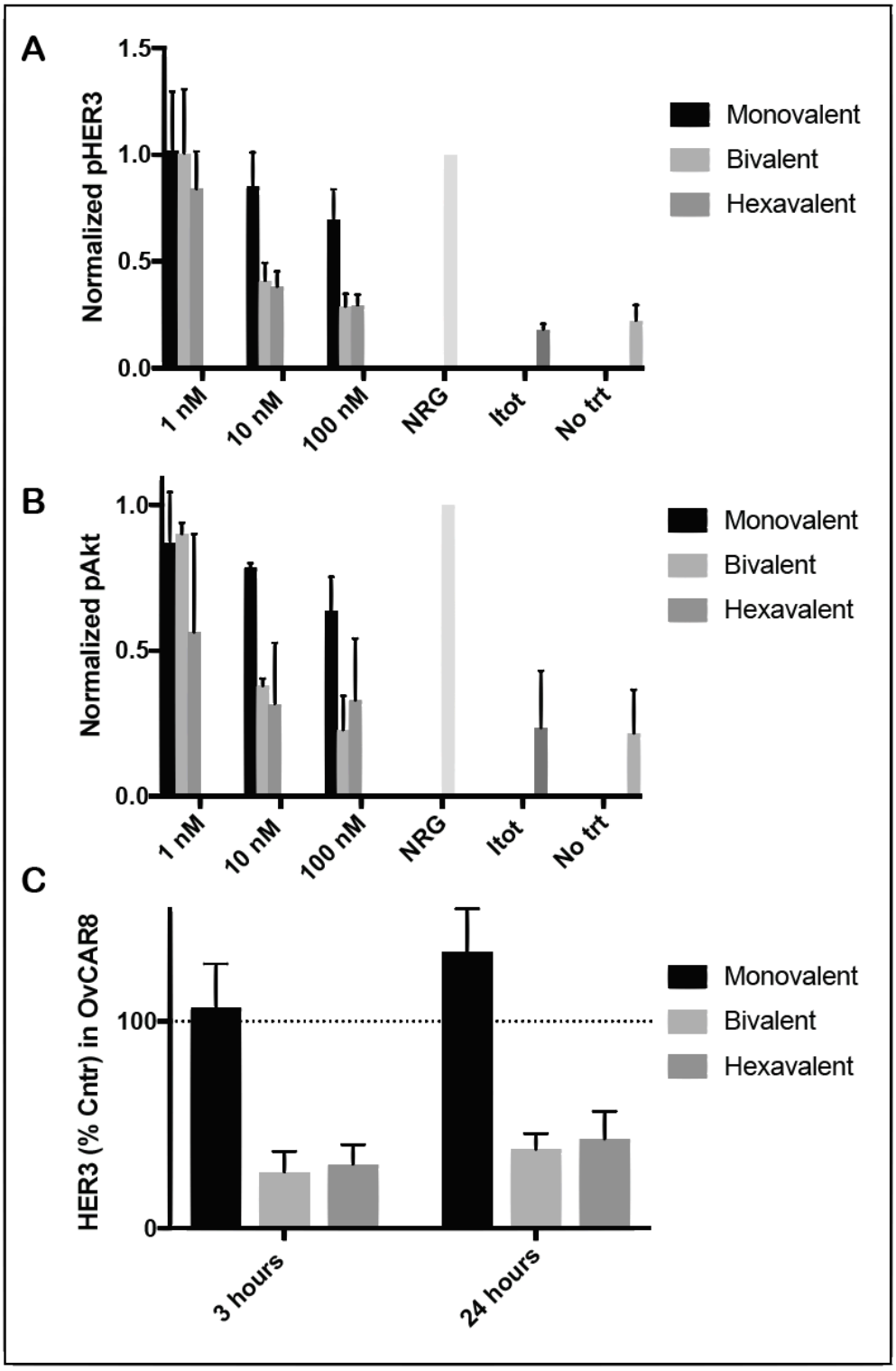

Figure 2.16: Immunoblot quantification of Figure 2.15. Quantified A. pHER3 B. pAkt and C. HER3 values are displayed for Figure 2. Blots were quantified using Odyssey CLx image system (Licor) Analysis Tool and normalized to β-actin. Results shown are mean +/- SEM of three independent experiments.

2.3.6 Arrangement of HER3 affibodies around an albumin-binding domain has minimal impact on bioactivity

Affibodies, despite their advantages over mAbs such as increased tissue penetration, stability, and ease of manufacturing, have pharmacokinetic limitations that are likely to hinder their therapeutic efficacy *in vivo* [62]. Albumin-binding domain (ABD) fusions have been widely exploited to extend circulating half-life by increasing molecular hydrodynamic radius, enabling FcRn-mediated recycling, and reducing renal clearance [62,80–82]. We generated various monovalent and bivalent HER3 affibody fusions with albumin-binding domains (**Figure 2.17A, B**). Specifically, we generated monovalent ligands HA and AH, and bivalent ligands HHA, HAH, AHH where 'H' denotes HER3 binding domain and 'A' denotes albumin-binding domain; molecular domains were connected by three-glycine minimal linkers. We selected ABD_{035} as the albumin-binding domain for this study [80]. The entire panel of HER3 affibody ABD fusions retained bioactivity similar to unmodified affibodies with regard to pHER3/pAkt inhibition (**Figure 2.17C, 2.18**) and HER3 downregulation, both in the presence and absence of bovine serum albumin (**Figure 2.17 4D, E, 2.18**). The retained bioactivity of HHA and AHH molecules indicates that HER3 receptor engagement is efficient even with a centralized HER3 binding domain, and thus the possible increased risk of the centralized HER3 binding domain being sterically inhibited from HER3 binding was not observed. Given that ABD fusion location had limited impact on protein bioactivity, we selected monovalent HA and bivalent HHA HER3 affibody ABD fusions for subsequent *in vivo* efficacy evaluation.

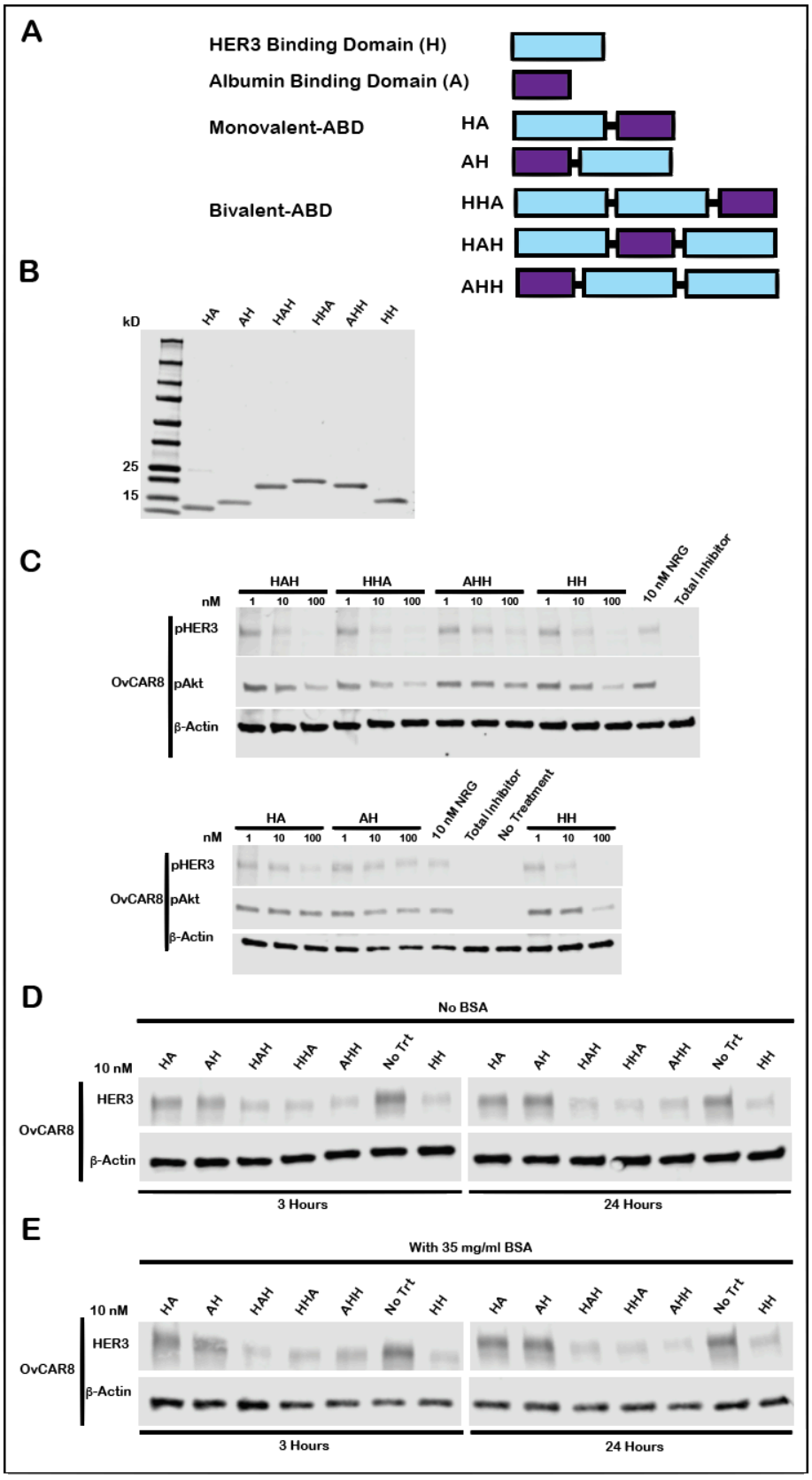
A
HER3 Binding Domain (H)
Albumin Binding Domain (A)
Monovalent-ABD
HA
AH
Bivalent-ABD
HHA
HAH
AHH
B
kD
HA
AH
HAH
HHA
AHH
HH
25
15
C
HAH
HHA
AHH
HH
nM
1
10
100
10 nM NRG
Total Inhibitor
pHER3
OvCAR8
pAkt
β-Actin
HA
AH
10 nM NRG
Total Inhibitor
No Treatment
HH
D
No BSA
10 nM
HER3
β-Actin
No Trt
3 Hours
24 Hours
E
With 35 mg/ml BSA

Figure 2.17: Arrangement of HER3 affibodies around an albumin-binding domain has minimal impact on bioactivity. A. Schematic representing monovalent and bivalent albumin binding domain fusion constructs where H denotes HER3 binding domain and A denotes Albumin binding domain **B**. Purified protein products are displayed on a Coomassie stained gel loaded at 10 mg/lane. Monovalent ABDs HA and AH have respective theoretical molecular weights of 12.9 and 13.0 kDa, bivalent ABDs HHA, HAH, and AHH have M.W. of 19.7, 19.7, and 19.8 kDa respectively, and HH - bivalent HER3 affibody positive control lacking ABD - has M.W. of 14.4 kDa **C.** OvCAR8 cells were treated with the indicated concentration affibody construct, or 100 nM pan HER kinase inhibitor (total inhibitor), or media alone (no treatment) for 30 minutes, then stimulated with 10 nM NRG for 10 minutes (except for no treatment negative control), lysed, and probed for pHER3, pAkt and b-actin by immunoblot. In the **D.** absence of bovine serum albumin (BSA), or **E.** presence of 35mg/ml BSA, OvCAR8 cells were treated with 10 nM of the indicated affibody construct, or media alone (no treatment), lysed at the indicated time points, and probed by immunoblot for HER3 and b-actin. All multivalent ligand concentrations refer to the concentration of individual affibody domains. Results shown are representative of three independent experiments. All blots were cropped.

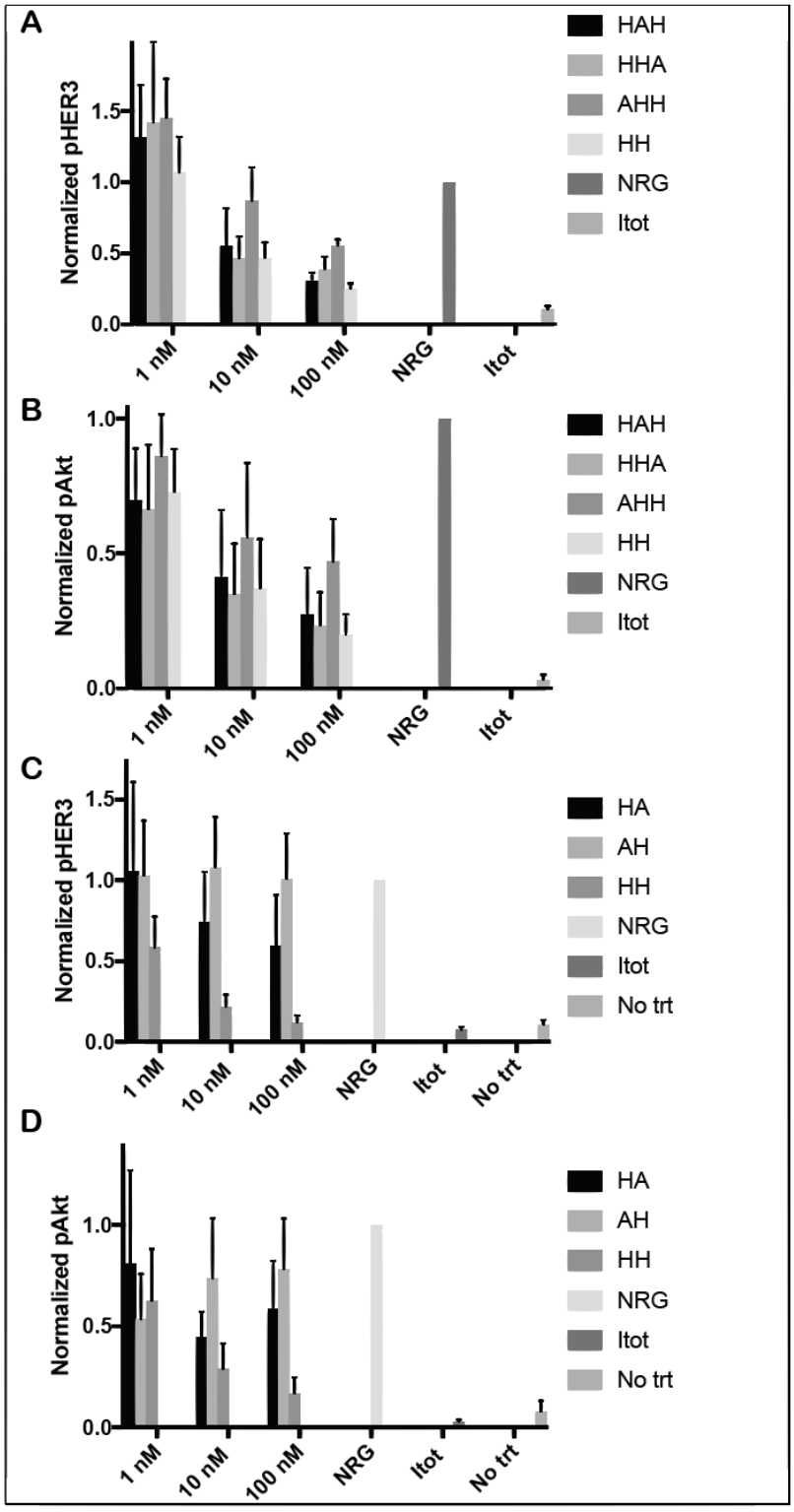

Figure 2.18: Immunoblot quantification of Figure 2.17 (pHER3 and pAkt). Quantified A., B. pHER3 and B., C. pAkt values are displayed for Figure 4. Blots were quantified using Odyssey CLx image system (Licor) Analysis Tool and normalized to β-actin. Results shown are mean +/- SEM of three independent experiments.

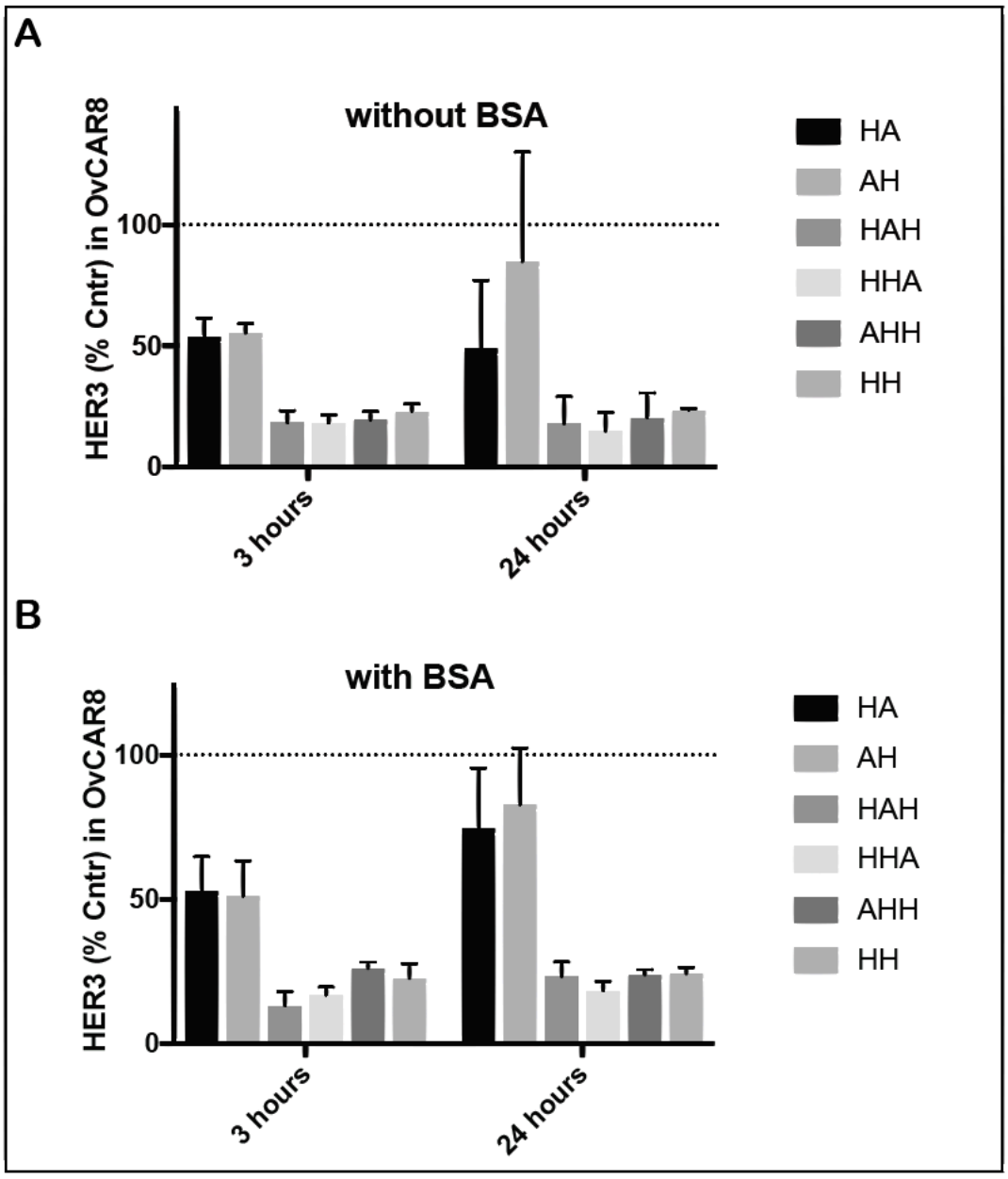

Figure 2.19: Immunoblot quantification of Figure 2.18 (HER3). Quantified A, B. HER3 values are displayed for Figure 4. Blots were quantified using Odyssey CLx image system (Licor) Analysis Tool and normalized to β-actin. Results shown are mean +/- SEM of three independent experiments.

2.4 Discussion

HER3, a potent activator of the PI3K/Akt pathway [9], and a mediator of resistance to ErbB and non-ErbB targeted therapies [21–25,45], is an important target for cancer therapy [19]. New and improved HER3-targeted therapeutics would provide additional treatment options for patients with cancers refractory to current therapies. In this study, we demonstrated that engineered multivalency could enhance the therapeutic potential of HER3-targeted affibodies. Further, we identified multivalent ligand-induced HER3 downregulation as a potential mechanism of action that could be exploited by other HER3-targeted therapeutics.

Cellular effects of various HER3 affibodies have previously been characterized, and the ability of monovalent affibodies to inhibit NRG-induced HER3 and Akt phosphorylation and cell growth is well established [49,50]. Bivalent and bispecific affibodies have also been described, with a bivalent HER3 affibody incorporating an albumin-binding domain shown to efficiently inhibit phosphorylation of both HER3 and HER2 [62]. The studies presented here significantly extend these findings to show that therapeutically relevant advantages of HER3-targeted affibodies endowed by multivalency are robust across multiple cancer cell lines, potentially independent of linker domain identity, and potentially the result of enhanced HER3 downregulation. These studies also extend our own previous work demonstrating the bioactivity of bivalent HER3 ligands [68,69], showing that multivalent engagement may be a generally useful strategy for HER3-targeted therapeutics that does not require employment of NRG. Given the potential for a NRG domain to initiate

undesired activation of HER3 as the result of unexpected proteolytic cleavage or unanticipated binding conformations, multivalent affibodies represent a lower risk approach to HER3-targeted therapy via engineered multivalent ligands.

In terms of efficacy, both NRG- and affibody-based multivalent ligands promote pHER3 inhibition and reduce cancer cell viability, however their mechanisms of action appear to be different. Multivalent affibodies had limited impact on HER2 phosphorylation in the BT474 cell line (**Figure 2.7**), whereas bivalent NRG efficacy is more closely associated with pHER2 inhibition in several cell lines [68], possibly via sequestering HER3 into homotypic interactions and preventing HER2/HER3 heterodimer formation. Alternatively, bivalent NRG, with the ability to bind both HER3 and HER4, could be inhibiting pHER2 as a result of blocking HER4-mediated signaling. In addition, we observed that bivalent affibodies with predicted linker domain lengths of less than 10 nm – theoretically too small to induce a HER3 dimer on a one molecule per dimer basis – exhibited similar pHER3 inhibition as constructs with longer predicted linker lengths (**Figure 2.11**). Taken together with the pHER2 data, pHER3 inhibition by multivalent affibodies may be independent of the ability of HER3 to interact with HER2. Another significant result of this study is the demonstration that HER3-targeted multivalent affibodies cause rapid and prolonged HER3 downregulation, whereas monovalent affibodies have little impact on HER3 levels (**Figure 2.9**). This finding that HER3-targeted multivalent affibody efficacy is due at least in part to enhanced post-translational receptor downregulation (**Figure 3.2**), and is not dependent on pHER2 inhibition, linker domain length, or increased

binding affinity to the target molecule provides evidence for potential broad utility of multivalent affibodies for targets beyond HER3.

Of course, any discussion of multivalent ligands should include monoclonal antibodies (mAbs), which are bivalent in nature. The capability of inducing HER3 downregulation is variable in HER3 mAbs described in the literature, however a tetravalent HER3 antibody has been shown to induce greater HER3 internalization compared to its bivalent counterpart [83]. This same study reported diminished efficacy of several mAbs against HER3 in the presence of NRG, in contrast to the data presented here and highlighting a potential limitation of targeting HER3 individually with mAbs. Nevertheless, it is notable that several mAbs targeting HER3 have reached later stage clinical trials [84]. Interestingly, a prior report has shown that combinations of two distinct HER3 antibodies did not induce an additive effect [85], as has been observed for EGFR [86] and other receptors. The same report indicated that acceleration of HER3 degradation is a potentially critical determinant of tumor growth inhibition by mAbs, reinforcing the significance of the multivalent affibody-induced HER3 downregulation observed in the present work. Complete understanding of the mechanistic differences between HER3-targeted multivalent affibodies (or other multivalent HER3 ligands) and antibodies requires further study, however such future studies could also incorporate evaluation of combinations of these molecules for potential therapeutic synergy.

Affibodies, like all molecules, have strengths and weaknesses with regard to their therapeutic potential. The structure of affibodies makes them highly stable and soluble [58], which is beneficial from a biomanufacturing perspective. The smaller size of affibodies relative to mAbs may increase their tumor penetration [87,88], although the circulating half-life of affibodies is much shorter than of the typical mAb. However, affibodies are easily amenable to formatting for improved pharmacokinetics, such as via fusion to an albumin-binding domain [62,89], and such constructs are compatible with multivalent presentation. Yet, the enhanced HER3 downregulation mediated by engineered multivalency reported here is a mechanism that can potentially be broadly exploited independently of specific HER3 binding domains, linker domain sizes and other molecular idiosyncrasies. Overall, these results position multivalent HER3-binding affibodies for further development and exemplify a general and versatile strategy to improve the efficacy of HER3-targeted cancer therapies.

Chapter 3: Mechanism of Action

Acknowledgements:

Figures 3.1-3.2 were adapted from:

Schardt JS; Oubaid JM, Williams SC; Howard JL; Aloimonos CM; Bookstaver ML; Lamichhane TN; Sokic S; Liyasova MS; O'Neill M; Andresson T; Hussain A; Lipkowitz S; Jay SM (2017) Engineered Multivalency Enhances Affibody-Based HER3 Inhibition for Cancer Therapy. Molecular Pharmaceutics. 14(4), 1047-1056.

Figures 3.3-3.4 were adapted from:

Schardt JS; Williams SC; Oubaid JM, Pottash AE, Noonan-Shueh MM, Ali RT, Goodman CA, Hussain A, Rena Lapidus RG, Lipkowitz S, Jay SM (2018). HER3-Targeted Affibodies with Optimized Formats Reduce Tumor Progression In Vivo in an Ovarian Cancer Model. In Review.

Fluorescence microscopy studies (Figure 3.6) were conducted by Jinan M. Oubaid and Dr. Melani Solomon in collaboration with Dr. Silvia Muro at University of Maryland.

3.1 Introduction

Knowledge of the mechanism of multivalent affibody-mediated HER3 downregulation is important for translation and further rational design. Receptor downregulation due to multivalent binding and induced receptor-receptor interactions is an established phenomenon. In this Chapter, we also seek to evaluate whether multivalent affibody-mediated HER3 downregulation is highly specific to HER3 or whether multivalent affibodies specific for other receptors can be employed to induce the downregulation of other ErbB receptor family members for therapeutic applications. In addition to knowledge regarding the trafficking of HER3, it is crucial to understand HER3-specific affibody trafficking, which has broad implications toward the rational design and development of HER3 affibodies to deliver toxic payloads to cancer.

3.2 Methods

3.2.1 Receptor downregulation inhibition studies

Cycloheximide pulse chase: OvCAR8 cells were treated with 10 nM trivalent, bivalent or monovalent affibody, or in combination with 178 mM cycloheximide, or 178 mM cycloheximide alone, lysed at the indicated time points, and probed by immunoblot for HER3 and b-Actin.

Proteosomal and Lysosomal Inhibition: OvCAR8 cells were pre-treated with 200 mM Leupeptin for 3 hours or no treatment, treated with 10 nM trivalent, bivalent or monovalent affibody or in combination with 200 mM Leupeptin, or 200 mM Leupeptin alone, lysed at the indicated time points, and probed by immunoblot for HER3 and b-Actin. OvCAR8 cells were pre-treated with 5 mM MG-132 for 3 hours or no treatment, treated with 10 nM trivalent, bivalent or monovalent affibody alone, or in combination with 5 mM MG-132, or 5 mM MG-132 alone, lysed at the indicated time points, and probed by immunoblot for HER3 and b-Actin.

3.2.2 HER3 and EGFR downregulation assays

To examine receptor levels, cells were treated with the indicated concentrations of affibody or no treatment (media alone) control, lysed at the indicated time points, and the immunoblots probed for HER3 and EGFR as previously described using primary antibodies (D22C5 HER3, C74B9 EGFR, and 13E5 b-actin; Cell Signaling Technology).

3.2.3 Affibody internalization studies

Internalization probed by fluorescence microscopy: OvCAR8 cells were seeded at 100,000 cells per well and stored at 37°C or 4°C. 5 uM of Bivalent HER3-GFP in 37°C or 4°C RPMI 1640 (ATCC) media was added to cells in the corresponding temperature conditions and a no treatment group (media only) was added to cells in the 37°C condition. All cells containing the factors or no treatment groups were incubated for 1 hour at their respective temperatures and then fixed using 2% paraformaldehyde (30525-89-4)(Sigma-Aldrich). Cells containing the Bivalent HER3-GFP affibodies were probed for fluorescence imaging with primary antibody (His-Tag Antibody #2365) obtained from Cell Signaling for 1 hour, followed by secondary antibody (Goat anti-Rabbit, Alexa Fluor 350 # A-11046) from ThermoFisher Scientific for 1 hour. Media only cells were not probed. Membranes of all cells were permeabilized using 0.1% Triton X-100 Detergent Solution (28314)(ThermoFisher Scientific). Endosomes of cells were then probed for fluorescence imaging with primary antibody (Mouse EEA1 MAB8047-SP) obtained from R&D Systems for 1 hour and then secondary antibody (Goat anti-Mouse, Texas Red-X # T-6390) from ThermoFisher Scientific for 1 hour. Media only cells were not probed. All cells were then imaged using fluorescence microscopy techniques.

3.3 Results

3.3.1 Multivalent affibody-mediated HER3 downregulation is at least in part post-translational

To verify whether the observed reduction in HER3 levels was post-translational in nature, cycloheximide, an inhibitor of protein synthesis, was used in a pulse-chase

assay. The half-life of HER3 was not significantly affected by cycloheximide treatment over 8 hours and multivalent affibodies induced HER3 downregulation after 2, 4, and 8-hour treatments. The downregulation of HER3 by multivalent ligands at a much faster rate than the HER3 half-life in OvCAR8 cells suggests that multivalent ligands cause reduced HER3 levels at least in part by post-translational downregulation (**Figures 3.1A, 3.2A**). To investigate the possibility of enhanced HER3 degradation, OvCAR8 cells were treated with multivalent affibodies in the presence or absence of the lysosomal inhibitor leupeptin or the proteasomal inhibitor MG-132 and HER3 protein levels were examined by immunoblot. Surprisingly, HER3 downregulation by multivalent affibody treatment persisted in the presence of leupeptin or MG-132, suggesting that HER3 receptor downregulation may occur via an alternative mechanism such as receptor shedding or cleavage (**Figures 3.1B-C, 3.2B-C**).

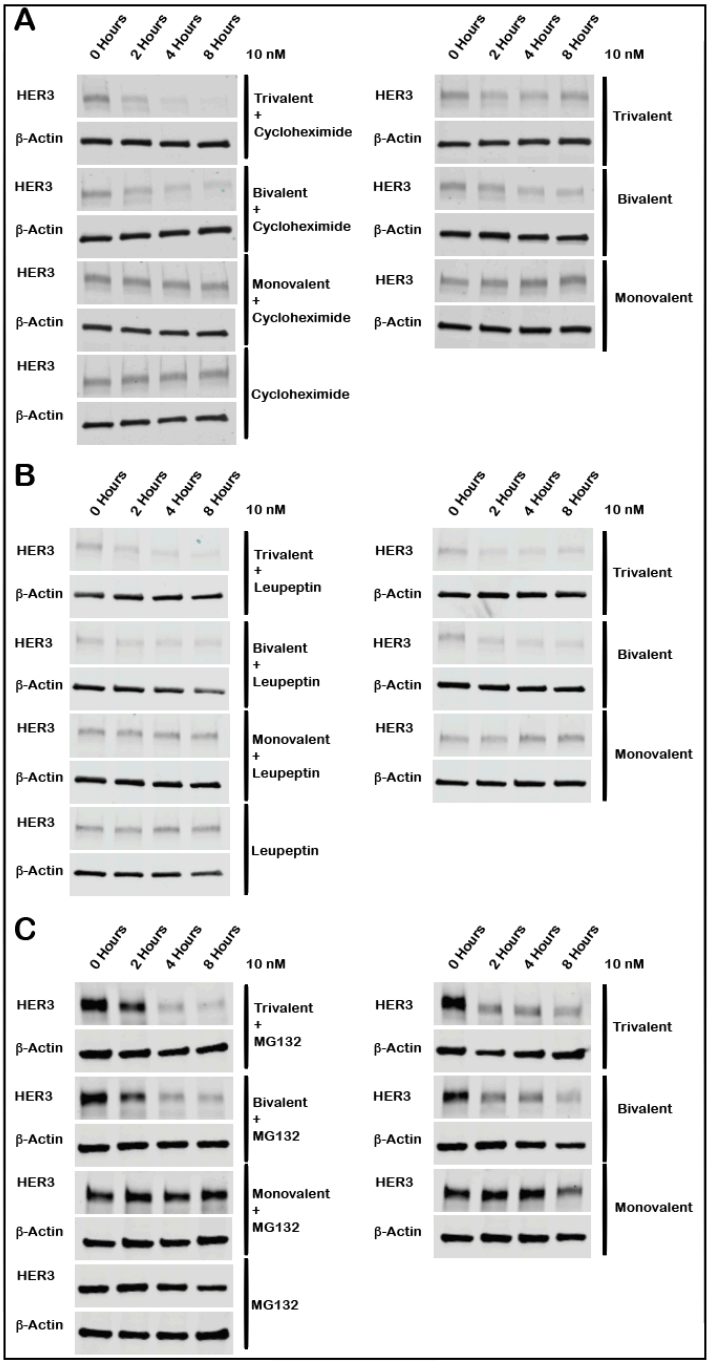

Figure 3.1: Multivalent affibody-mediated HER3 downregulation is at least in part post-translational. A. OvCAR8 cells were treated with 10 nM trivalent, bivalent or monovalent affibody, or in combination with 178 mM cycloheximide, or 178 mM cycloheximide alone, lysed at the indicated time points, and probed by immunoblot for HER3 and b-Actin. **B.** OvCAR8 cells were pre-treated with 200 mM Leupeptin for 3 hours or no treatment, treated with 10 nM trivalent, bivalent or monovalent affibody or in combination with 200 mM Leupeptin, or 200 mM Leupeptin alone, lysed at the indicated time points, and probed by immunoblot for HER3 and b-Actin. **C.** OvCAR8 cells were pre-treated with 5 mM MG-132 for 3 hours or no treatment, treated with 10 nM trivalent, bivalent or monovalent affibody alone, or in combination with 5 mM MG-132, or 5 mM MG-132 alone, lysed at the indicated time points, and probed by immunoblot for HER3 and b-Actin. Results shown are representative of two independent experiments. All blots were cropped.

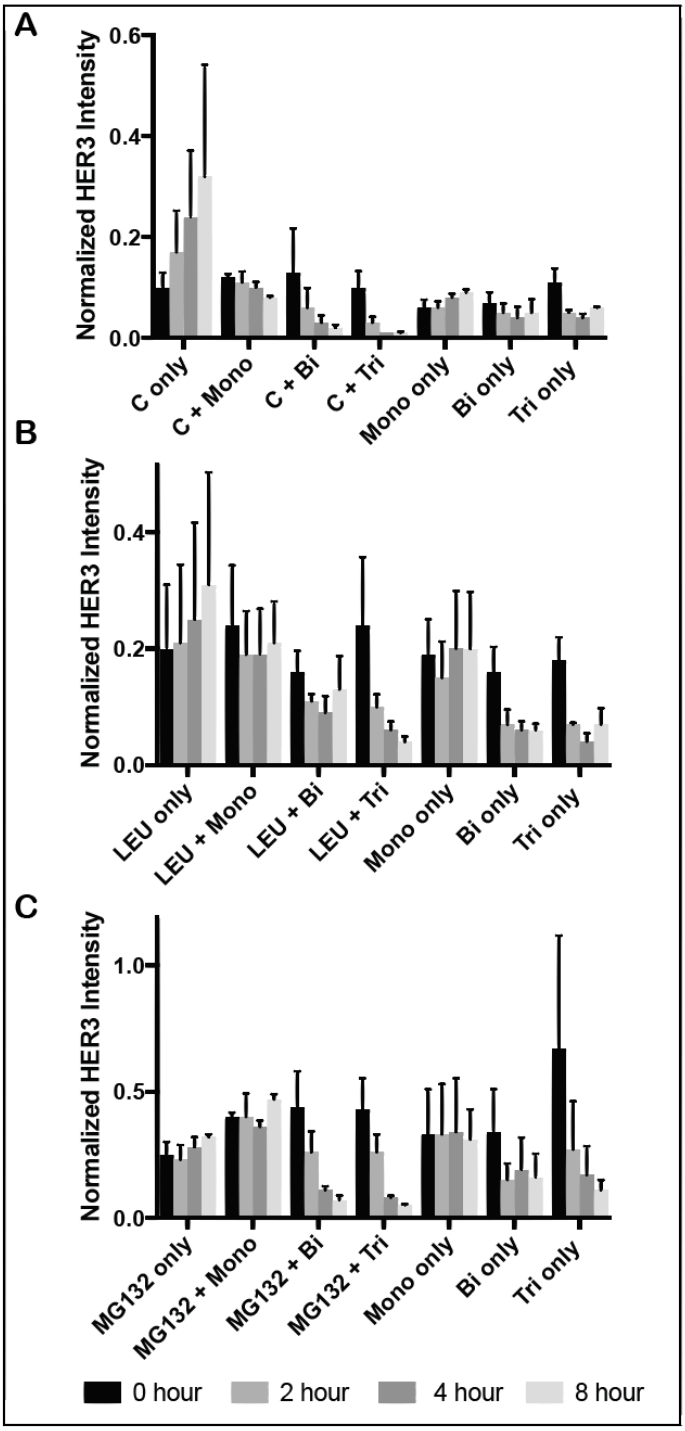

Figure 3.2: Immunoblot quantification Figure 3.1: Multivalent affibody-mediated HER3 downregulation is at least in part post-translational. Quantified HER3 values are displayed for the following experiments in OvCAR8 cells: **A.** cycloheximide pulse chase, and HER3 degradation inhibition experiments with **B.** Leupeptin and **C.** MG132. Blots were quantified using Odyssey CLx image system (Licor) Analysis Tool and normalized to b-actin. Results shown are averages of two independent experiments.

3.3.2 Bivalent affibody-mediated HER3 downregulation is a specific phenomenon

Given that multivalent HER3 affibodies promote HER3 receptor downregulation, we sought to examine to what extent multivalency can be employed as a general tool to induce ErbB receptor downregulation. Using a Z-EGFR$_{1907}$ domain developed by Friedman et al. [90], we generated bivalent EGFR-EGFR affibodies as well as bispecific, bivalent HER3-EGFR affibody molecules (**Figure 3.3A, B**) and assessed their ability to downregulate HER3 and EGFR receptors (by immunoblot in the absence of NRG and EGF) compared to bivalent HER3 affibodies. We observed that only positive control HER3 bivalent ligands induced HER3 receptor downregulation, while EGFR levels were unaffected by any of the molecules (**Figure 3.3C, D, 3.4**), indicating that HER3 downregulation by multivalent ligands is a specific phenomenon. HER3 and EGFR levels were normalized to b-actin levels and the results of three independent experiments were quantified in **Figure 3.4**.

Further, we hypothesized that HER3 downregulation by multivalent ligands is a direct result of HER3 sequestration by simultaneous engagement of multiple HER3 receptors. However, one general mechanism for HER3 inhibition is the blockade of heterodimer formation, and the possibility exists that multivalent ligands demonstrate improved bioactivity compared to monovalent analogs due to engagement of a single HER3 receptor by one HER3 affibody domain, while the un-engaged HER3 binding domain acts through HER3-independent steric blockade to inhibit receptor heterodimerization and induce HER3 downregulation. To test our hypothesis, we assessed the activity of a bivalent HER3-wild type (WT) affibody that incorporated

one HER3-binding domain as well as a structurally similar WT affibody domain that does not have affinity for HER3 (**Figure 3.3C, D, 3.4**). HER3 downregulation was not observed with HER3-WT affibody, nor with a control monovalent HER3 affibody with an attached linker domain, suggesting that HER3 downregulation is not idiosyncratic to bivalent molecules but rather requires simultaneous engagement of multiple HER3 receptors (**Figure 3.3C, D, 3.4**).

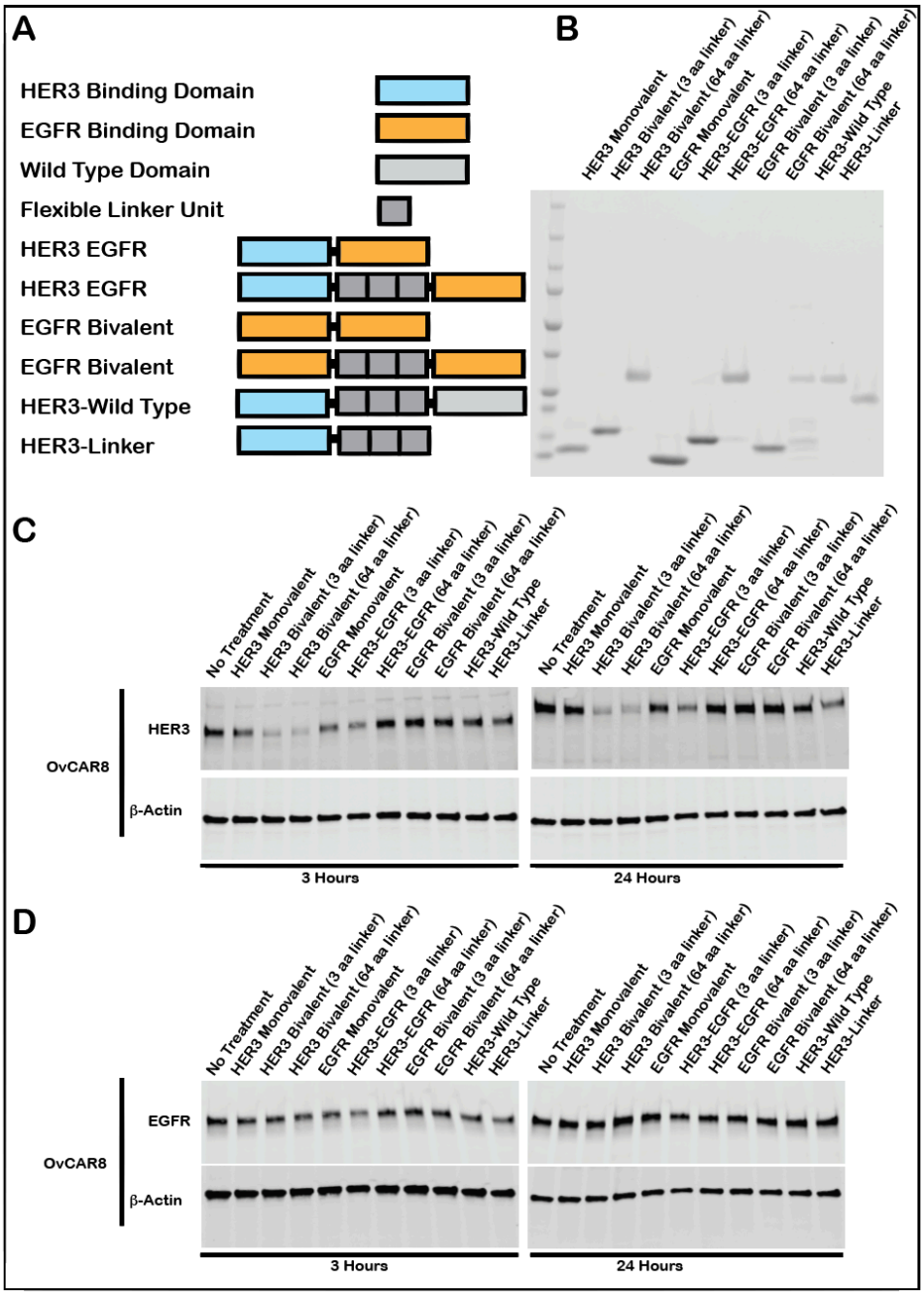

Figure 3.3: HER3 downregulation by multivalent ligands is a specific phenomenon. A. Schematic of various affibody constructs: monovalent HER3 (7.6 kDa), HER3 bivalent affibody with 3 or 64 amino acid linker (14.4 and 19.1 kDa), monovalent EGFR (7.6 kDa), HER3 EGFR bivalent bispecific affibody with 3 and 64 aa linker (14.3 and 18.9 kDa), EGFR bivalent affibody with 3 or 64 aa linker (14.4 and 18.2 kDa), bivalent bispecific HER3 wild type affibody with 64 aa linker (19.1 kDa), monovalent HER3 affibody with 64 aa linker tail (12.5 kDa). **B**. Purified protein products are displayed on a Coomassie stained gel loaded at 10 mg/lane with respective molecular weights listed in Figure 3A. **C.** OvCAR8 cells were treated with 10 nM of the indicated affibody construct, or media alone (no treatment), lysed at the indicated time points, and probed by immunoblot for HER3 and b-actin or **D.** EGFR and b-actin. All multivalent ligand concentrations refer to the concentration of individual affibody domains. Results shown are representative of three independent experiments. All blots were cropped.

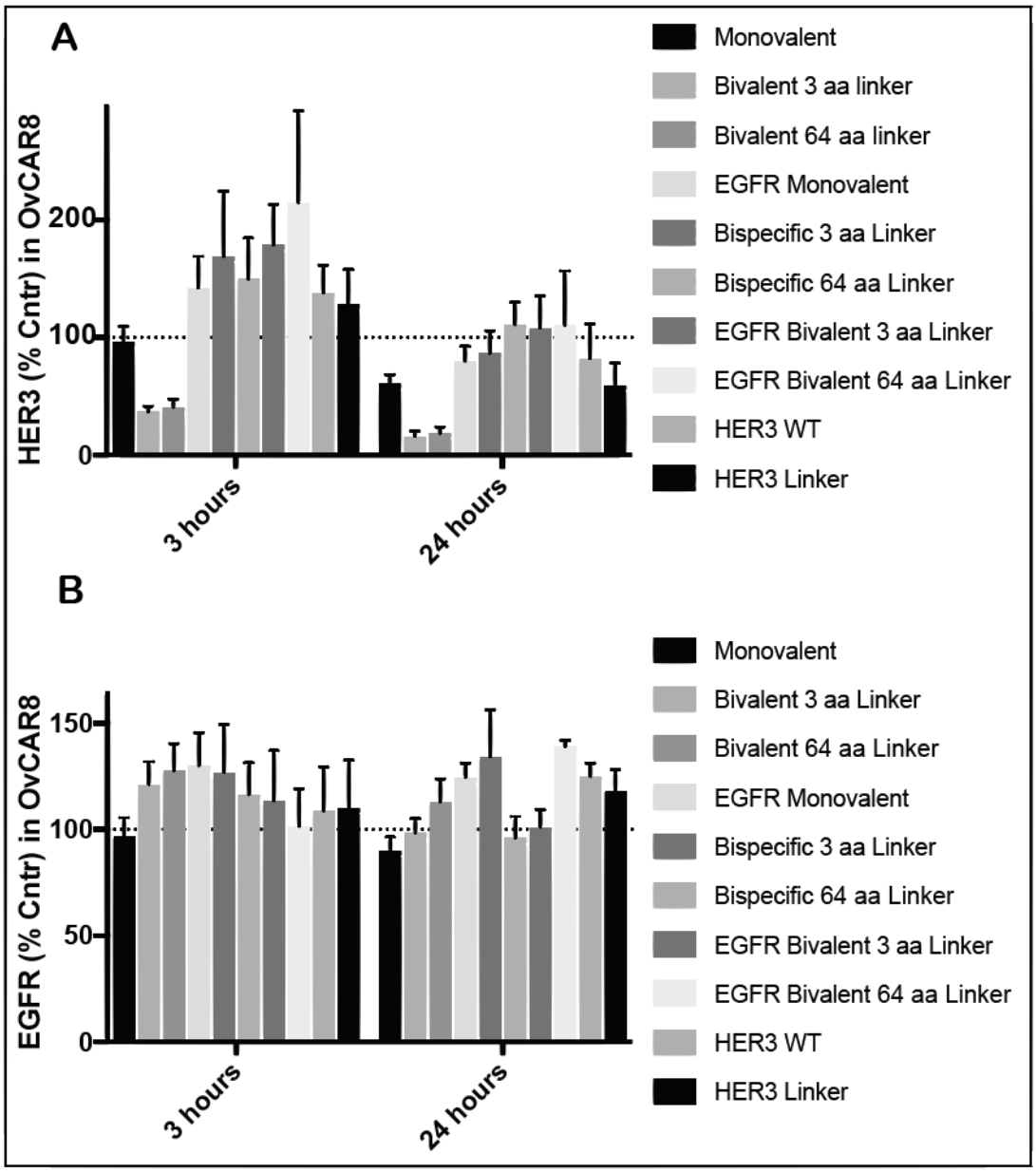

Figure 3.4: Immunoblot quantification of Figure 3.3. Quantified A. HER3 and B. EGFR values are displayed for Figure 3. Blots were quantified using Odyssey CLx image system (Licor) Analysis Tool and normalized to β-actin. Results shown are mean +/- SEM of three independent experiments.

3.3.3 Affibody internalization probed with GFP fusion proteins

To examine if HER3 affibodies are internalized by OvCAR8 cells, we generated HER3 affibody C-terminal GFP fusion constructs **(Figure 3.5A)**. Constructs were engineered, recombinantly expressed in BL21 (DE3) *E. coli*, and purified by immobilized metal affinity and size exclusion chromatography **(Figure 3.5B)**. Bivalent HER3 affibodies retained bioactivity upon fusion with GFP in regard to binding to HER3 positive cells **(Figure 3.5C,D)**, and inducing HER3 downregulation **(Figure 3.5E,F)**. To determine if bivalent HER3 affibody GFP fusion constructs were internalized, OvCAR8 cells were treated with GFP fusion construct for 1 hour at either 37C or 4C, and examined by fluorescence microscopy **(Figure 3.6)**. Composite images of 37C condition reveal colocalization (yellow) of HER3 affibody GFP fusions (green) and endosomes (red), suggesting HER3 affibodies are internalized in endosomes. Quantitative analysis revealed approximately 36% of green signal is colocalized with endosomes compared with approximately only 5% colocalization at 4C condition **(Figure 3.6)**. Blue signal indicates affibody binding at the cell surface probed by secondary antibody for His Tag present on bivalent GFP fusion proteins **(Figure 3.6).** In support of our observations from these fluorescence microscopy studies, incubation of OvCAR8 cells treated with 10 nM bivalent affibody for 3 hours caused complete inhibition of HER3 downregulation **(Figure 3.7).** Together these data suggest that bivalent HER3 affibodies are internalized by OvCAR8 cells via endocytosis.

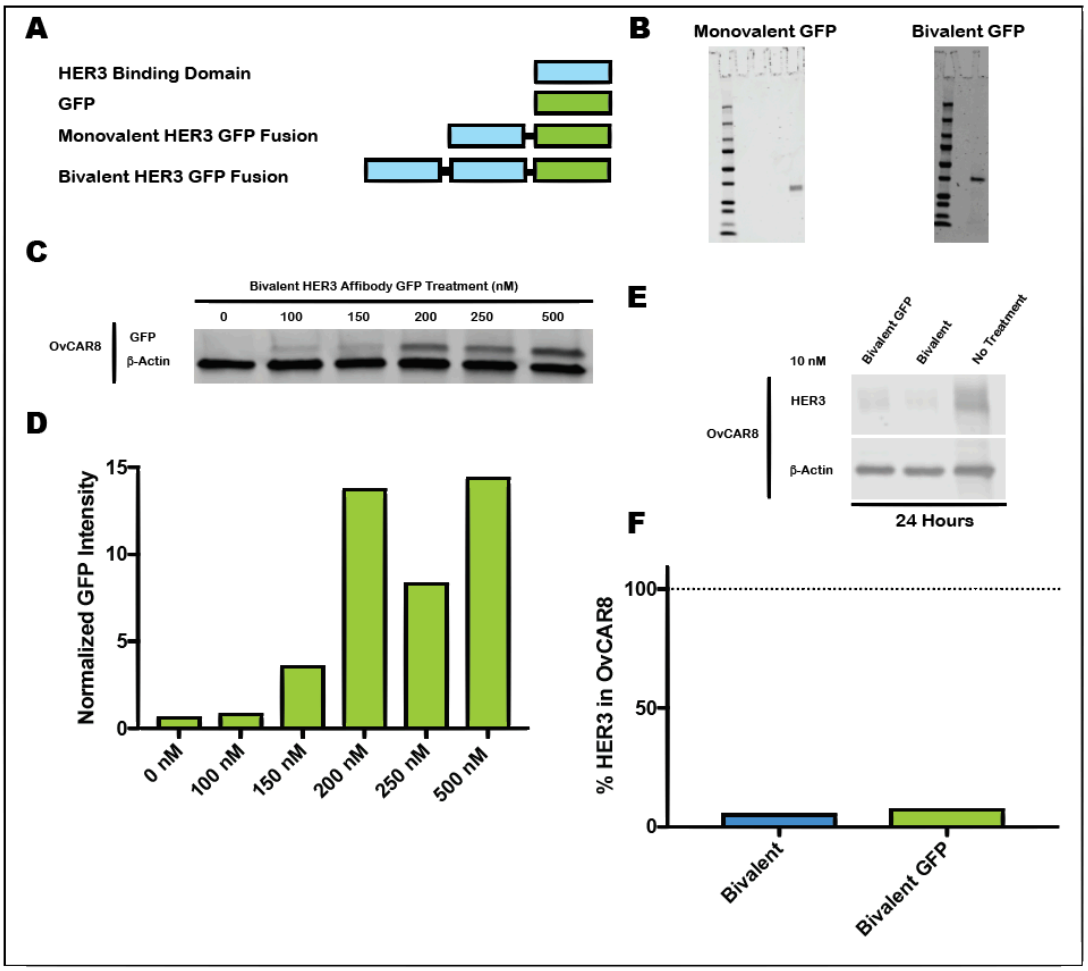

Figure 3.5: Bivalent HER3 affibodies retain bioactivity upon fusion with GFP. A. Schematic of HER3 affibody GFP fusion constructs **B.** Coomassie gel of purified bivalent and monovalent GFP fusion constructs **C.** OvCAR8 cells were treated with the indicated concentration of bivalent GFP affibody construct, or media alone (no treatment), lysed after 5 minutes, and probed by immunoblot for GFP and b-actin. **D.** Immunoblot quantification of C **E.** OvCAR8 cells were treated with 10 nM of the indicated affibody construct, or media alone (no treatment), lysed at the indicated time points, and probed by immunoblot for HER3 and b-actin or All multivalent ligand concentrations refer to the concentration of individual affibody domains. All blots were cropped. **F.** Immunoblot quantification of E**.**

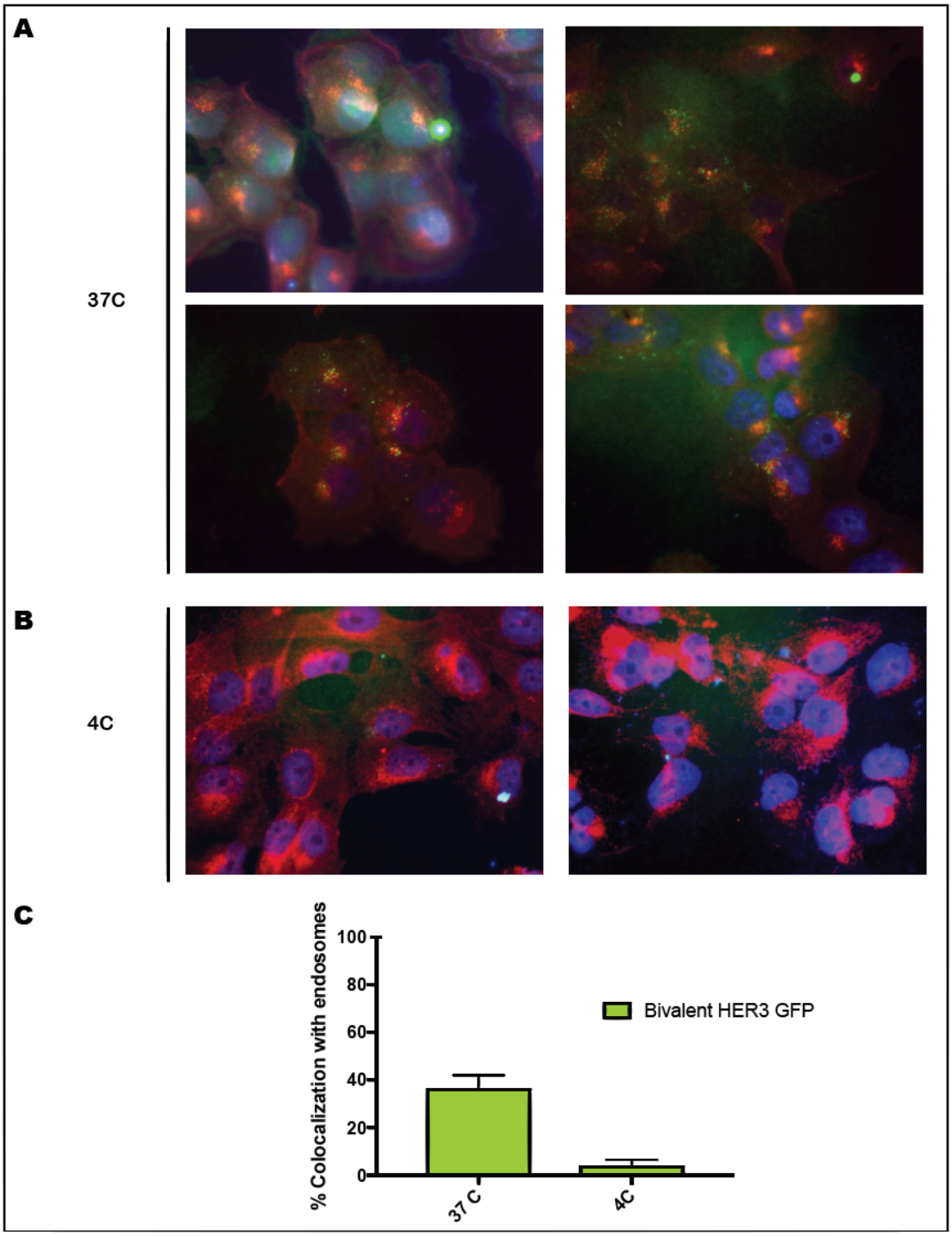

Figure 3.6: Bivalent affibody GFP fusion proteins are internalized by OvCAR8 cells. A. Composite images of OvCAR8 cells incubated with bivalent affibody GFP at 37C. **B.** Composite images of OvCAR8 cells incubated with bivalent affibody GFP at 4C. **C.** Quantifications of green/red (yellow) colocalization indicating overlay of bivalent GFP with endosomes**. Color Guide:** Blue (cell surface – secondary antibody for His Tag present on bivalent GFP fusion), Green (GFP), Red (endosomes). OvCAR8 cells were seeded at 100,000 cells per well and stored at 37°C or 4°C. 5 uM of Bivalent HER3-GFP in 37°C or 4°C RPMI 1640 media was added to cells in the corresponding temperature conditions and a no treatment group (media only) was added to cells in the 37°C condition. All cells containing the factors or no treatment groups were incubated for 1 hour at their respective temperatures and then fixed using 2% paraformaldehyde. Cells containing the Bivalent

HER3-GFP affibodies were probed for fluorescence imaging with primary antibody (His-Tag Antibody #2365) for 1 hour, followed by secondary antibody (Goat anti-Rabbit, Alexa Fluor 350 # A-11046) for 1 hour. Media only cells were not probed. Membranes of all cells were permeabilized using 0.1% Triton X-100 Detergent Solution (28314). Endosomes of cells were then probed by fluorescence imaging with primary antibody (Mouse EEA1 MAB8047-SP) for 1 hour and then secondary antibody (Goat anti-Mouse, Texas Red-X # T-6390) for 1 hour. All cells were then imaged using fluorescence microscopy.

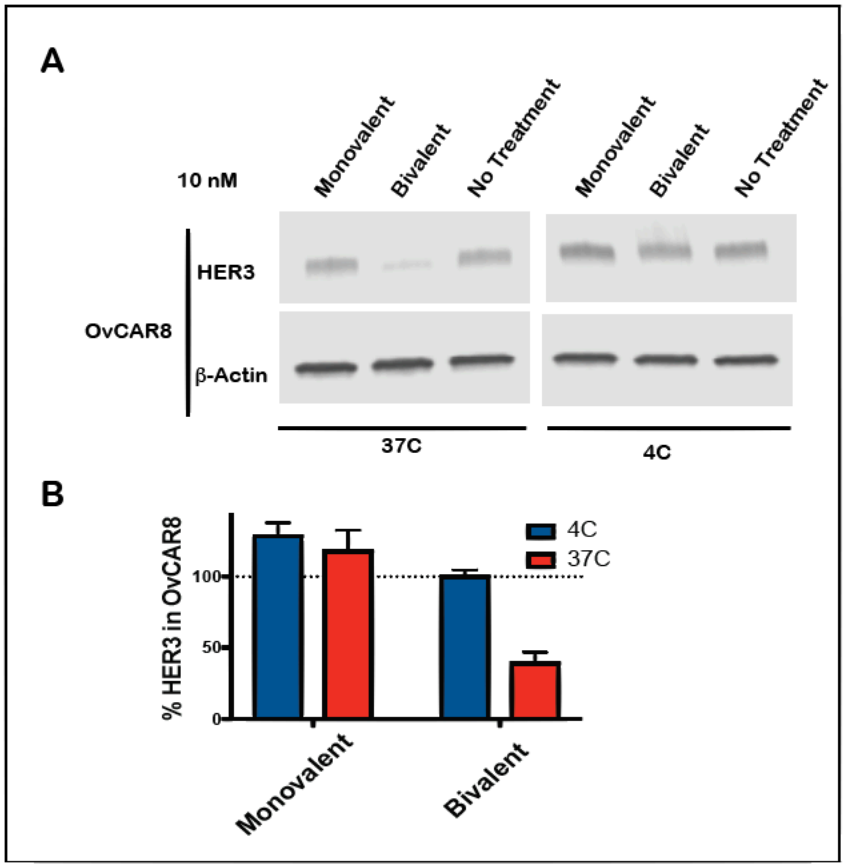

Figure 3.7: Bivalent affibody-mediated HER3 downregulation is inhibited at 4C. A. OvCAR8 cells were treated with 10 nM of the indicated affibody construct, or media alone (no treatment), lysed at the indicated time points, and probed by immunoblot for HER3 and b-actin. All multivalent ligand concentrations refer to the concentration of individual affibody domains. Results shown are representative of two independent experiments. All blots were cropped. **B.** Immunoblot quantification of A.

3.4 Discussion

We demonstrate HER3-targeted multivalent affibodies cause rapid and prolonged HER3 downregulation, whereas monovalent affibodies have little impact on HER3 levels (**Figure 2.9**). This finding that HER3-targeted multivalent affibody efficacy is due at least in part to enhanced post-translational receptor downregulation (**Figure**

3.1), and is not dependent on pHER2 inhibition, linker domain length, or increased binding affinity to the target molecule provides evidence for potential broad utility of multivalent affibodies for targets beyond HER3.

Mechanistically, our data (**Figure 3.3C, D 3.4A, B**) provide valuable insights into the effects of multivalency on enhanced downregulation of HER3 and other receptors. The possibility exists that receptor downregulation is a result of enhanced avidity effects, endowed through multivalency, and not necessarily a result of simultaneous engagement of multiple receptors. In opposition to this possibility, our previous results indicate that increasing ligand valency does not increase K_D as measured by Surface Plasmon Resonance [79]. In the current study, neither monovalent nor bivalent EGFR ligands had an effect on total EGFR levels, suggesting that enhanced avidity is not a general mechanism enabling ErbB receptor downregulation, and indeed HER3 downregulation requires simultaneous engagement of multiple HER3 receptors. The HER3 and EGFR affibodies used in this study were observed to be inhibitory toward their respective receptors, and here multivalent EGFR ligands were not rationally designed to promote EGFR downregulation, but rather to assess whether downregulation by multivalent ligands was a receptor specific event.

In addition, future work is necessary to understand the link between HER3 receptor downregulation by multivalent ligands and cancer cell survival. For example, HER3 downregulation may not have a substantial effect on cancer cell death, but instead may induce vulnerability due to reduction in Akt-mediated pro-survival signaling,

prompting cancer cells to become more susceptible to standard treatments such as chemotherapeutics and ErbB-targeted therapies beyond HER3. The majority of clinical trials for HER3 antibodies involve their use in combination therapies, for example MM-121 combined with docetaxel for non-small cell lung cancer. Future investigation of HER3 affibodies in combination with other drugs as well as development of HER3-targeting ligands engineered to deliver toxic payloads such as chemotherapeutic agents or toxins could represent promising avenues for ovarian cancer treatment.

Considering previous reports of receptor downregulation by multivalent ErbB therapeutics, to our knowledge, evidence of receptor downregulation by bispecific ligands is limited. Neither the HER2-HER3 bivalent bispecific antibody MM-111 [55], nor the two-in-one antibody HER3-EGFR MEHD7945A [91] were reported to induce downregulation or degradation of either target receptor. However, the HER3 IGF-1R tetravalent bispecific antibody MM-141 was observed to promote degradation of both HER3 and IGF-1R, as well as HER2 and insulin receptor [56]. In our experiments, monospecific, bivalent EGFR affibodies did not induce EGFR downregulation, suggesting that engineered multivalency cannot be applied universally as a strategy to downregulate ErbB family target receptors. However, it should be noted that previous investigations indicate that multivalency can be used as tool to induce EGFR downregulation on a case-by-case basis [13]. Interestingly, MM-151, a mixture of three monoclonal EGFR antibodies, each binding a unique non-overlapping epitope on EGFR, was observed to induce EGFR downregulation in

multiple cell lines, whereas the combination of MM-151 Fab fragments was not, thus demonstrating that multivalency is required for EGFR downregulation in this case [13]. In this study, Kearns et al. further demonstrated that each of the three antibody components of MM-151 individually promoted EGFR downregulation, with the most significant single agent-induced downregulation observed upon treatment with an antibody specific for the cetuximab-like epitope on domain III of EGFR extracellular domain, yet interestingly, the EGFR monoclonal antibody cetuximab was not observed to induce EGFR downregulation [13]. Overall, these data taken altogether indicate that multivalency is likely required for EGFR downregulation, however this phenomenon appears highly dependent on molecular idiosyncrasies beyond the degree of valency, and may include affinity, avidity, binding epitope, degree of epitopes targeted, and degree of EGFR crosslinking.

Chapter 4: HER3 Affibody Efficacy

Acknowledgements:

Figure 4.1 was adapted from:

Schardt JS; Oubaid JM, Williams SC; Howard JL; Aloimonos CM; Bookstaver ML; Lamichhane TN; Sokic S; Liyasova MS; O'Neill M; Andresson T; Hussain A; Lipkowitz S; Jay SM (2017) Engineered Multivalency Enhances Affibody-Based HER3 Inhibition for Cancer Therapy. Molecular Pharmaceutics. 14(4), 1047-1056.

Figure 4.4 was adapted from:

Schardt JS; Williams SC; Oubaid JM, Pottash AE, Noonan-Shueh MM, Ali RT, Goodman CA, Hussain A, Rena Lapidus RG, Lipkowitz S, Jay SM (2018). HER3-Targeted Affibodies with Optimized Formats Reduce Tumor Progression In Vivo in an Ovarian Cancer Model. In Review.

In vivo studies (Figures 4.3 and 4.4) were conducted in collaboration with Dr. Rena G. Lapidus at Marlene and Stewart Greenebaum Comprehensive Cancer Center, and the Translational Laboratory Shared Service, University of Maryland School of Medicine in Baltimore.

4.1 Introduction

We aim to develop HER3-directed therapeutics specifically for the treatment of ovarian cancer, the fifth leading cause of death in woman with an estimated 14,000 ovarian cancer-related deaths, and an estimated 22,000 new cases of ovarian cancer in 2017 [92]. The five-year survival rate for ovarian cancer patients is 46.5% [92] and HER3 expression is negatively correlated with ovarian cancer patient survival [93]. Furthermore, HER3 overexpression has been identified in 16% of patients with ovarian cancer [19]. NRG-HER3 autocrine signaling has been identified as a key driver of some ovarian cancers, thus HER3 inhibition may be effective in this setting [16]. Current treatment options for ovarian cancer are limited and include surgery, chemotherapy, hormone therapy, targeted therapy, and radiation therapy [94]. Specifically, these targeted therapies include: small molecule PARP inhibitors, and VEGF antibodies for angiogenesis inhibition (*e.g.* Avastin) [94]. HER3 therapies would fill a critical clinical need for the treatment of ovarian cancer, and could be employed in combination with approved therapies.

4.2 Methods

4.2.1 Cell proliferation assays

OvCAR8, Du145, and H1975 cells were seeded at 9,000 cells per well, and BT474 cells were seeded at 80,000 cells per well in media supplemented with 2% FBS, 1% Pen-Strep, and 200 pM NRG in a 24 well plate (VWR 10062-900), treated with the indicated concentrations of affibody, PI3K inhibitor NVP-BKM120, combination, or

no treatment control (media alone), incubated in 5% CO_2 at 37ºC for 5 days, and analyzed using Alamar Blue (Bio-Rad) following the manufacturer's protocol.

4.2.2 Combination treatments

OvCAR8 cells were seeded at 18,000 cells per well in media supplemented with 2% FBS, 1% Pen-Strep, and 200 pM NRG in 24 well plates, treated with the indicated concentration of drug **(**carboplatin, cisplatin, doxorubicin, paclitaxel) or combination with 10 nM monovalent or bivalent affibody, and analyzed using Alamar Blue assay five days post-treatment.

4.2.3 Du145 xenograft study

24 NSG mice were injected with 3 million Du145 cells in media or PBS (no FCS) and 33% matrigel. Mice were sorted into 3 groups when tumors reached ~ 100 mm^3 to ensure similar initial mean tumor volume per group. Du145 xenograft bearing mice were injected by IP with 80 micrograms bivalent affibody, an equivalent dose of monovalent affibody, or PBS alone (8 mice per group) three times weekly every 3 days for 18 days, and weighed twice weekly. Tumor volume was assessed using calipers twice weekly. Mice were sacrificed after 39 days once tumor burden exceeded 1500 mm^3, and tumors were excised and frozen.

4.2.4 ADR RES Study

15 NOD.Cg-*Prkdc*^{scid} *Il2rg*^{tm1Wjl}/SzJ NOD SCID gamma (NSG) mice were injected with 15x10^6 luciferase expressing ADR-RES cancer cells by intraperitoneal injection (i.p.). Ten days after injection, mice were imaged with IVIS Xenogen In Vivo

Imaging System (Perkin Elmer, Bridgeport CT) to monitor disease burden using bioluminescence and then the mice were sorted into groups with equivalent mean tumor volumes. Mice were injected with 80 micrograms bivalent affibody, an equivalent dose of monovalent affibody, or PBS alone (5 mice per group) three times weekly via i.p. injection. Tumor burden was monitored weekly by bioluminescent imaging using IVIS (Xenogen).

4.3 Results

4.3.1 Multivalency increases HER3 affibody-mediated inhibition of cancer cell growth

We examined the effect of multivalent ligands on *in vitro* cell viability in comparison to monovalent affibody treatment. Interestingly, despite the observation of HER3 signaling inhibition by multivalent affibodies in all cell lines tested, cell viability was differentially impacted. In OvCAR8 cells, both bivalent and trivalent HER3 affibodies (10 nM and 50 nM) significantly reduced viability compared to monovalent affibodies (**Figure 4.1A**). In Du145 cells, multivalent and monovalent ligands significantly reduced cell viability compared to untreated controls (**Figure 4.1**B). In H1975 cells, multivalent affibody treatment had more limited anti-proliferative effects compared to monovalent treatment and untreated controls, as only the trivalent affibodies caused statistically significant growth inhibition (**Figure 4C**). In BT474 cells, neither multivalent nor monovalent treatment reduced proliferation below control levels (**Figure 4.1D**).

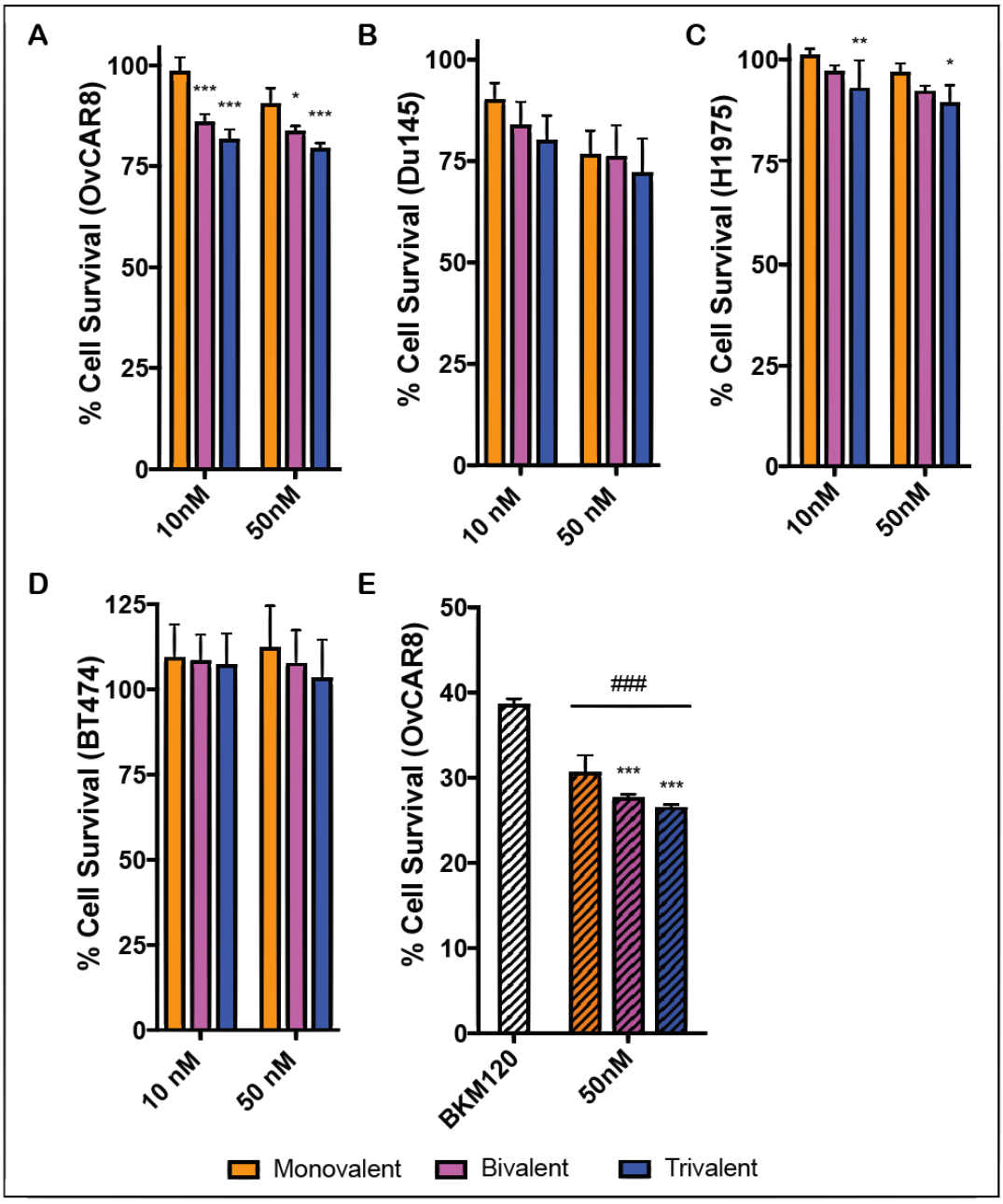

Figure 4.1: Multivalency increases functional efficacy of HER3 affibodies as single agents and as part of combination therapy. A. OvCAR8 **B.** Du145 **C.** H1975 **D.** BT474 cells were exposed to 200 pM NRG and treated with the indicated concentrations of trivalent, bivalent or monovalent affibodies, incubated for 5 days and analyzed using the Alamar Blue assay following the manufacturer's protocol. **E.** OvCAR8 cells were treated with 50nM of the indicated affibodies in combination with 1mM BKM120 (BKM), or with 1mM BKM alone, and incubated and analyzed as above. Results shown are mean +/- SD and are representative of three independent experiments; n=10, ***P<0.001, **P<0.01 *P<0.05 in reference to the equivalent dosage monovalent affibody group, ###P<0.001 in reference to the BKM only group by one way ANOVA with Bonferroni post-hoc test.

4.3.2 Multivalency improves therapeutic efficacy of FDA approved chemotherapy drugs

We explored the utility of bivalent HER3 affibodies in combination therapy with various chemotherapeutic drugs: carboplatin, cisplatin, doxorubicin, and paclitaxel. Combination with bivalent HER3 affibodies significantly reduced the IC50 values of these drugs in OvCAR8 cells compared to monovalent affibody combination treatment and single agent chemotherapeutic treatment. Dose curves are shown in **Figure 4.2.**

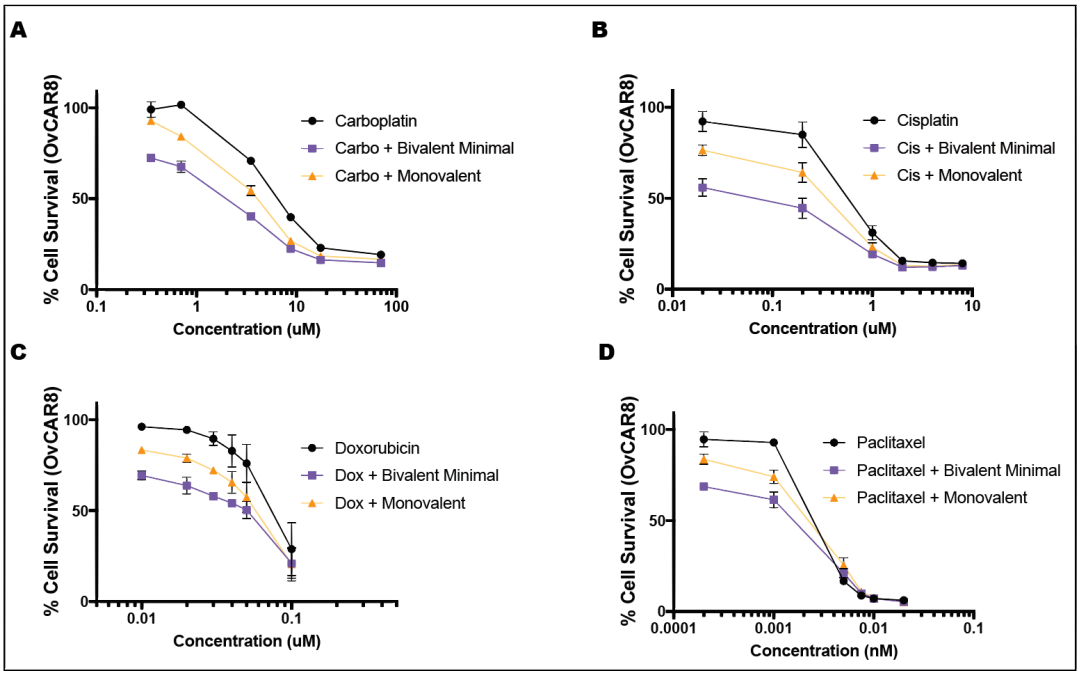

Figure 4.2: Multivalency improves therapeutic efficacy of FDA approved chemotherapy drugs. OvCAR8 cells were seeded at 18,000 cells per well in media supplemented with 2% FBS, 1% Pen-Strep, and 200 pM NRG in 24 well plates, treated with the indicated concentration of drug or combination with 10 nM monovalent or bivalent affibody **A.** carboplatin, **B.** cisplatin, **C.** doxorubicin, **D.** paclitaxel, and analyzed using Alamar Blue assay five days post-treatment.

4.3.3 HER3 affibodies slow tumor progression in vivo in a Du145 xenograft model

We assessed ligand efficacy *in vivo* in a Du145 xenograft model (**Figure 4.3**). Bivalent HER3 ABDs significantly slowed tumor progression, albeit modestly, compared to PBS control, and this trend persisted even after dosing had been terminated. *In vivo* efficacy was similar between bivalent and monovalent ABD fusions in this model.

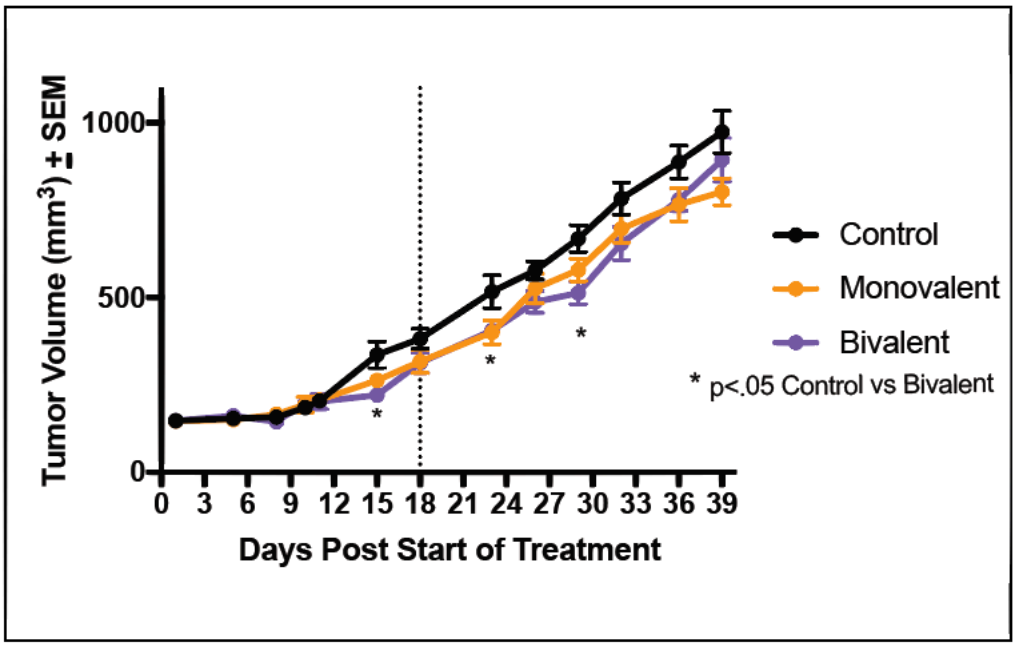

Figure 4.3: HER3 ABD fusions slow tumor progression *in vivo* in Du145 xenograft model. Mean tumor volume over time (Vertical dashed line indicates last treatment day). 24 NSG mice were injected with 3 million Du145 cells in media or PBS (no FCS) and 33% matrigel. Mice were sorted into 3 groups when tumors reached ~ 100 mm^3 to ensure similar initial mean tumor volume per group. Du145 xenograft bearing mice were injected by IP with 80 micrograms bivalent affibody, an equivalent dose of monovalent affibody, or PBS alone (8 mice per group) three times weekly every 3 days for 18 days, and weighed twice weekly. Tumor volume was assessed using calipers twice weekly. Mice were sacrificed after 39 days once tumor burden exceeded 1500 mm^3, and tumors were excised and frozen. Results shown are mean +/- SE; n=8, *P<0.05 in reference to bivalent versus PBS only treatment at the indicated time point by one way ANOVA with Bonferroni post-hoc test.

4.3.4 HER3 affibodies reduce tumor progression in vivo in an ovarian cancer xenograft model

We assessed the effect of the affibodies at slowing tumor growth in an orthotopic human ovarian cancer model. The ADR-RES cell line was chosen for this study as it is a derivative of the OvCAR8 cell line (from the same patient donor) [95]. NSG mice were injected i.p. with 15 million luciferase-expressing ADR-RES cancer cells; 10 days after injection, mice were i.p. injected with 80 micrograms bivalent affibody, an equivalent dose of monovalent affibody, or PBS alone (5 mice per group) three times weekly for 28 days. Note, treatment started ten days after cell injection, thus the tumors were already engrafted. Bivalent HER3 ABDs significantly reduced tumor levels as measured by photon intensity compared to PBS control at days 21 and 28-post start of treatment. The monovalent HER3 ABDs significantly reduced tumor levels compared to PBS control only at day 28 (**Figure 4.4A, B**).

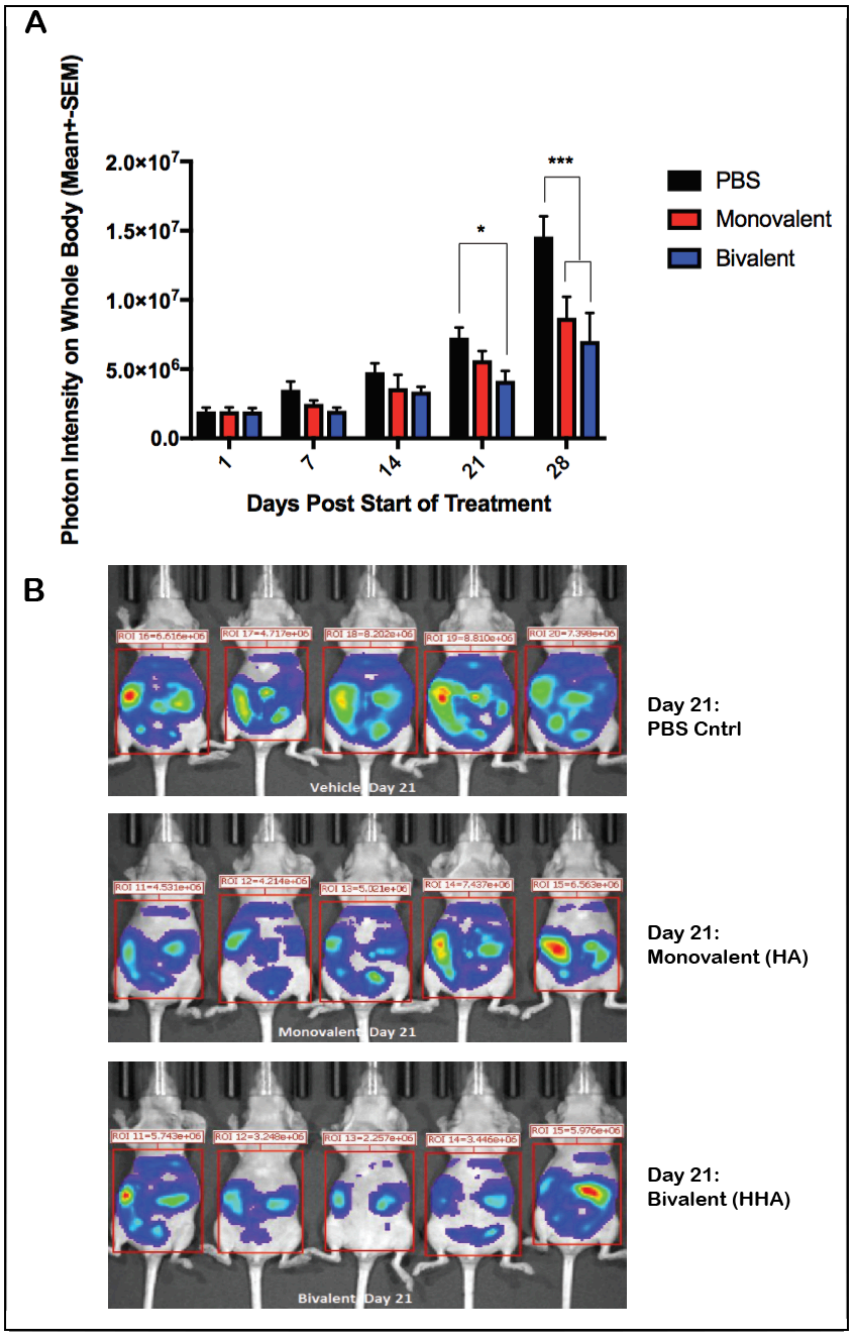

Figure 4.4: HER3-ABD fusions reduce tumor progression in vivo in an ADR-RES xenograft model. A. Whole body photon intensity at indicated time points post treatment. **B.** Raw IVIS images Day 21 post treatment. For **A** and **B**, 15 NSG mice were injected with 15 million luciferase expressing ADR-RES cancer cells by i.p.. 10 days after injection, mice were imaged with IVIS (Xenogen) to monitor disease burden and sorted into groups of equivalent mean tumor volumes. Mice were injected i.p. with 80 micrograms bivalent affibody, an equivalent dose of monovalent affibody, or PBS alone (5 mice per group) three times weekly. Tumor burden was monitored weekly by bioluminescent imaging using IVIS (Xenogen). Results shown are mean +/- SE; n=5, ***P<0.001 and *P<0.05 indicate significance compared to PBS only (control) group by one way ANOVA with Bonferroni post-hoc test.

4.3.3 Discussion

The therapeutic potential of any cancer drug could be further enhanced by selective deployment against the most vulnerable cancer types. Our results revealed disparate efficacies on the cell lines used in this study, despite the fact that these cells were chosen based on biological features that were expected to correlate with HER3-targeted affibody efficacy. The BT474 cancer cell line is reported to have moderate to high levels of HER2 and HER3 [43,78], which together form the most potent mitogenic unit of the HER family [20]. The H1975 cell line expresses HER2 and HER3 and was previously shown to be susceptible to HER3 biasing by bivalent NRG treatment[68]. Additionally, high basal NRG expression has been demonstrated as a biomarker for HER3 oncogenic addiction and susceptibility to HER3-targeted therapies [43]; both the OvCAR8 and Du145 cell lines are reported to have high basal NRG expression [43], and the OvCAR8 cell line has been documented to depend on a HER3/NRG autocrine loop [16]. In our studies, multivalent affibodies induced significant reductions in cell viability in the OvCAR8, H1975 and Du145 cell lines, while BT474 cells were not significantly affected (**Figure 4.1**). In BT474 cells, this lack of efficacy occurred despite enhanced HER3 degradation (**Figure 2.9**). Thus, our data support previous work indicating that HER3 targeted therapies are most efficacious as single agents against cancers that exhibit NRG autocrine signaling [43]. However, the ability of multivalent affibodies to induce HER3 downregulation indicates therapeutic potential for combination therapy approaches, for example, with HER2-targeted drugs, as well as potential utility in drug conjugate approaches.

Development of new therapeutic approaches for ovarian cancer is imperative due to the generally high rate of recurrence and poor prognosis associated with this disease. HER3 is well established as a compelling therapeutic target in numerous cancers, including ovarian cancer, yet, conventional small molecule- and monoclonal antibody-based approaches have so far failed to yield a widely used therapeutic that directly targets HER3. Here, we report the potential of an alternative approach, HER3-targeted affibodies. We identify a streamlined and specific molecular format for optimal pHER3 inhibition and HER3 downregulation: a bivalent affibody with minimal three-glycine linker separating binding domains. We further report significant mechanistic evidence supporting HER3 downregulation as a highly specific phenomenon prompted by HER3 sequestration by multivalent ligands. Most importantly, we show that both monovalent and bivalent HER3 affibody-ABD fusion proteins significantly reduce tumor burden in an ADR-RES ovarian cancer model in mice, suggesting further exploration of HER3 affibodies as ovarian cancer therapeutics.

Taken together with the repertoire of work in the field, the results reported here further highlight the translational promise of multivalent ligands for HER3-directed cancer therapy. Previous work from the Lofblom group showed that a bivalent affibody of molecular format Z_{HER3}-ABD-Z_{HER3} (3A3), where domains are separated by a $(S_4G)_4$ linker domain, is capable of simultaneously binding both molecular targets HER3 and albumin [62]. Further, 3A3 showed improved pHER3 inhibition compared to monovalent affibody [62], in agreement with our own findings that

affibody multivalency improves pHER3 inhibition [79]. 3A3 was also shown to significantly reduce pancreatic cancer BxPC-3 xenograft tumor progression in mice approximately 26 days post-treatment when dosed at 80 μg treatment 3 times weekly [96], and allowed for tumor growth inhibition comparable to monoclonal antibody MM-121 when each were dosed at 600 ug 3 times weekly in a similar BxPC-3 *in vivo* model [97]. This report also supports the idea that the efficacy of multivalent HER3 affibodies can be retained in a variety of formats [97]. Thus, overall, multivalent HER3 ligands are versatile and show *in vivo* therapeutic potential against cancers from a variety of source tissues.

Our work here, together with our previous investigation of HER3 multivalent affibodies, reveals disparity between *in vitro* bioactivity versus *in vivo* efficacy. Specifically, *in vitro* multivalent affibody treatment promotes dramatic reduction in HER3 receptor levels and reduced pHER3 levels compared to monovalent affibody treatment, whereas *in vivo* efficacy of multivalent affibodies is comparable to monovalent ligands (**Figures 4.3 and 4.4**). The luciferase expressing ADR-RES model used in this work is not a solid tumor model and was therefore not amenable to biopsy for the assessment of HER3 levels post-treatment. Thus, it remains to be definitively shown whether multivalent affibodies induce similar HER3 downregulation as observed *in vitro*. Regardless, further investigation is likely required in order to realize the full potential of multivalent ligands compared to monovalent ligands *in vivo* through exploration of alternative dosing levels, treatment regimens, and cancer models.

Beyond our focus here on multivalent HER3 affibodies for ovarian cancer therapy and induced receptor downregulation, it is important to highlight that affibodies and alternative protein scaffolds in general represent an emerging field of significant industrial and clinical interest for myriad therapeutic applications. Numerous alternative scaffold-based therapies are in on-going clinical trials for treatment of a variety of pathologic conditions, including the affibody therapeutic AB-035, an IL-17A-specific affibody for the treatment of psoriasis, and AB7-25, a HER2 specific affibody for cancer PET imaging [98–100]. Affibodies possess inherent strengths and weaknesses compared to the standard IgG antibody therapeutics. Affibodies have superior tissue penetration (due to their small size), enhanced stability, ease of manufacturing and expression in bacterial systems, and low immunogenicity [98–100]. The limitations of affibody therapeutics, namely their short half-life and lack of immune effector function, can easily be overcome through molecular engineering approaches tailored to the specific application of interest. For instance, affibodies incorporating albumin-binding domain fusion partners are reported to display extended half-life of up to 12 days [98]. HER3 affibodies proved highly amenable to molecular engineering approaches, as modulation of linker length, valency, and ABD fusion placement allowed for robust retention of HER3 affibody bioactivity. Thus, the versatility and modular potential of affibody molecules are advantageous toward the development of sophisticated, multi-functional, and multi-domain, next-generation molecular therapeutics.

Regarding the treatment of ovarian cancer, this work provides proof of principle for multivalent ligands as a promising strategy to limit *in vivo* ovarian cancer progression. OvCAR8 and ADR-RES cell lines are representative models of high-grade serous ovarian cancer (HGSOC), a highly aggressive and common ovarian cancer subtype. The results herein encourage a more extensive evaluation of multivalent HER3 ligands against a broad panel of HGSOC cell models, which may help identify biomarkers of susceptibility to HER3-targeted therapies, and enable the strategic deployment of such therapeutics against ovarian cancer in a more personalized medicine approach.

Chapter 5: Delivering Toxic Payloads via Next Generation HER3 Affibody Anti-Cancer Therapeutics

Acknowledgements:

All studies in this chapter were conducted in collaboration with Dr. Ira Pastan, Dr. Tapan Bera, and Matthew Williams at Laboratory of Molecular Biology, National Institute of Health in Bethesda, Maryland.

5.1 Introduction

Recombinant immunotoxins have emerged as promising therapeutic modalities for the treatment of cancer. This technology combines the natural potency of protein toxins to induce apoptosis and kill cells with the targeting ability of antibodies (and other high affinity binding domains) towards the ultimate goal of selective delivery of toxic payload to cancer cells without deleterious off-target effects on healthy cells and tissue [101–103].

Pseudomonas exotoxin A (PE) is a 613 amino acid protein with molecular weight of 66.7 kDa. Structurally, it contains three major domains: a cell-binding domain (Domain 1 – Residues 1-252), a translocation domain (Domain 2 – Residues 253-364), and a protein synthesis arrest and programmed cell death induction domain (Domain 3 – Residues 396-613) [103]. Initial efforts in developing immunotoxins involved the incorporation of full-length toxins, which caused severe toxicity in *in vivo* pre-clinical models [102,104]. This limitation led to the engineering of PE38, a 38 kDa truncated PE format with reduced off target toxicity. Specifically, PE38 was engineered with a deletion of the domain 1 cell-binding moiety; PE38 contains amino acids 251-364 followed by amino acids 381-613 of PE based on Protein Data Bank structure 1IKQ [105]. To generate recombinant immunotoxin, an antibody fragment (or other high affinity binding domain) can traditionally be engineered as an N-terminal fusion protein to direct toxin to the cells overexpressing a specific target of interest.

For immunotoxin to induce cell death, an orchestrated succession of molecular therapeutic trafficking events must occur. First, the immunotoxin must enter endocytic compartments within the target cell [102]. Notably, the truncated PE38 lacks a cellular binding domain (domain I), and it is therefore requisite that the antibody or high affinity-binding domain endows the immunotoxin with the function of cellular uptake into endocytic compartments [102]. Once, the immunotoxin enters the endocytic compartment, PE38 is cleaved into two fragments [102]. The C-terminal domain, composed of domain III and a portion of domain II, translocates

into the ER, and then to the cytosol [102]. There, the cell death induction domain (Domain III) exerts its adenosine diphosphate (ADP)-ribosylation enzymatic activity by modifying elongation factor 2 with ADP ribose, ultimately causing protein synthesis arrest and cell death [102].

The first immunotoxin to be granted FDA-approval was denileukin diftitox (ONTAK) (approved in 1999) [104,106]. ONTAK is a diphtheria toxin IL-2 fusion protein, which has been employed clinically for the treatment of cutaneous T cell lymphoma (CTCL), Non-Hodgkin lymphoma (NHL), and chronic lymphocytic leukemia (CLL) [104,106]. Diphtheria toxin induces cell death by near analogous mechanism to that of PE38. There are several immunotoxins in clinical trial incorporating diphtheria toxin, PE38, and other toxin moieties [106]. Immunotoxins incorporating PE38 in clinical trial include: (1) BL22, which contains a CD22 mAb, for the treatment of hairy cell leukemia (HCL), and (2) LMB-2, which contains the variable region of an anti-CD25 mAb, for the treatment of T cell malignancies and HCL [106]. While immunotoxins have most frequently been investigated as therapies for hematologic cancers, there are several on-going clinical trials pursuing immunotoxins for the treatment of solid tumors and metastatic cancers *e.g.* LBM-100, a mesothelin specific antibody-PE38 toxin fusion, for the treatment of mesothelioma [106]. Solid tumors present considerable added challenge compared to hematologic cancers toward effective treatment with immunotoxins [106]. Solid tumors are naturally less accessible to targeted therapy. Further, patients with solid tumors are generally less immunocompromised (compared with patient's with hematological malignancies)

and are therefore more likely to develop acquired immunotoxin resistance – by mechanism of neutralizing antibody production [106].

5.2 Methods

5.2.1 Preparation of Recombinant Immunotoxin

Cloning of HER3 bivalent affibody PE38 Fusion Protein: DNA gene block (IDT) encoding HER3 bivalent affibody was ligated into pRK79 protein expression vector immediately upstream of DNA encoding truncated Pseudomonas exotoxin (PE38) using Gibson cloning strategy. Briefly, Gene block:

5'- **taactttaagaaggagatatacatatg**

VDNKFNKERYLAYYEIWQLPNLNRTQKAAFIGSLQDDPSQSANLLAEAKKLN

DAQAPKGGGVDNKFNKERYLAYYEIWQLPNLNRTQKAAFIGSLQDDPSQSA

NLLAEAKKLNDAQAPK

aaagcttccggaggtcccgagggcg-3'

and expression vector pRK79 were each digested with HindIII and Nde1 restriction enzymes following manufacturer's protocol (NEB), and ligated using Gibson assembly reagent (NEB). Positive clones were examined by DNA digest, and sequences were confirmed by Sanger Sequencing at NCI Core Facility.

Transformation: BL21 (DE3) *E. Coli* Cells were transformed following manufacturer's protocol with 200 ng plasmid DNA. Transformed cells were plated on five LB/Chloramphenicol agar plates (200ul per plate) and incubated overnight at 32^{o}C for 16 hours, resulting in at least 100 colonies per plate.

Fermentation: Super Broth was prepared (1 Liter of Terrific Broth was supplemented with 8.9 mL of 45% glucose solution, 1.68 mL of 1M MgSO4, and chloramphenicol). All colonies from five plates were dislodged with 5 mL Super Broth, and used to inoculate 2-500mL cultures in baffled, 1L Erlenmeyer flasks in an environment of 37C, shaken at 250 RPM. Cultures were monitored for approximately two hours until OD600nm was between 2.0-2.5, and then induced with a final concentration of 1mM IPTG. Culture continued to shake at 37C for an additional 2 hours after induction. Bacteria were harvested by centrifugation at 3500 rpm for 20 minutes, supernatant was discarded, and cell pellet was stored at -80C. Samples of pre- and post- induction of both soluble and insoluble fractions were analyzed via SDS-PAGE gel stained with coomassie.

Inclusion body preparation: Pellet was resuspended in 160mL of TES (50 mM Tris-HCl, pH 8.0, 20 mM EDTA, 100 mM NaCl), and treated with 6.5 mL of lysozyme (5 mg/ml in water). Solution was mixed using Tissuemizer probe and incubated at room temperature for 30 minutes, shaken manually every 10 minutes. 20 mL of 25% Triton X100 solution (in water) was added to the solution, and it was mixed using the Tissuemizer to sheer DNA. The solution was incubated at room temperature for 30 minutes, shaken by hand every 10 minutes. The solution was centrifuged at 12,000 rpm at 4C for 20 minutes, and the supernatant was discarded. The process of suspension in TES, incubation with 25% Triton X100, mixing, centrifugation, and discarding of supernatant was repeated two more times, and then this process was

repeated three times washing *without* Triton X100. Finally, the inclusion body was pelleted by centrifugation and stored at -80C.

Solubilization and denaturation: The inclusion body was resuspended in 5 mL GTE buffer (6 M guanidine HCl, 100 mM Tris-HCl, pH 8.0, 2 mM EDTA), incubated at room temperature for two hours, and then centrifuged at 12,000 rpm. The solubilized protein in the supernatant was collected, and quantified for protein content by Pierce Coomassie Plus reagent. Then, protein solution was diluted to 10 mg/ml in GTE buffer supplemented with 10 mg/ml dithioerythritol to reduce disulfide bonds on the toxin domain, and incubated at room temperature for 5 hours, protected from light.

Refolding: Denatured protein was added dropwise to 1 L chilled refolding buffer (100 mM Tris-HCl, 1 mM EDTA, 0.5 M arginine, pH 9.5, 551 mg/L oxidized glutathione – added just before use) and incubated for 24 hours. Then, folded protein solution was dialyzed against 50L dialysis buffer (20 mM Tris-HCl, pH 7.4, chilled to 4°C, 100 mM urea – added just before use.

Chromatography: Q-Sepharose ion exchange column was equilibrated with 10 column volumes chromatography buffer A (20 mM Tris-HCl, pH 7.4, 1 mM EDTA), 10 column volumes chromatography buffer B (1 M NaCl in Chromatography buffer A), and then 10 column volumes chromatography buffer B. Q-Sepharose column was loaded with protein solution. Q-Sepharose column was then connected to AKTA chromatography system, and protein was eluted by 50% buffer B gradient over 30

minutes. Fractions were assessed for protein content and purity by coomassie gel. Selected fractions were consolidated and loaded onto an 8 mL Mono-Q ion exchange column (equilibrated in Buffer A as described for Q-Sepharose column). Mono-column was connected to AKTA chromatography system, and eluted by 50% buffer B gradient over 60 minutes. Fractions were assessed for protein content and purity by coomassie gel, and selected fractions were further purified, and buffer exchanged to Phosphate-buffered saline (20 mM KH2PO4, 50 mM Na2HPO4, 0.15 M NaCl, pH 7.4) using Progel TSK G3000SW size exclusion column.

The methods outlined in *Section 5.2.1* are adapted from *Pastan et al. Recombinant Immunotoxins in the Treatment of Cancer. 2004* [103].

5.2.2 Assessment of recombinant immunotoxin in vitro bioactivity

OvCAR8 cells were seeded at 18,000 cells per well in media supplemented with 2% FBS, 1% Pen-Strep, and 200 pM NRG in a 24 well plate (VWR 10062-900), treated with the indicated concentrations of bivalent HER3 PE38 immunotoxin, HB21 immunotoxin (positive control), or no treatment negative control (media alone), incubated in 5% CO_2 at 37ºC for 5 days, and analyzed using Alamar Blue (Bio-Rad) following the manufacturer's protocol.

5.3 Results and Discussion

5.3.1 Preparation of bivalent HER3-PE38 toxin fusion

DNA encoding Bivalent HER3 affibody was cloned upstream of PE38 toxin in plasmid pRK79. The protein was expressed in BL21 (DE3) *E. coli* in 2-500mL cultures. Bivalent HER3 affibody-PE38 toxin fusion was identified in the insoluble protein fraction, only after induction of protein expression with IPTG as indicated by a distinct band of expected size (theoretical molecular weight of 51.453 kDa) by SDS-PAGE gel stained with coomassie (**Figure 5.1**). This approximately 50 kDa band was visible only in the insoluble fraction post-IPTG induction. To purify the recombinant immunotoxin, the insoluble protein fraction was isolated, cells were lysed, and the inclusion body was washed extensively to remove contaminates *e.g.* DNA. Coomassie stained SDS-PAGE gel of washed inclusion body revealed a distinct band of expected size (**Figure 5.2**). The isolated inclusion body was solubilized by suspension in guanidine rich buffer and homogenization using Tissuemizer probe. The solubilized protein yield was approximately 70 milligrams (per 2-500mL cultures) as determined by Pierce Coomassie Plus reagent following manufacturer's protocol and in reference to BSA standard curve. To isolate bioactive, recombinant immunotoxin, the solubilized protein was denatured, refolded, dialyzed, and purified via three stages of chromatography. First, Q-Sepharose ion exchange chromatography was employed as a cost-effective initial step to remove crude high molecular weight contaminants and aggregates. Q-Sepharose gradient chromatography introducing high salt buffer resulted in protein elution as a single peak for absorbance at 280nm, and the corresponding fractions were examined for

purity and protein content by Coomassie stained SDS-PAGE gel. The results revealed that the majority of fractions contained thick bands at expected molecular weight approximately 50 kDa (indicative of the recombinant immunotoxin), but also several higher molecular bands (indicative of aggregates and impurities) (**Figure 5.3**). Fractions illustrated with 'X' were discarded based on low concentration and high impurity relative to the level of 50 kDa band (**Figure 5.3**). Total approximate protein content determined by Nanodrop (E=12.43 for our recombinant immunotoxin) was 70 mg, indicating limited loss of protein product during Q-Sepharose chromatography. To more stringently purify the immunotoxin, Mono-Q ion exchange chromatography was employed again introducing a gradient of high salt to elute the protein, resulting in the elution of two distinct peaks. Coomassie stained SDS-PAGE gel of fractions B9-B5 (peak 1) and C1-C6 (peak 2) collected after Mono-Q chromatography indicate that Mono-Q separated with high purity bivalent HER3 affibody-PE38 toxin fusion protein (peak 1) from higher molecular weight aggregates and impurities (peak 2) (Figure 5.4). Total approximate protein content determined by Nanodrop was approximately 35 mg, indicating that approximately half of solubilized inclusion body proteins were recombinant immunotoxin monomer, assuming limited loss of total protein during Mono-Q chromatography stage. As a final polishing and buffer exchange step to PBS (for the peak 1 Mono-Q fractions), size exclusion chromatography was employed, and resulted in the elution of a single peak at absorbance 280nm. Coomassie stained SDS-PAGE gel and Nanodrop respectively confirmed high purity fractions (**Figure 5.5**) and total protein content approximately 30 mgs. The purified recombinant immunotoxin fractions were consolidated and

examined on a Coomassie stained SDS-PAGE gel at 2.5 ug/lane in reference to control well loaded with 2.5 ug BSA (**Figure 5.6**), reinforcing the result of a high purity product of expected molecular weight and band intensity comparable to that of BSA control (to confirm concentration).

5.3.2 Assessment of recombinant immunotoxin in vitro bioactivity

To assess *in vitro* bioactivity of bivalent HER3-PE38 toxin fusion protein, OvCAR8 cells were treated with indicated concentrations of bivalent HER3 PE38 immunotoxin, HB21 immunotoxin (positive control), or no treatment negative control (media alone), incubated for 5 days and analyzed using the Alamar Blue assay. The results indicate that bivalent HER3 PE38 immunotoxins exhibit potent bioactivity, reducing cell survival to approximately 10% of no treatment negative control at dosing around 200 nM, and 35% of negative control value at 20 nM treatment (**Figure 5.7)**. Bivalent HER3 Affibody PE38 did, however, exhibit significantly lower bioactivity than positive control HB21, a PE40 immunotoxin directed to human transferrin receptor (expressed on OvCAR8 and many cancer cell types) by monoclonal antibody variable region fusion. HB21 showed substantial cell killing (around 10% of negative control no treatment cells) even at subnanomolar concentrations (**Figure 5.7)**. Overall, these results – confirming potent cell death induction by bivalent HER3 affibody PE38 immunotoxin – provide crucial proof of concept for effective intracellular delivery of toxic payload to cancer cells. It is well established that PE38 alone has limited toxicity because it is not readily internalized by cells [101]. Thus, HER3 affibodies successfully traffic PE38 inside OvCAR8 cells. These results encourage further evaluation of bivalent HER3 PE38 affibodies for

HER3-positive cancer treatment, and crucially indicate promise for HER3 affibodies to be employed for intracellular delivery of various therapeutic cargo (*e.g.* chemotherapeutic small molecule drugs) in HER3 affibody-drug conjugate approaches.

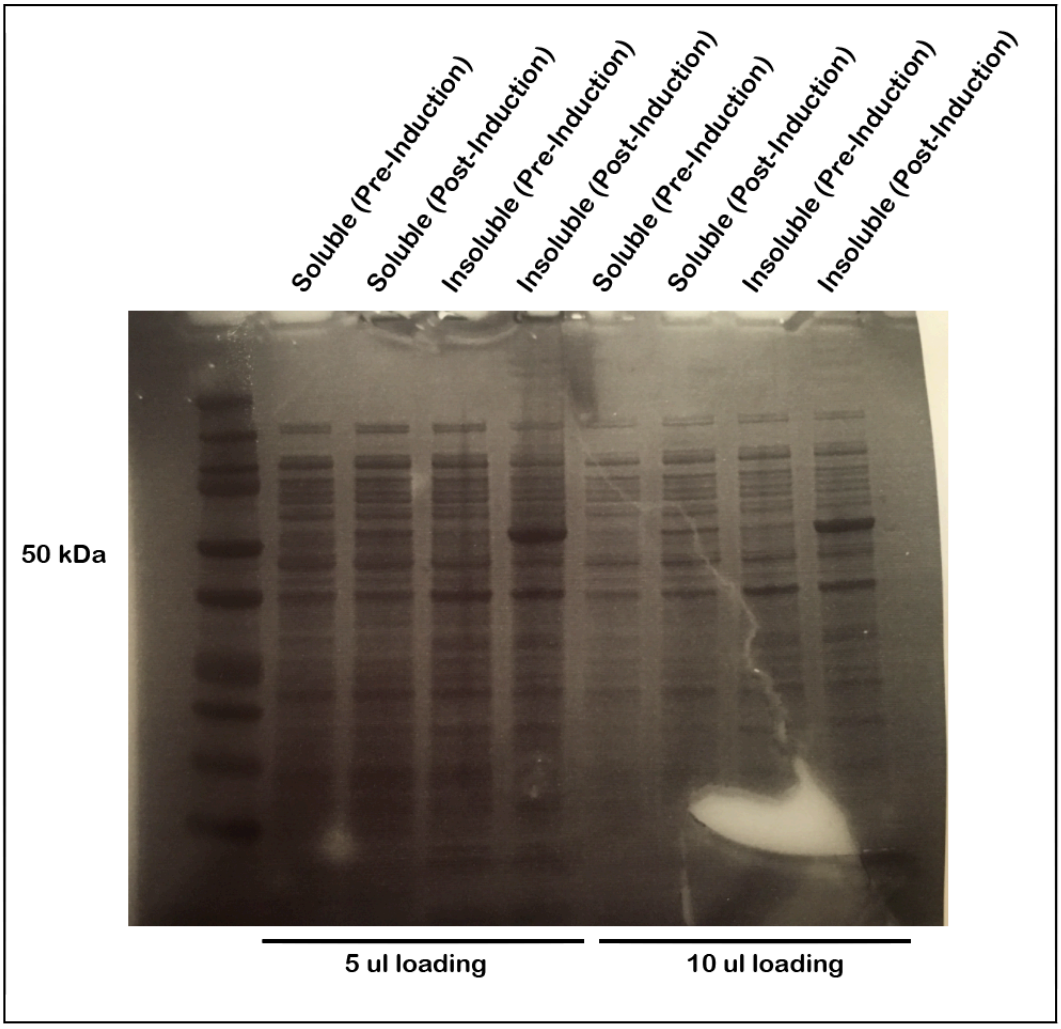

Figure 5.1: Bivalent HER3 affibody PE38 toxin fusion is identified as insoluble protein. Coomassie stained SDS-PAGE gel of soluble and insoluble protein fractions before and after induction of protein expression with IPTG; samples were loaded at 5 ul (first four lanes to the right of the ladder) and 10 ul (last four lanes on the right) total volumes. Bivalent HER3 affibody PE38 toxin fusion protein has theoretical molecular weight of 51.453 kDa. A distinct band of expected size is visible in the insoluble protein fraction only after induction of protein expression. Briefly, 2-500mL cultures were inoculated in an environment of 37C, shaken at 250 RPM. Cultures were monitored for approximately two hours until OD600nm was between 2.0-2.5, and then induced with a final concentration of 1mM IPTG. Cultures continued to shake at 37C for an additional 2 hours after induction.

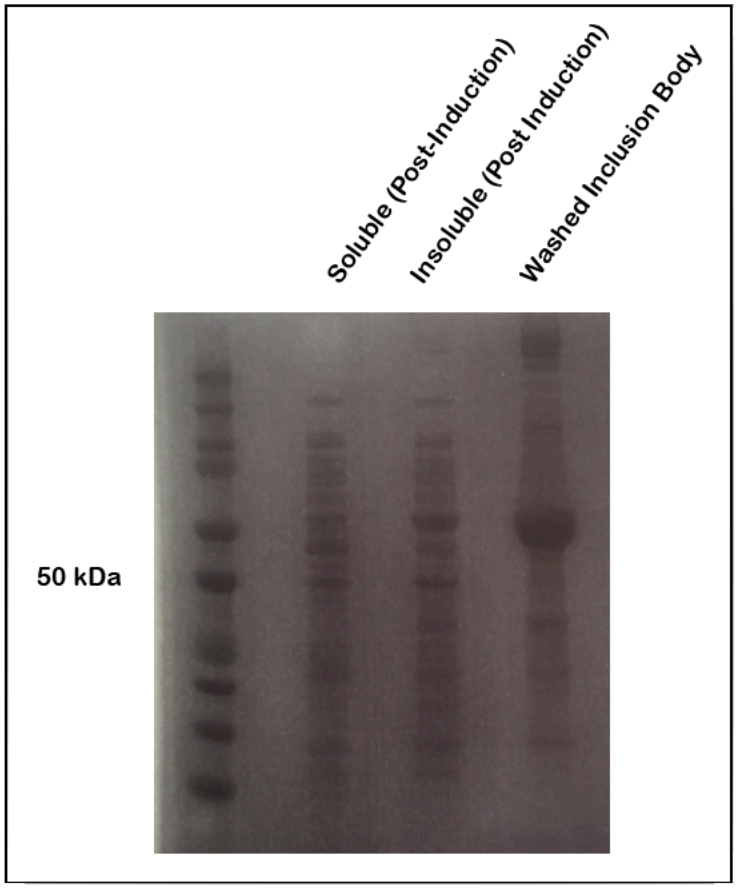

Figure 5.2: Bivalent HER3 affibody-PE38 toxin fusion protein is identified in washed inclusion body. Coomassie stained SDS-PAGE gel of soluble and insoluble protein fractions before and after induction of protein expression with IPTG, and washed inclusion body. Bivalent HER3 affibody-PE38 toxin fusion protein has theoretical molecular weight of 51.453 kDa. A distinct band of expected size is visible in the washed inclusion body. Briefly, pelleted insoluble protein fraction was resuspended in 160mL of TES buffer, and treated with 6.5 mL of lysozyme (5 mg/ml in water). Solution was mixed using Tissuemizer probe and incubated at room temperature for 30 minutes, shaken manually every 10 minutes. 20 mL of 25% Triton X100 solution (in water) was added to the solution, and it was mixed using the Tissuemizer to sheer DNA. The solution was incubated at room temperature for 30 minutes, shaken by hand every 10 minutes. The solution was centrifuged at 12,000 rpm at 4C for 20 minutes, and the supernatant was discarded. The process of suspension in TES, incubation with 25% Triton X100, mixing, centrifugation, and discarding of supernatant was repeated two more times, and then this process was repeated three times washing *without* Triton X100.

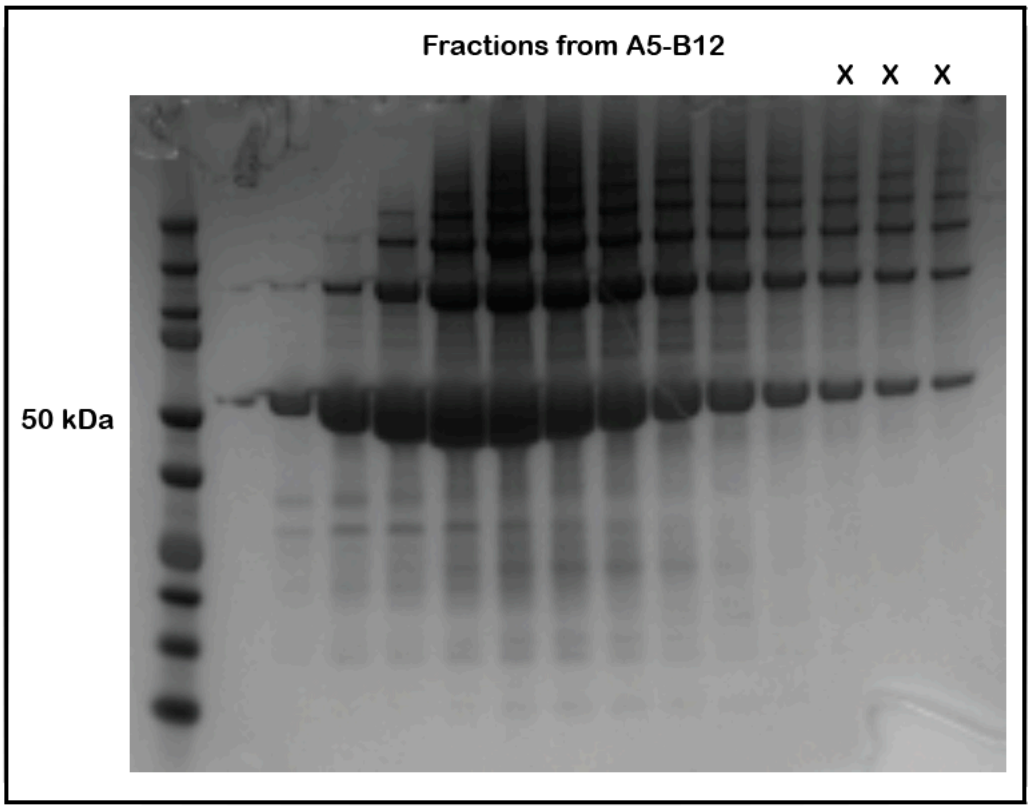

Figure 5.3: Purification of refolded protein (from inclusion body fraction) via Q-Sepharose ion exchange column. Coomassie stained SDS-PAGE gel of fractions A5-B12 corresponding with A280 chromatography peak reveals that fractions contain thick band of expected molecular weight approximately 50 kDa, but also several higher molecular bands indicative of aggregates/impurities. Fractions illustrated with 'X' were discarded based on low concentration and high impurity relative to 50 kDa band. Briefly, Q-Sepharose column was loaded with refolded inclusion body protein solution. Column was then connected to AKTA chromatography system, and protein was eluted by 50% buffer B gradient over 30 minutes.

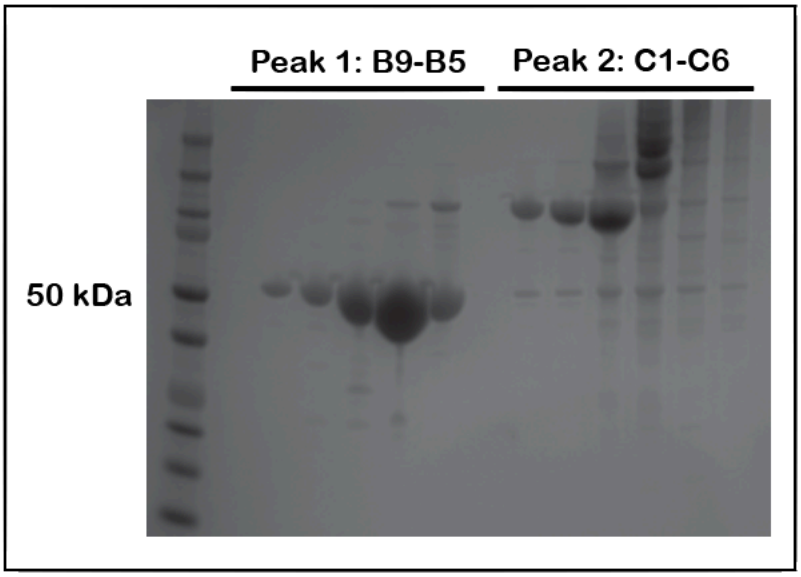

Figure 5.4: Purification of selected, consolidated fractions by Mono-Q ion exchange chromatography. Coomassie stained SDS-PAGE gel of fractions B9-B5 (peak 1) and C1-C6 (peak 2) collected after Mono-Q chromatography. The results indicate that Mono-Q successfully separates bivalent HER3 affibody PE38 toxin fusion protein (expected molecular weight approximately 50 kDa) from higher molecular weight aggregates and impurities. Briefly, Mono-Q column was loaded with selected fractions, column was connected to AKTA chromatography system, and protein was eluted by 50% buffer B gradient over 60 minutes.

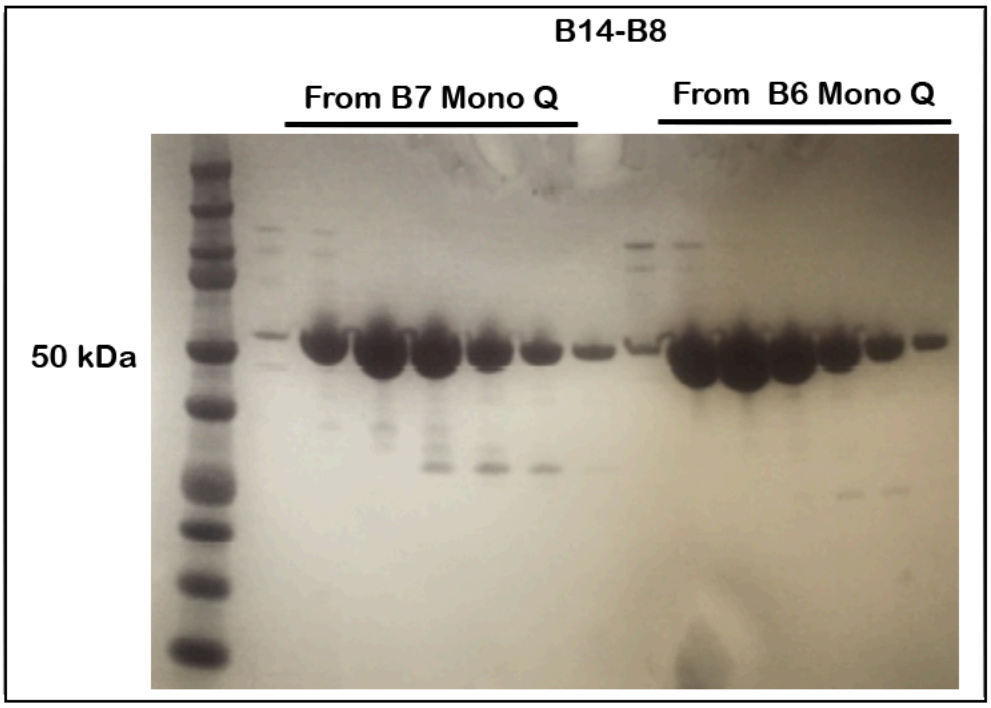

Figure 5.5: Size exclusion purification and buffer exchange of bivalent HER3 affibody-PE38 toxin fusion. Coomassie stained SDS-PAGE gel of fractions collected after size exclusion chromatography corresponding with A280 single peak. Briefly, selected fractions post Mono-Q chromatography (B7 and B6) were buffer exchanged to Phosphate-buffered saline (20 mM KH2PO4, 50 mM Na2HPO4, 0.15 M NaCl, pH 7.4) using Progel TSK G3000SW size exclusion column connected to AKTA chromatography system.

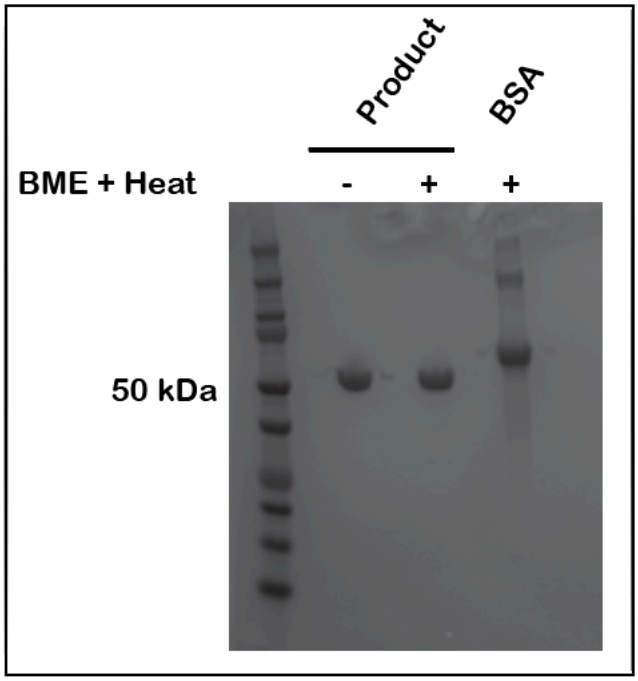

Figure 5.6: Bivalent HER3-PE38 toxin fusion protein – Purified product. Coomassie stained SDS-PAGE gel of final, consolidated protein product loaded at 2.5 ug/lane in both non-denaturing and denaturing (BME treatment and 5 minute incubation at 95C) compared against reference standard of 2.5 ug denatured bovine serum albumin.

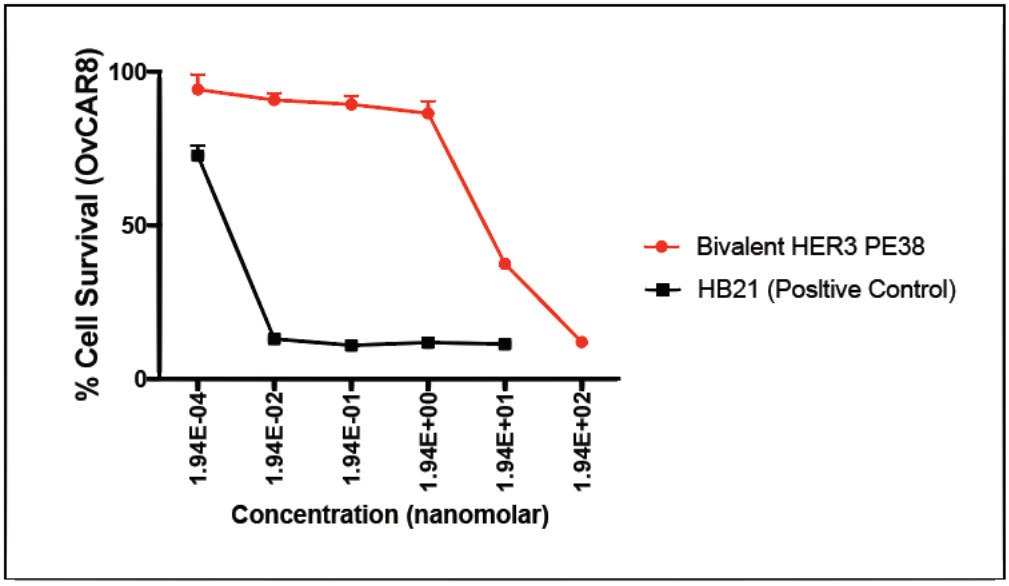

Figure 5.7: Assessment of *in vitro* bioactivity of bivalent HER3-PE38 toxin fusion protein. OvCAR8 cells were exposed to 200 pM NRG and treated with the indicated concentrations of treated with the indicated concentrations of bivalent HER3 PE38 immunotoxin, HB21 immunotoxin (positive control), or no treatment negative control (media alone), incubated for 5 days and analyzed using the Alamar Blue assay following the manufacturer's protocol. Results shown are mean +/- SE, n=3.

Chapter 6: Future Directions

The results herein demonstrate HER3 multivalent ligands as promising molecular therapeutics for improved cancer treatment. Yet, further investigation of HER3 affibodies is needed in order to realize the full potential of these molecules. HER3 affibodies should be engineered for optimized efficacy and employed against the most vulnerable cancers. We show that bivalent affibodies with small glycine linker separating affibody domains allow for optimized HER3 downregulation, pHER3 inhibition. HER3 affibodies show modest cancer cell proliferation inhibition and can foreseeable be applied in combination, conjugation, and toxin fusion protein based approaches to enhance overall therapeutic efficacy. We demonstrate that bivalent HER3 PE38 toxin fusions exhibit potent OvCAR8 cancer cell killing.

A key next step is to more rigorously investigate the potential of our toxin delivery approach. First, we plan to confirm that multivalent HER3 affibody PE38 fusions retain the ability to downregulate HER3 receptor (assessed by immunoblot). We next plan to engineer monovalent PE38 toxin fusions to examine any differential effects. Notably, multivalent but not monovalent HER3 affibodies induce HER3 downregulation. If multivalent HER3 ligands are endocytosed as a result of HER3 receptor internalization due to multivalent binding events, we would expect to see differential *in vitro* bioactivity comparing monovalent and bivalent PE38 fusion ligands. Albumin binding domains have been employed by our research group and others to improve HER3 affibody half-life and *in vivo* efficacy. We will generate HER3 affibody – albumin binding domain – PE38 fusion proteins and evaluate these molecules *in vivo* in ovarian cancer xenograft models. One potential pitfall is that HER3 PE38 toxin fusions may exhibit low tolerability due to toxicity when evaluated *in vivo*. The pilot study of HER3 affibody PE38 immunotoxin (Chapter 5) has provided valuable proof of concept for effective intracellular delivery of toxic payload to cancer cells. If dose-limiting toxicity thwarts the promise of our immunotoxin approach, we will pursue HER3 affibody-drug conjugate approaches for the targeted delivery of chemotherapeutic agents to cancer cells.

Beyond engineering of affibodies in fusion and conjugation-based approaches to improve overall efficacy, another key objective of our on-going research is to conclusively elucidate the mechanism of HER3 downregulation by multivalent

ligands. Understanding this mechanism will provide fundamental knowledge on HER3 receptor biology; this knowledge can ultimately be applied toward the improved rational design of cancer therapies against HER3. Thus far, we know that HER3 downregulation by multivalent ligands is at least in part post-translational in nature, however classic inhibitors of degradation pathways and combinations thereof have shown limited ability to inhibit the observed downregulation phenomenon. We are able to inhibit HER3 downregulation by multivalent ligands by incubation at 4C indicating an active mechanism of downregulation. However, this result does not provide conclusive evidence toward differentiating between either (i) receptor shedding or (ii) receptor endocytosis, since incubation at 4C could foreseeable inhibit either process. Further, we present evidence that multivalent HER3 affibodies are internalized via endocytosis, suggesting that HER3 receptors are also internalized by this mechanism. A key next step is to examine HER3 downregulation by multivalent ligands in the context of comparison with HER3 downregulation by native ligand neuregulin, a process that is well-understood [107,108]. For instance, HER3 downregulation induced by NRG results in upregulation of Nrdp1, a cytoplasmic HER3 interaction partner [107]. By carefully examining HER3 downregulation in relationship to NRG-mediated HER3 downregulation in MCF-7 cells as a control system, we hope to gain new insights into HER3 downregulation by multivalent ligands, and potentially uncover a novel mechanism of action for HER3 downregulation by multivalent affibodies.

Beyond gaining fundamental understanding in HER3 receptor biology as a future aim of our research, we will continue to identify the most vulnerable cell types to HER3 multivalent affibodies. Our *in vivo* efficacy data support that HER3 affibodies are promising toward the treatment of ovarian cancer. We hypothesize that HER3 expression and NRG expression will be key indicators of susceptibility to HER3 affibodies. We are conducting on-going research to examine the utility of HER3 multivalent ligands in ovarian cancer cell models that best recapitulate ovarian cancer patient tumors. Specifically, we are screening HGSOC and clear cell ovarian cancers for HER3 and NRG and evaluating this data in relationship in vitro cancer cell survival data in response to HER3 affibody treatment.

The overarching goal of our continued research is to position HER3 therapeutics for ultimate clinical translational toward improved cancer therapy.

Appendix A: Affibody Construct Protein and DNA Sequences

1. Monovalent HER3 Affibody:

Protein:

AHHHHHHVVDNKFNKERYLAYYEIWQLPNLNRTQKAAFIGSLQDDPSQSAN

LLAEAKKLNDAQAPK

DNA:

GCACATCACCACCACCATCACGTGGTCGATAACAAATTCAACAAAGAACG

CTACTTAGCATATTACGAGATTTGGCAGTTACCGAACCTGAACCGGACCC

AAAAAGCTGCGTTTATTGGCAGCTTGCAAGACGACCCGTCACAGAGCGCC

AACCTGCTGGCCGAAGCGAAGAAGCTGAATGATGCGCAAGCACCCAAA

2. Bivalent HER3 Affibody (64 Amino Acid Linker):

Protein:

AHHHHHHVVDNKFNKERYLAYYEIWQLPNLNRTQKAAFIGSLQDDPSQSAN

LLAEAKKLNDAQAPKGGASGAGGSEGGGSEGGTSGATASGAGGSEGGGSEG

GTSGATASGAGGSEGGGSEGGTSGATGGVDNKFNKERYLAYYEIWQLPNLN

RTQKAAFIGSLQDDPSQSANLLAEAKKLNDAQAPK

DNA:

GCACATCACCACCACCATCACGTGGTCGATAACAAATTCAACAAAGAACG

CTACTTAGCATATTACGAGATTTGGCAGTTACCGAACCTGAACCGGACCC

AAAAAGCTGCGTTTATTGGCAGCTTGCAAGACGACCCGTCACAGAGCGCC

AACCTGCTGGCCGAAGCGAAGAAGCTGAATGATGCGCAAGCACCCAAAG

GCGGTGCCTCGGGCGCAGGGGGTAGCGAAGGCGGGGGCTCCGAAGGTGG

CACCTCGGGAGCCACCGCATCAGGGGCAGGGGGCAGCGAAGGCGGCGGT
TCGGAAGGGGGTACGTCAGGCGCGACCGCATCTGGGGCGGGTGGGAGCG
AAGGCGGAGGGTCCGAGGGTGGCACATCAGGCGCTACCGGTGGTGTAGA
CAACAAATTTAACAAAGAGCGTTACCTGGCCTATTACGAAATTTGGCAAC
TGCCGAATCTGAACCGGACGCAGAAAGCTGCTTTCATTGGCAGCCTGCAG
GATGACCCAAGCCAGTCGGCGAATCTTCTGGCTGAAGCGAAAAAGCTCA
ACGATGCACAAGCCCCTAAA

3. Bivalent HER3 Affibody (GGG Linker):

Protein:

AHHHHHHVVDNKFNKERYLAYYEIWQLPNLNRTQKAAFIGSLQDDPSQSAN
LLAEAKKLNDAQAPKGGGVDNKFNKERYLAYYEIWQLPNLNRTQKAAFIGS
LQDDPSQSANLLAEAKKLNDAQAPK

DNA:

GCACATCACCACCACCATCACGTGGTCGATAACAAATTCAACAAAGAACG
CTACTTAGCATATTACGAGATTTGGCAGTTACCGAACCTGAACCGGACCC
AAAAAGCTGCGTTTATTGGCAGCTTGCAAGACGACCCGTCACAGAGCGCC
AACCTGCTGGCCGAAGCGAAGAAGCTGAATGATGCGCAAGCACCCAAAG
GCGGTGGTGTAGACAACAAATTTAACAAAGAGCGTTACCTGGCCTATTAC
GAAATTTGGCAACTGCCGAATCTGAACCGGACGCAGAAAGCTGCTTTCAT
TGGCAGCCTGCAGGATGACCCAAGCCAGTCGGCGAATCTTCTGGCTGAAG
CGAAAAAGCTCAACGATGCACAAGCCCCTAAA

4. Hexavalent Linear

Protein:

AHHHHHHVVDNKFNKERYLAYYEIWQLPNLNRTQKAAFIGSLQDDPSQSAN

LLAEAKKLNDAQAPKGGGVDNKFNKERYLAYYEIWQLPNLNRTQKAAFIGS

LQDDPSQSANLLAEAKKLNDAQAPKGGGVDNKFNKERYLAYYEIWQLPNLN

RTQKAAFIGSLQDDPSQSANLLAEAKKLNDAQAPKGGGVDNKFNKERYLAY

YEIWQLPNLNRTQKAAFIGSLQDDPSQSANLLAEAKKLNDAQAPKGGGVDN

KFNKERYLAYYEIWQLPNLNRTQKAAFIGSLQDDPSQSANLLAEAKKLNDAQ

APKGGGVDNKFNKERYLAYYEIWQLPNLNRTQKAAFIGSLQDDPSQSANLL

AEAKKLNDAQAPK

DNA:

GCACATCACCACCACCATCACGTGGTCGATAACAAATTCAACAAAGAACG

CTACTTAGCATATTACGAGATTTGGCAGTTACCGAACCTGAACCGGACCC

AAAAAGCTGCGTTTATTGGCAGCTTGCAAGACGACCCGTCACAGAGCGCC

AACCTGCTGGCCGAAGCGAAGAAGCTGAATGATGCGCAAGCACCCAAAG

GCGGTGGTGTAGACAACAAATTTAACAAAGAGCGTTACCTGGCCTATTAC

GAAATTTGGCAACTGCCGAATCTGAACCGGACGCAGAAAGCTGCTTTCAT

TGGCAGCCTGCAGGATGACCCAAGCCAGTCGGCGAATCTTCTGGCTGAAG

CGAAAAAGCTCAACGATGCACAAGCCCCTAAAGGCGGTGGTGTCGATAA

CAAATTCAACAAAGAACGCTACTTAGCATATTACGAGATTTGGCAGTTAC

CGAACCTGAACCGGACCCAAAAAGCTGCGTTTATTGGCAGCTTGCAAGAC

GACCCGTCACAGAGCGCCAACCTGCTGGCCGAAGCGAAGAAGCTGAATG

ATGCGCAAGCACCCAAAGGCGGTGGTGTAGACAACAAATTTAACAAAGA

GCGTTACCTGGCCTATTACGAAATTTGGCAACTGCCGAATCTGAACCGGA

CGCAGAAAGCTGCTTTCATTGGCAGCCTGCAGGATGACCCAAGCCAGTCG

GCGAATCTTCTGGCTGAAGCGAAAAAGCTCAACGATGCACAAGCCCCTAA

AGGCGGTGGTGTCGATAACAAATTCAACAAAGAACGCTACTTAGCATATT

ACGAGATTTGGCAGTTACCGAACCTGAACCGGACCCAAAAAGCTGCGTTT

ATTGGCAGCTTGCAAGACGACCCGTCACAGAGCGCCAACCTGCTGGCCGA

AGCGAAGAAGCTGAATGATGCGCAAGCACCCAAAGGCGGTGGTGTAGAC

AACAAATTTAACAAAGAGCGTTACCTGGCCTATTACGAAATTTGGCAACT

GCCGAATCTGAACCGGACGCAGAAAGCTGCTTTCATTGGCAGCCTGCAGG

ATGACCCAAGCCAGTCGGCGAATCTTCTGGCTGAAGCGAAAAAGCTCAAC

GATGCACAAGCCCCTAAA

5. Monovalent EGFR Affibody:

Protein:

AHHHHHHGGVDNKFNKEMWAAWEEIRNLPNLNGWQMTAFIASLVDDPSQS

ANLLAEAKKLNDAQAPK

DNA:

GCACATCACCACCACCATCACGGTGGTGTGGATAACAAATTTAACAAAGA

GATGTGGGCGGCATGGGAAGAGATCCGTAATTTGCCTAACCTGAATGGCT

GGCAAATGACCGCGTTTATCGCTAGTTTGGTTGATGACCCGAGTCAATCG

GCGAACTTACTTGCAGAGGCGAAGAAATTAAACGACGCGCAGGCTCCGA

AA

6. Bispecific HER3-EGFR Bivalent Affibody (64 AA Linker):

Protein:

AHHHHHHVVDNKFNKERYLAYYEIWQLPNLNRTQKAAFIGSLQDDPSQSAN

LLAEAKKLNDAQAPKGGASGAGGSEGGGSEGGTSGATASGAGGSEGGGSEG

GTSGATASGAGGSEGGGSEGGTSGATGGVDNKFNKEMWAAWEEIRNLPNL

NGWQMTAFIASLVDDPSQSANLLAEAKKLNDAQAPK

DNA:

GCACATCACCACCACCATCACGTGGTCGATAACAAATTCAACAAAGAACG

CTACTTAGCATATTACGAGATTTGGCAGTTACCGAACCTGAACCGGACCC

AAAAAGCTGCGTTTATTGGCAGCTTGCAAGACGACCCGTCACAGAGCGCC

AACCTGCTGGCCGAAGCGAAGAAGCTGAATGATGCGCAAGCACCCAAAG

GCGGTGCCTCGGGCGCAGGGGGTAGCGAAGGCGGGGGCTCCGAAGGTGG

CACCTCGGGAGCCACCGCATCAGGGGCAGGGGGCAGCGAAGGCGGCGGT

TCGGAAGGGGGTACGTCAGGCGCGACCGCATCTGGGGCGGGTGGGAGCG

AAGGCGGAGGGTCCGAGGGTGGCACATCAGGCGCTACCGGTGGTGTGGA

TAACAAATTTAACAAAGAGATGTGGGCGGCATGGGAAGAGATCCGTAAT

TTGCCTAACCTGAATGGCTGGCAAATGACCGCGTTTATCGCTAGTTTGGTT

GATGACCCGAGTCAATCGGCGAACTTACTTGCAGAGGCGAAGAAATTAA

ACGACGCGCAGGCTCCGAAA

7. Bispecific HER3-EGFR Bivalent Affibody (GGG Linker):

Protein:

AHHHHHHVVDNKFNKERYLAYYEIWQLPNLNRTQKAAFIGSLQDDPSQSAN

LLAEAKKLNDAQAPKGGGVDNKFNKEMWAAWEEIRNLPNLNGWQMTAFIA

SLVDDPSQSANLLAEAKKLNDAQAPK

DNA:

GCACATCACCACCACCATCACGTGGTCGATAACAAATTCAACAAAGAACG

CTACTTAGCATATTACGAGATTTGGCAGTTACCGAACCTGAACCGGACCC

AAAAAGCTGCGTTTATTGGCAGCTTGCAAGACGACCCGTCACAGAGCGCC

AACCTGCTGGCCGAAGCGAAGAAGCTGAATGATGCGCAAGCACCCAAAG

GCGGTGGTGTGGATAACAAATTTAACAAAGAGATGTGGGCGGCATGGGA

AGAGATCCGTAATTTGCCTAACCTGAATGGCTGGCAAATGACCGCGTTTA

TCGCTAGTTTGGTTGATGACCCGAGTCAATCGGCGAACTTACTTGCAGAG

GCGAAGAAATTAAACGACGCGCAGGCTCCGAAA

8. Bivalent EGFR Affibody (64 AA Linker):

Protein:

AHHHHHHVVDNKFNKEMWAAWEEIRNLPNLNGWQMTAFIASLVDDPSQSA

NLLAEAKKLNDAQAPKGGASGAGGSEGGGSEGGTSGATASGAGGSEGGGSE

GGTSGATASGAGGSEGGGSEGGTSGATGGVDNKFNKEMWAAWEEIRNLPN

LNGWQMTAFIASLVDDPSQSANLLAEAKKL

DNA:

GCACATCACCACCACCATCACGTGGTGGATAACAAATTTAACAAAGAGAT

GTGGGCGGCATGGGAAGAGATCCGTAATTTGCCTAACCTGAATGGCTGGC

AAATGACCGCGTTTATCGCTAGTTTGGTTGATGACCCGAGTCAATCGGCG

AACTTACTTGCAGAGGCGAAGAAATTAAACGACGCGCAGGCTCCGAAAG
GCGGTGCCTCGGGCGCAGGGGGTAGCGAAGGCGGGGGCTCCGAAGGTGG
CACCTCGGGAGCCACCGCATCAGGGGCAGGGGGCAGCGAAGGCGGCGGT
TCGGAAGGGGGTACGTCAGGCGCGACCGCATCTGGGGCGGGTGGGAGCG
AAGGCGGAGGGTCCGAGGGTGGCACATCAGGCGCTACCGGTGGTGTGGA
TAACAAATTTAACAAAGAGATGTGGGCGGCATGGGAAGAGATCCGTAAT
TTGCCTAACCTGAATGGCTGGCAAATGACCGCGTTTATCGCTAGTTTGGTT
GATGACCCGAGTCAATCGGCGAACTTACTTGCAGAGGCGAAGAAATTAA
A

9. Bivalent EGFR Affibody (GGG Linker):

Protein:

AHHHHHHVVDNKFNKEMWAAWEEIRNLPNLNGWQMTAFIASLVDDPSQSA
NLLAEAKKLNDAQAPKGGGVDNKFNKEMWAAWEEIRNLPNLNGWQMTAFI
ASLVDDPSQSANLLAEAKKLNDAQAPK

DNA:

GGCACATCACCACCACCATCACGTGGTGGATAACAAATTTAACAAAGAG
ATGTGGGCGGCATGGGAAGAGATCCGTAATTTGCCTAACCTGAATGGCTG
GCAAATGACCGCGTTTATCGCTAGTTTGGTTGATGACCCGAGTCAATCGG
CGAACTTACTTGCAGAGGCGAAGAAATTAAACGACGCGCAGGCTCCGAA
AGGCGGTGGTGTGGATAACAAATTTAACAAAGAGATGTGGGCGGCATGG
GAAGAGATCCGTAATTTGCCTAACCTGAATGGCTGGCAAATGACCGCGTT
TATCGCTAGTTTGGTTGATGACCCGAGTCAATCGGCGAACTTACTTGCAG
AGGCGAAGAAATTAAACGACGCGCAGGCTCCGAAA

10. Bivalent Affibody HER3-Zwt (64 AA Linker)

Protein:

AHHHHHHVVDNKFNKERYLAYYEIWQLPNLNRTQKAAFIGSLQDDPSQSAN

LLAEAKKLNDAQAPKGGASGAGGSEGGGSEGGTSGATASGAGGSEGGGSEG

GTSGATASGAGGSEGGGSEGGTSGATGGVDNKFNKEQQNAFYEILHLPNLNE

EQRNAFIQSLKDDPSQSANLLAEAKKLNDAQAPK

DNA:

GCACATCACCACCACCATCACGTGGTCGATAACAAATTCAACAAAGAACG

CTACTTAGCATATTACGAGATTTGGCAGTTACCGAACCTGAACCGGACCC

AAAAAGCTGCGTTTATTGGCAGCTTGCAAGACGACCCGTCACAGAGCGCC

AACCTGCTGGCCGAAGCGAAGAAGCTGAATGATGCGCAAGCACCCAAAG

GCGGTGCCTCGGGCGCAGGGGGTAGCGAAGGCGGGGGCTCCGAAGGTGG

CACCTCGGGAGCCACCGCATCAGGGGCAGGGGGCAGCGAAGGCGGCGGT

TCGGAAGGGGGTACGTCAGGCGCGACCGCATCTGGGGCGGGTGGGAGCG

AAGGCGGAGGGTCCGAGGGTGGCACATCAGGCGCTACCGGTGGTGTAGA

CAACAAATTTAACAAAGAGCAGCAGAACGCTTTCTATGAAATACTGCACT

TACCGAACCTGAACGAGGAGCAGCGGAATGCTTTTATACAGTCGTTGAAG

GATGACCCAAGCCAGTCGGCGAATCTTCTGGCTGAAGCGAAAAAGCTCA

ACGATGCACAAGCCCCTAAA

11. Monovalent HER3-ABD

Protein:

AHHHHHHVVDNKFNKERYLAYYEIWQLPNLNRTQKAAFIGSLQDDPSQSAN

LLAEAKKLNDAQAPKGGGLAEAKVLANRELDKYGVSDFYKRLINKAKTVEG

VEALKLHILAALP

DNA:

GCACATCACCACCACCATCACGTGGTCGATAACAAATTCAACAAAGAACG

CTACTTAGCATATTACGAGATTTGGCAGTTACCGAACCTGAACCGGACCC

AAAAAGCTGCGTTTATTGGCAGCTTGCAAGACGACCCGTCACAGAGCGCC

AACCTGCTGGCCGAAGCGAAGAAGCTGAATGATGCGCAAGCACCCAAAG

GAGGGGGACTTGCAGAAGCCAAAGTCTTAGCGAATAGAGAACTGGATAA

ATATGGCGTGTCCGACTTCTATAAGCGTCTGATAAATAAAGCGAAGACCG

TTGAGGGAGTTGAAGCCCTGAAGTTGCATATTTTGGCTGCCCTTCCA

12. Monovalent ABD-HER3

Protein:

AHHHHHHGGGLAEAKVLANRELDKYGVSDFYKRLINKAKTVEGVEALKLHI

LAALPGGGVDNKFNKERYLAYYEIWQLPNLNRTQKAAFIGSLQDDPSQSANL

LAEAKKLNDAQAPK

DNA:

GCACATCACCACCACCATCACGGCGGTGGTCTTGCAGAAGCCAAAGTCTT

AGCGAATAGAGAACTGGATAAATATGGCGTGTCCGACTTCTATAAGCGTC

TGATAAATAAAGCGAAGACCGTTGAGGGAGTTGAAGCCCTGAAGTTGCAT

ATTTTGGCTGCCCTTCCAGGAGGGGGAGTCGATAACAAATTCAACAAAGA

ACGCTACTTAGCATATTACGAGATTTGGCAGTTACCGAACCTGAACCGGA

CCCAAAAAGCTGCGTTTATTGGCAGCTTGCAAGACGACCCGTCACAGAGC

GCCAACCTGCTGGCCGAAGCGAAGAAGCTGAATGATGCGCAAGCACCCA

AA

13. Bivalent HER3-HER3-ABD

Protein:

AHHHHHHVVDNKFNKERYLAYYEIWQLPNLNRTQKAAFIGSLQDDPSQSAN

LLAEAKKLNDAQAPKGGGVDNKFNKERYLAYYEIWQLPNLNRTQKAAFIGS

LQDDPSQSANLLAEAKKLNDAQAPKGGGLAEAKVLANRELDKYGVSDFYK

RLINKAKTVEGVEALKLHILAALP

DNA:

GCACATCACCACCACCATCACGTGGTCGATAACAAATTCAACAAAGAACG

CTACTTAGCATATTACGAGATTTGGCAGTTACCGAACCTGAACCGGACCC

AAAAAGCTGCGTTTATTGGCAGCTTGCAAGACGACCCGTCACAGAGCGCC

AACCTGCTGGCCGAAGCGAAGAAGCTGAATGATGCGCAAGCACCCAAAG

GCGGTGGTGTAGACAACAAATTTAACAAAGAGCGTTACCTGGCCTATTAC

GAAATTTGGCAACTGCCGAATCTGAACCGGACGCAGAAAGCTGCTTTCAT

TGGCAGCCTGCAGGATGACCCAAGCCAGTCGGCGAATCTTCTGGCTGAAG

CGAAAAAGCTCAACGATGCACAAGCCCCTAAAGGAGGGGGACTTGCAGA

AGCCAAAGTCTTAGCGAATAGAGAACTGGATAAATATGGCGTGTCCGACT

TCTATAAGCGTCTGATAAATAAAGCGAAGACCGTTGAGGGAGTTGAAGCC

CTGAAGTTGCATATTTTGGCTGCCCTTCCA

14. Bivalent ABD-HER3-HER3

Protein:

AHHHHHHGGGLAEAKVLANRELDKYGVSDFYKRLINKAKTVEGVEALKLHI

LAALPGGGVDNKFNKERYLAYYEIWQLPNLNRTQKAAFIGSLQDDPSQSANL

LAEAKKLNDAQAPKGGGVDNKFNKERYLAYYEIWQLPNLNRTQKAAFIGSL

QDDPSQSANLLAEAKKLNDAQAPK

DNA:

GCACATCACCACCACCATCACGGCGGTGGTCTTGCAGAAGCCAAAGTCTT

AGCGAATAGAGAACTGGATAAATATGGCGTGTCCGACTTCTATAAGCGTC

TGATAAATAAAGCGAAGACCGTTGAGGGAGTTGAAGCCCTGAAGTTGCAT

ATTTTGGCTGCCCTTCCAGGAGGGGGAGTCGATAACAAATTCAACAAAGA

ACGCTACTTAGCATATTACGAGATTTGGCAGTTACCGAACCTGAACCGGA

CCCAAAAAGCTGCGTTTATTGGCAGCTTGCAAGACGACCCGTCACAGAGC

GCCAACCTGCTGGCCGAAGCGAAGAAGCTGAATGATGCGCAAGCACCCA

AAGGCGGTGGTGTAGACAACAAATTTAACAAAGAGCGTTACCTGGCCTAT

TACGAAATTTGGCAACTGCCGAATCTGAACCGGACGCAGAAAGCTGCTTT

CATTGGCAGCCTGCAGGATGACCCAAGCCAGTCGGCGAATCTTCTGGCTG

AAGCGAAAAAGCTCAACGATGCACAAGCCCCTAAA

15. Bivalent HER3-ABD-HER3

Protein:

AHHHHHHVVDNKFNKERYLAYYEIWQLPNLNRTQKAAFIGSLQDDPSQSAN

LLAEAKKLNDAQAPKGGGLAEAKVLANRELDKYGVSDFYKRLINKAKTVEG

VEALKLHILAALPGGGVDNKFNKERYLAYYEIWQLPNLNRTQKAAFIGSLQD

DPSQSANLLAEAKKLNDAQAPK

DNA:

GCACATCACCACCACCATCACGTGGTCGATAACAAATTCAACAAAGAACG

CTACTTAGCATATTACGAGATTTGGCAGTTACCGAACCTGAACCGGACCC

AAAAAGCTGCGTTTATTGGCAGCTTGCAAGACGACCCGTCACAGAGCGCC

AACCTGCTGGCCGAAGCGAAGAAGCTGAATGATGCGCAAGCACCCAAAG

GCGGTGGTCTTGCAGAAGCCAAAGTCTTAGCGAATAGAGAACTGGATAA

ATATGGCGTGTCCGACTTCTATAAGCGTCTGATAAATAAAGCGAAGACCG

TTGAGGGAGTTGAAGCCCTGAAGTTGCATATTTTGGCTGCCCTTCCAGGA

GGGGGAGTAGACAACAAATTTAACAAAGAGCGTTACCTGGCCTATTACGA

AATTTGGCAACTGCCGAATCTGAACCGGACGCAGAAAGCTGCTTTCATTG

GCAGCCTGCAGGATGACCCAAGCCAGTCGGCGAATCTTCTGGCTGAAGCG

AAAAAGCTCAACGATGCACAAGCCCCTAAA

Bibliography

[1] Cancer Facts & Figures 2016 | American Cancer Society, n.d.

[2] U.S. cancer survival rates improving | Reuters, (n.d.). http://www.reuters.com/article/us-cancer-survival-idUSKBN0NE2KD20150423 (accessed March 13, 2016).

[3] A.C. Society, Cancer facts & figures, 2008.

[4] Types of Cancer Treatment | American Cancer Society, (n.d.). http://www.cancer.org/treatment/treatmentsandsideeffects/treatmenttypes/ (accessed March 12, 2016).

[5] Types of Cancer Treatment - National Cancer Institute, (n.d.). http://www.cancer.gov/about-cancer/treatment/types (accessed March 12, 2016).

[6] Biomarker Testing, (n.d.). http://pathology.jhu.edu/breast/biomarker-testing.php (accessed March 13, 2016).

[7] Genentech: The Tissue Is Still The Issue, (n.d.). http://www.gene.com/stories/the-tissue-is-still-the-issue (accessed March 13, 2016).

[8] H.-S. Cho, D.J. Leahy, Structure of the extracellular region of HER3 reveals an interdomain tether., Science. 297 (2002) 1330–3. doi:10.1126/science.1074611.

[9] N. Jiang, N. Saba, Z. Chen, Advances in targeting HER3 as an anticancer therapy, Chemother. Res. …. (2012).

[10] Y. Yarden, M.X. Sliwkowski, Untangling the ErbB signalling network., Nat. Rev. Mol. Cell Biol. 2 (2001) 127–37. doi:10.1038/35052073.

[11] I.H. Koumakpayi, J.-S. Diallo, C. Le Page, L. Lessard, M. Gleave, L.R. Bégin, A.-M. Mes-Masson, F. Saad, Expression and nuclear localization of ErbB3 in prostate cancer., Clin. Cancer Res. 12 (2006) 2730–7. doi:10.1158/1078-0432.CCR-05-2242.

[12] N. Tebbutt, M.W. Pedersen, T.G. Johns, Targeting the ERBB family in cancer: couples therapy., Nat. Rev. Cancer. 13 (2013) 663–73. doi:10.1038/nrc3559.

[13] S. Arena, G. Siravegna, B. Mussolin, J.D. Kearns, B.B. Wolf, S. Misale, L. Lazzari, A. Bertotti, L. Trusolino, A.A. Adjei, C. Montagut, F. Di Nicolantonio, R. Nering, A. Bardelli, MM-151 overcomes acquired resistance to cetuximab and panitumumab in colorectal cancers harboring EGFR extracellular domain mutations., Sci. Transl. Med. 8 (2016) 324ra14. doi:10.1126/scitranslmed.aad5640.

[14] D. Graus-Porta, R.R. Beerli, J.M. Daly, N.E. Hynes, ErbB-2, the preferred heterodimerization partner of all ErbB receptors, is a mediator of lateral signaling., EMBO J. 16 (1997) 1647–55. doi:10.1093/emboj/16.7.1647.

[15] R. Landgraf, D. Eisenberg, Heregulin Reverses the Oligomerization of HER3 †, Biochemistry. 39 (2000) 8503–8511. doi:10.1021/bi000953+.

[16] Q. Sheng, X. Liu, E. Fleming, K. Yuan, H. Piao, J. Chen, Z. Moustafa, R.K. Thomas, H. Greulich, A. Schinzel, S. Zaghlul, D. Batt, S. Ettenberg, M. Meyerson, B. Schoeberl, A.L. Kung, W.C. Hahn, R. Drapkin, D.M. Livingston, J.F. Liu, An activated ErbB3/NRG1 autocrine loop supports in

vivo proliferation in ovarian cancer cells., Cancer Cell. 17 (2010) 298–310. doi:10.1016/j.ccr.2009.12.047.
[17] A.P. Garner, C.U. Bialucha, E.R. Sprague, J.T. Garrett, Q. Sheng, S. Li, O. Sineshchekova, P. Saxena, C.R. Sutton, D. Chen, Y. Chen, H. Wang, J. Liang, R. Das, R. Mosher, J. Gu, A. Huang, N. Haubst, C. Zehetmeier, M. Haberl, W. Elis, C. Kunz, A.B. Heidt, K. Herlihy, J. Murtie, A. Schuller, C.L. Arteaga, W.R. Sellers, S.A. Ettenberg, An antibody that locks HER3 in the inactive conformation inhibits tumor growth driven by HER2 or neuregulin., Cancer Res. 73 (2013) 6024–35. doi:10.1158/0008-5472.CAN-13-1198.
[18] E. Singer, R. Landgraf, T. Horan, D. Slamon, D. Eisenberg, Identification of a heregulin binding site in HER3 extracellular domain., J. Biol. Chem. 276 (2001) 44266–74. doi:10.1074/jbc.M105428200.
[19] L. Aurisicchio, E. Marra, G. Roscilli, R. Mancini, G. Ciliberto, The promise of anti-ErbB3 monoclonals as new cancer therapeutics., Oncotarget. 3 (2012) 744–58. doi:10.18632/oncotarget.550.
[20] J. Baselga, S.M. Swain, Novel anticancer targets: revisiting ERBB2 and discovering ERBB3., Nat. Rev. Cancer. 9 (2009) 463–75. doi:10.1038/nrc2656.
[21] J.S. Poovassery, J.C. Kang, D. Kim, R.J. Ober, E.S. Ward, Antibody targeting of HER2/HER3 signaling overcomes heregulin-induced resistance to PI3K inhibition in prostate cancer., Int. J. Cancer. 137 (2015) 267–77. doi:10.1002/ijc.29378.
[22] D. Carrión-Salip, C. Panosa, J.A. Menendez, T. Puig, G. Oliveras, A. Pandiella, R. De Llorens, A. Massaguer, Androgen-independent prostate cancer cells circumvent EGFR inhibition by overexpression of alternative HER receptors and ligands, Int. J. Oncol. 41 (2012) 1128–1138.
[23] N. V Sergina, M. Rausch, D. Wang, J. Blair, B. Hann, K.M. Shokat, M.M. Moasser, Escape from HER-family tyrosine kinase inhibitor therapy by the kinase-inactive HER3., Nature. 445 (2007) 437–41. doi:10.1038/nature05474.
[24] L. Chen, B.A. Mooso, M.K. Jathal, A. Madhav, S.D. Johnson, E. van Spyk, M. Mikhailova, A. Zierenberg-Ripoll, L. Xue, R.L. Vinall, R.W. deVere White, P.M. Ghosh, Dual EGFR/HER2 inhibition sensitizes prostate cancer cells to androgen withdrawal by suppressing ErbB3., Clin. Cancer Res. 17 (2011) 6218–28. doi:10.1158/1078-0432.CCR-11-1548.
[25] A. Jain, E. Penuel, S. Mink, J. Schmidt, A. Hodge, K. Favero, C. Tindell, D.B. Agus, HER kinase axis receptor dimer partner switching occurs in response to EGFR tyrosine kinase inhibition despite failure to block cellular proliferation., Cancer Res. 70 (2010) 1989–99. doi:10.1158/0008-5472.CAN-09-3326.
[26] F. Musa, R. Schneider, Targeting the PI3K/AKT/mTOR pathway in ovarian cancer, Transl. Cancer Res. 4 (n.d.) 97–106.
[27] B. Cheaib, A. Auguste, A. Leary, The PI3K/Akt/mTOR pathway in ovarian cancer: therapeutic opportunities and challenges., Chin. J. Cancer. 34 (2015) 4–16. doi:10.5732/cjc.014.10289.
[28] R. Torka, K. Pénzes, S. Gusenbauer, C. Baumann, I. Szabadkai, L. Őrfi, G. Kéri, A. Ullrich, Activation of HER3 interferes with antitumor effects of Axl receptor tyrosine kinase inhibitors: suggestion of combination therapy.,

Neoplasia. 16 (2014) 301–18. doi:10.1016/j.neo.2014.03.009.
[29] G.M. Krishnamurthy, V. M., Estroff, L. A., & Whitesides, Multivalency in ligand design, 2006.
[30] C. Liu, J. Cochran, Engineering Multivalent and Multispecific Protein Therapeutics, Eng. Transl. Med. (2014).
[31] C. Fasting, C.A. Schalley, M. Weber, O. Seitz, S. Hecht, B. Koksch, J. Dernedde, C. Graf, E.-W. Knapp, R. Haag, Multivalency as a chemical organization and action principle., Angew. Chem. Int. Ed. Engl. 51 (2012) 10472–98. doi:10.1002/anie.201201114.
[32] W. Yan, Binding time--not just affinity--gains stature in drug design., Nat. Med. 21 (2015) 545. doi:10.1038/nm0615-545.
[33] G. Vauquelin, S.J. Charlton, Exploring avidity: understanding the potential gains in functional affinity and target residence time of bivalent and heterobivalent ligands., Br. J. Pharmacol. 168 (2013) 1771–85. doi:10.1111/bph.12106.
[34] ClinicalTrials.gov, (n.d.). https://clinicaltrials.gov/ (accessed March 11, 2016).
[35] Merrimack Pharmaceuticals Announces Initiation of a Phase 2 Front-line Clinical Trial of... -- CAMBRIDGE, Mass., May 5, 2015 /PRNewswire/ --, (n.d.). http://www.prnewswire.com/news-releases/merrimack-pharmaceuticals-announces-initiation-of-a-phase-2-front-line-clinical-trial-of-mm-141-in-biomarker-selected-patients-with-metastatic-pancreatic-cancer-300076816.html (accessed March 11, 2016).
[36] V.M. Krishnamurthy, V. Semetey, P.J. Bracher, N. Shen, G.M. Whitesides, Dependence of effective molarity on linker length for an intramolecular protein-ligand system., J. Am. Chem. Soc. 129 (2007) 1312–20. doi:10.1021/ja066780e.
[37] S. Liese, R.R. Netz, Influence of length and flexibility of spacers on the binding affinity of divalent ligands., Beilstein J. Org. Chem. 11 (2015) 804–16. doi:10.3762/bjoc.11.90.
[38] G.P. Adams, R. Schier, A.M. McCall, H.H. Simmons, E.M. Horak, R.K. Alpaugh, J.D. Marks, L.M. Weiner, High Affinity Restricts the Localization and Tumor Penetration of Single-Chain Fv Antibody Molecules, Cancer Res. 61 (2001) 4750–4755.
[39] A.M. Scott, J.D. Wolchok, L.J. Old, Antibody therapy of cancer., Nat. Rev. Cancer. 12 (2012) 278–87. doi:10.1038/nrc3236.
[40] P. Wu, T.E. Nielsen, M.H. Clausen, FDA-approved small-molecule kinase inhibitors., Trends Pharmacol. Sci. 36 (2015) 422–439. doi:10.1016/j.tips.2015.04.005.
[41] B.S. Jaiswal, N.M. Kljavin, E.W. Stawiski, E. Chan, C. Parikh, S. Durinck, S. Chaudhuri, K. Pujara, J. Guillory, K.A. Edgar, V. Janakiraman, R.-P. Scholz, K.K. Bowman, M. Lorenzo, H. Li, J. Wu, W. Yuan, B.A. Peters, Z. Kan, J. Stinson, M. Mak, Z. Modrusan, C. Eigenbrot, R. Firestein, H.M. Stern, K. Rajalingam, G. Schaefer, M.A. Merchant, M.X. Sliwkowski, F.J. de Sauvage, S. Seshagiri, Oncogenic ERBB3 mutations in human cancers., Cancer Cell. 23 (2013) 603–17. doi:10.1016/j.ccr.2013.04.012.
[42] Overview of Targeted Therapies for Cancer - My Cancer Genome, (n.d.).

https://www.mycancergenome.org/content/molecular-medicine/overview-of-targeted-therapies-for-cancer/ (accessed March 16, 2016).
[43] B. Schoeberl, A.C. Faber, D. Li, M.-C. Liang, K. Crosby, M. Onsum, O. Burenkova, E. Pace, Z. Walton, L. Nie, A. Fulgham, Y. Song, U.B. Nielsen, J.A. Engelman, K.-K. Wong, An ErbB3 antibody, MM-121, is active in cancers with ligand-dependent activation., Cancer Res. 70 (2010) 2485–94. doi:10.1158/0008-5472.CAN-09-3145.
[44] B. Schoeberl, E.A. Pace, J.B. Fitzgerald, B.D. Harms, L. Xu, L. Nie, B. Linggi, A. Kalra, V. Paragas, R. Bukhalid, V. Grantcharova, N. Kohli, K.A. West, M. Leszczyniecka, M.J. Feldhaus, A.J. Kudla, U.B. Nielsen, Therapeutically targeting ErbB3: a key node in ligand-induced activation of the ErbB receptor-PI3K axis., Sci. Signal. 2 (2009) ra31. doi:10.1126/scisignal.2000352.
[45] M. Soler, F. Mancini, O. Meca-Cortés, L. Sánchez-Cid, N. Rubio, S. López-Fernández, J.J. Lozano, J. Blanco, P.L. Fernández, T.M. Thomson, HER3 is required for the maintenance of neuregulin-dependent and -independent attributes of malignant progression in prostate cancer cells., Int. J. Cancer. 125 (2009) 2565–75. doi:10.1002/ijc.24651.
[46] N. Kronqvist, M. Malm, L. Göstring, E. Gunneriusson, M. Nilsson, I. Höidén Guthenberg, L. Gedda, F.Y. Frejd, S. Ståhl, J. Löfblom, Combining phage and staphylococcal surface display for generation of ErbB3-specific Affibody molecules., Protein Eng. Des. Sel. 24 (2011) 385–96. doi:10.1093/protein/gzq118.
[47] P.K. Foreman, M. Gore, P.A. Kobel, L. Xu, H. Yee, C. Hannum, H. Ho, S.M. Wang, H. V Tran, M. Horowitz, L. Horowitz, R.R. Bhatt, ErbB3 inhibitory surrobodies inhibit tumor cell proliferation in vitro and in vivo., Mol. Cancer Ther. 11 (2012) 1411–20. doi:10.1158/1535-7163.MCT-12-0068.
[48] J. Nilvebrant, M. Astrand, J. Löfblom, S. Hober, Development and characterization of small bispecific albumin-binding domains with high affinity for ErbB3., Cell. Mol. Life Sci. 70 (2013) 3973–85. doi:10.1007/s00018-013-1370-9.
[49] M. Malm, N. Kronqvist, H. Lindberg, L. Gudmundsdotter, T. Bass, F.Y. Frejd, I. Höidén-Guthenberg, Z. Varasteh, A. Orlova, V. Tolmachev, S. Ståhl, J. Löfblom, Inhibiting HER3-mediated tumor cell growth with affibody molecules engineered to low picomolar affinity by position-directed error-prone PCR-like diversification., PLoS One. 8 (2013) e62791. doi:10.1371/journal.pone.0062791.
[50] L. Göstring, M. Malm, I. Höidén-Guthenberg, F.Y. Frejd, S. Ståhl, J. Löfblom, L. Gedda, Cellular effects of HER3-specific affibody molecules., PLoS One. 7 (2012) e40023. doi:10.1371/journal.pone.0040023.
[51] Merrimack, (n.d.). http://www.merrimack.com/ (accessed March 11, 2016).
[52] C. Mirschberger, C.B. Schiller, M. Schräml, N. Dimoudis, T. Friess, C.A. Gerdes, U. Reiff, V. Lifke, G. Hoelzlwimmer, I. Kolm, K.-P. Hopfner, G. Niederfellner, B. Bossenmaier, RG7116, a therapeutic antibody that binds the inactive HER3 receptor and is optimized for immune effector activation., Cancer Res. 73 (2013) 5183–94. doi:10.1158/0008-5472.CAN-13-0099.
[53] G. Meneses-Lorente, T. Friess, I. Kolm, G. Hölzlwimmer, S. Bader, C. Meille,

M. Thomas, B. Bossenmaier, Preclinical pharmacokinetics, pharmacodynamics, and efficacy of RG7116: a novel humanized, glycoengineered anti-HER3 antibody., Cancer Chemother. Pharmacol. 75 (2015) 837–50. doi:10.1007/s00280-015-2697-8.

[54] Merrimack's MM-111 Fails in Gastric Cancer, Securing Roche/Genentech's Monopoly in the HER2-Positive Space | GlobalData Healthcare, (n.d.). http://healthcare.globaldata.com/resources/expert-insights/pharmaceuticals/merrimacks-mm111-fails-in-gastric-cancer-securing-rochegenentechs-monopoly-in-the-her2positive-space (accessed March 11, 2016).

[55] C. McDonagh, A. Huhalov, B. Harms, Antitumor activity of a novel bispecific antibody that targets the ErbB2/ErbB3 oncogenic unit and inhibits heregulin-induced activation of ErbB3, Mol. Cancer …. (2012).

[56] J.B. Fitzgerald, B.W. Johnson, J. Baum, S. Adams, S. Iadevaia, J. Tang, V. Rimkunas, L. Xu, N. Kohli, R. Rennard, M. Razlog, Y. Jiao, B.D. Harms, K.J. Olivier, B. Schoeberl, U.B. Nielsen, A.A. Lugovskoy, MM-141, an IGF-IR- and ErbB3-directed bispecific antibody, overcomes network adaptations that limit activity of IGF-IR inhibitors., Mol. Cancer Ther. 13 (2014) 410–25. doi:10.1158/1535-7163.MCT-13-0255.

[57] R. Vazquez-Lombardi, T.G. Phan, C. Zimmermann, D. Lowe, L. Jermutus, D. Christ, Challenges and opportunities for non-antibody scaffold drugs., Drug Discov. Today. 20 (2015) 1271–1283. doi:10.1016/j.drudis.2015.09.004.

[58] J. Löfblom, J. Feldwisch, V. Tolmachev, J. Carlsson, S. Ståhl, F.Y. Frejd, Affibody molecules: engineered proteins for therapeutic, diagnostic and biotechnological applications., FEBS Lett. 584 (2010) 2670–80. doi:10.1016/j.febslet.2010.04.014.

[59] D.L. Nielsen, I. Kümler, J.A.E. Palshof, M. Andersson, Efficacy of HER2-targeted therapy in metastatic breast cancer. Monoclonal antibodies and tyrosine kinase inhibitors., Breast. 22 (2013) 1–12. doi:10.1016/j.breast.2012.09.008.

[60] A.L. Nelson, Antibody fragments: hope and hype., MAbs. 2 77–83.

[61] N. Moran, Boehringer splashes out on bispecific antibody platforms., Nat. Biotechnol. 29 (2011) 5–6. doi:10.1038/nbt0111-5.

[62] M. Malm, T. Bass, L. Gudmundsdotter, M. Lord, F.Y. Frejd, S. Ståhl, J. Löfblom, Engineering of a bispecific affibody molecule towards HER2 and HER3 by addition of an albumin-binding domain allows for affinity purification and in vivo half-life extension., Biotechnol. J. 9 (2014) 1215–22. doi:10.1002/biot.201400009.

[63] A.L. Nelson, J.M. Reichert, Development trends for therapeutic antibody fragments., Nat. Biotechnol. 27 (2009) 331–7. doi:10.1038/nbt0409-331.

[64] P. Caliceti, Pharmacokinetic and biodistribution properties of poly(ethylene glycol)–protein conjugates, Adv. Drug Deliv. Rev. 55 (2003) 1261–1277. doi:10.1016/S0169-409X(03)00108-X.

[65] C.-H.B. Chen, G.A. Chernis, V.Q. Hoang, R. Landgraf, Inhibition of heregulin signaling by an aptamer that preferentially binds to the oligomeric form of human epidermal growth factor receptor-3., Proc. Natl. Acad. Sci. U. S. A. 100

(2003) 9226–31. doi:10.1073/pnas.1332660100.
[66] A.D. Keefe, S. Pai, A. Ellington, Aptamers as therapeutics., Nat. Rev. Drug Discov. 9 (2010) 537–50. doi:10.1038/nrd3141.
[67] E. Park, R. Baron, R. Landgraf, Higher-order association states of cellular ERBB3 probed with photo-cross-linkable aptamers., Biochemistry. 47 (2008) 11992–2005. doi:10.1021/bi8004208.
[68] S.M. Jay, E. Kurtagic, L.M. Alvarez, S. de Picciotto, E. Sanchez, J.F. Hawkins, R.N. Prince, Y. Guerrero, C.L. Treasure, R.T. Lee, L.G. Griffith, Engineered bivalent ligands to bias ErbB receptor-mediated signaling and phenotypes., J. Biol. Chem. 286 (2011) 27729–40. doi:10.1074/jbc.M111.221093.
[69] S.M. Jay, A.C. Murthy, J.F. Hawkins, J.R. Wortzel, M.L. Steinhauser, L.M. Alvarez, J. Gannon, C.A. Macrae, L.G. Griffith, R.T. Lee, An engineered bivalent neuregulin protects against doxorubicin-induced cardiotoxicity with reduced proneoplastic potential., Circulation. 128 (2013) 152–61. doi:10.1161/CIRCULATIONAHA.113.002203.
[70] D.J. Katzmann, G. Odorizzi, S.D. Emr, Receptor downregulation and multivesicular-body sorting., Nat. Rev. Mol. Cell Biol. 3 (2002) 893–905. doi:10.1038/nrm973.
[71] J.W. D'Souza, S. Reddy, L.E. Goldsmith, I. Shchaveleva, J.D. Marks, S. Litwin, M.K. Robinson, Combining anti-ERBB3 antibodies specific for domain I and domain III enhances the anti-tumor activity over the individual monoclonal antibodies., PLoS One. 9 (2014) e112376. doi:10.1371/journal.pone.0112376.
[72] L. Fattore, D. Malpicci, E. Marra, F. Belleudi, A. Noto, C. De Vitis, M.E. Pisanu, P. Coluccia, R. Camerlingo, G. Roscilli, A. Ribas, A. Di Napoli, M.R. Torrisi, L. Aurisicchio, P.A. Ascierto, R. Mancini, G. Ciliberto, Combination of antibodies directed against different ErbB3 surface epitopes prevents the establishment of resistance to BRAF/MEK inhibitors in melanoma., Oncotarget. 6 (2015) 24823–41. doi:10.18632/oncotarget.4485.
[73] F. Shi, S.E. Telesco, Y. Liu, R. Radhakrishnan, M.A. Lemmon, ErbB3/HER3 intracellular domain is competent to bind ATP and catalyze autophosphorylation., Proc. Natl. Acad. Sci. U. S. A. 107 (2010) 7692–7. doi:10.1073/pnas.1002753107.
[74] S.P. Soltoff, K.L. Carraway, S.A. Prigent, W.G. Gullick, L.C. Cantley, ErbB3 is involved in activation of phosphatidylinositol 3-kinase by epidermal growth factor., Mol. Cell. Biol. 14 (1994) 3550–3558. doi:10.1128/MCB.14.6.3550.
[75] S.A. Prigent, W.J. Gullick, Identification of c-erbB-3 binding sites for phosphatidylinositol 3'-kinase and SHC using an EGF receptor/c-erbB-3 chimera., EMBO J. 13 (1994) 2831–41.
[76] S.-Y. Hsieh, J.-R. He, C.-Y. Hsu, W.-J. Chen, R. Bera, K.-Y. Lin, T.-C. Shih, M.-C. Yu, Y.-J. Lin, C.-J. Chang, W.-H. Weng, S.-F. Huang, Neuregulin/erythroblastic leukemia viral oncogene homolog 3 autocrine loop contributes to invasion and early recurrence of human hepatoma., Hepatology. 53 (2011) 504–16. doi:10.1002/hep.24083.
[77] Q. Li, S. Ahmed, J.A. Loeb, Development of an autocrine neuregulin signaling loop with malignant transformation of human breast epithelial cells., Cancer

Res. 64 (2004) 7078–85. doi:10.1158/0008-5472.CAN-04-1152.
[78] R.M. Neve, K. Chin, J. Fridlyand, J. Yeh, F.L. Baehner, T. Fevr, L. Clark, N. Bayani, J.-P. Coppe, F. Tong, T. Speed, P.T. Spellman, S. DeVries, A. Lapuk, N.J. Wang, W.-L. Kuo, J.L. Stilwell, D. Pinkel, D.G. Albertson, F.M. Waldman, F. McCormick, R.B. Dickson, M.D. Johnson, M. Lippman, S. Ethier, A. Gazdar, J.W. Gray, A collection of breast cancer cell lines for the study of functionally distinct cancer subtypes, Cancer Cell. 10 (2006) 515–527. doi:10.1016/j.ccr.2006.10.008.
[79] J. Schardt, J. Oubaid, S. Williams, J. Howard, C. Aloimonos, M. Bookstaver, T. Lamichhane, S. Sokic, M. Liyasova, A. Hussain, S. Lipkowitz, S. Jay, Engineered Multivalency Enhances Affibody-Based HER3 Inhibition and Downregulation in Cancer Cells, Mol. Pharm. (2017).
[80] J. Nilvebrant, S. Hober, The albumin-binding domain as a scaffold for protein engineering., Comput. Struct. Biotechnol. J. 6 (2013) e201303009. doi:10.5936/csbj.201303009.
[81] M. Werle, A. Bernkop-Schnürch, Strategies to improve plasma half life time of peptide and protein drugs, Amino Acids. 30 (2006) 351–367. doi:10.1007/s00726-005-0289-3.
[82] R.E. Kontermann, Strategies to Extend Plasma Half-Lives of Recombinant Antibodies, BioDrugs. 23 (2009) 93–109. doi:10.2165/00063030-200923020-00003.
[83] J.C. Kang, J.S. Poovassery, P. Bansal, S. You, I.M. Manjarres, R.J. Ober, E.S. Ward, Engineering multivalent antibodies to target heregulin-induced HER3 signaling in breast cancer cells, MAbs. 6 (2014) 340–353. doi:10.4161/mabs.27658.
[84] M. Malm, F.Y. Frejd, S. Ståhl, J. Löfblom, Targeting HER3 using mono- and bispecific antibodies or alternative scaffolds, MAbs. 8 (2016) 1195–1209. doi:10.1080/19420862.2016.1212147.
[85] N. Gaborit, A. Abdul-Hai, M. Mancini, M. Lindzen, S. Lavi, O. Leitner, L. Mounier, M. Chentouf, S. Dunoyer, M. Ghosh, C. Larbouret, T. Chardès, H. Bazin, A. Pèlegrin, M. Sela, Y. Yarden, Examination of HER3 targeting in cancer using monoclonal antibodies., Proc. Natl. Acad. Sci. U. S. A. 112 (2015) 839–44. doi:10.1073/pnas.1423645112.
[86] J.B. Spangler, J.R. Neil, S. Abramovitch, Y. Yarden, F.M. White, D.A. Lauffenburger, K.D. Wittrup, Combination antibody treatment down-regulates epidermal growth factor receptor by inhibiting endosomal recycling., Proc. Natl. Acad. Sci. U. S. A. 107 (2010) 13252–7. doi:10.1073/pnas.0913476107.
[87] A. Orlova, M. Malm, M. Rosestedt, Z. Varasteh, K. Andersson, R.K. Selvaraju, M. Altai, H. Honarvar, J. Strand, S. Ståhl, V. Tolmachev, J. Löfblom, Imaging of HER3-expressing xenografts in mice using a 99mTc(CO)3-HEHEHE-ZHER3:08699 affibody molecule, Eur. J. Nucl. Med. Mol. Imaging. 41 (2014) 1450–1459. doi:10.1007/s00259-014-2733-7.
[88] M. Rosestedt, K.G. Andersson, B. Mitran, V. Tolmachev, J. Löfblom, A. Orlova, S. Ståhl, Affibody-mediated PET imaging of HER3 expression in malignant tumours., Sci. Rep. 5 (2015) 15226. doi:10.1038/srep15226.
[89] D. Dong, G. Xia, Z. Li, Z. Li, Human Serum Albumin and HER2-Binding

Affibody Fusion Proteins for Targeted Delivery of Fatty Acid-Modified Molecules and Therapy, Mol. Pharm. 13 (2016) 3370–3380. doi:10.1021/acs.molpharmaceut.6b00265.
[90] M. Friedman, A. Orlova, E. Johansson, T.L.J. Eriksson, I. Höidén-Guthenberg, V. Tolmachev, F.Y. Nilsson, S. Ståhl, Directed evolution to low nanomolar affinity of a tumor-targeting epidermal growth factor receptor-binding affibody molecule., J. Mol. Biol. 376 (2008) 1388–402. doi:10.1016/j.jmb.2007.12.060.
[91] G. Schaefer, L. Haber, L.M. Crocker, S. Shia, L. Shao, D. Dowbenko, K. Totpal, A. Wong, C. V Lee, S. Stawicki, R. Clark, C. Fields, G.D. Lewis Phillips, R.A. Prell, D.M. Danilenko, Y. Franke, J.-P. Stephan, J. Hwang, Y. Wu, J. Bostrom, M.X. Sliwkowski, G. Fuh, C. Eigenbrot, A two-in-one antibody against HER3 and EGFR has superior inhibitory activity compared with monospecific antibodies., Cancer Cell. 20 (2011) 472–86. doi:10.1016/j.ccr.2011.09.003.
[92] Statistics - Ovarian Cancer Research Fund Alliance, (n.d.). https://ocrfa.org/patients/about-ovarian-cancer/statistics/?gclid=EAIaIQobChMI7ee7z6yd2gIVyUwNCh2yKQbyEAAYAiAAEgLAu_D_BwE (accessed April 3, 2018).
[93] B. Tanner, D. Hasenclever, K. Stern, W. Schormann, M. Bezler, M. Hermes, M. Brulport, A. Bauer, I.B. Schiffer, S. Gebhard, M. Schmidt, E. Steiner, J. Sehouli, J. Edelmann, J. Läuter, R. Lessig, K. Krishnamurthi, A. Ullrich, J.G. Hengstler, ErbB-3 predicts survival in ovarian cancer., J. Clin. Oncol. 24 (2006) 4317–23. doi:10.1200/JCO.2005.04.8397.
[94] Treating Ovarian Cancer, (n.d.). https://www.cancer.org/cancer/ovarian-cancer/treating.html (accessed April 3, 2018).
[95] L.A. Garraway, H.R. Widlund, M.A. Rubin, G. Getz, A.J. Berger, S. Ramaswamy, R. Beroukhim, D.A. Milner, S.R. Granter, J. Du, C. Lee, S.N. Wagner, C. Li, T.R. Golub, D.L. Rimm, M.L. Meyerson, D.E. Fisher, W.R. Sellers, Integrative genomic analyses identify MITF as a lineage survival oncogene amplified in malignant melanoma, Nature. 436 (2005) 117–122. doi:10.1038/nature03664.
[96] T.Z. Bass, M. Rosestedt, B. Mitran, F.Y. Frejd, J. Löfblom, V. Tolmachev, S. Ståhl, A. Orlova, In vivo evaluation of a novel format of a bivalent HER3-targeting and albumin-binding therapeutic affibody construct, Sci. Rep. 7 (2017) 43118. doi:10.1038/srep43118.
[97] A. Orlova, T.Z. Bass, C. Atterby, M. Rosestedt, L. Gudmundsdotter, C. Dahlsson Leitao, F.Y. Frejd, J. Löfblom, V. Tolmachev, S. Ståhl, Evaluating the therapeutic potential of a dimeric HER3-binding affibody construct in comparison with a monoclonal antibody, seribantumab, Digit. Vetenskapliga Ark. (2017).
[98] B. Owens, Faster, deeper, smaller—the rise of antibody-like scaffolds, Nat. Biotechnol. 35 (2017) 602–603. doi:10.1038/nbt0717-602.
[99] S. Ståhl, T. Gräslund, A. Eriksson Karlström, F.Y. Frejd, P.-Å. Nygren, J. Löfblom, Affibody Molecules in Biotechnological and Medical Applications., Trends Biotechnol. 35 (2017) 691–712. doi:10.1016/j.tibtech.2017.04.007.
[100] F.Y. Frejd, K.-T. Kim, Affibody molecules as engineered protein drugs, Exp.

Mol. Med. 49 (2017) e306. doi:10.1038/emm.2017.35.
[101] C. Alewine, R. Hassan, I. Pastan, Advances in anticancer immunotoxin therapy., Oncologist. 20 (2015) 176–85. doi:10.1634/theoncologist.2014-0358.
[102] I. Pastan, R. Hassan, D.J. FitzGerald, R.J. Kreitman, Immunotoxin therapy of cancer, Nat. Rev. Cancer. 6 (2006) 559–565. doi:10.1038/nrc1891.
[103] I. Pastan, R. Beers, T.K. Bera, Recombinant Immunotoxins in the Treatment of Cancer, in: Antib. Eng., Humana Press, New Jersey, 2004: pp. 503–518. doi:10.1385/1-59259-666-5:503.
[104] D. Hendriks, G. Choi, M. de Bruyn, V.R. Wiersma, E. Bremer, Antibody-Based Cancer Therapy: Successful Agents and Novel Approaches, Int. Rev. Cell Mol. Biol. 331 (2017) 289–383. doi:10.1016/BS.IRCMB.2016.10.002.
[105] M. Onda, S. Nagata, D.J. FitzGerald, R. Beers, R.J. Fisher, J.J. Vincent, B. Lee, M. Nakamura, J. Hwang, R.J. Kreitman, R. Hassan, I. Pastan, Characterization of the B cell epitopes associated with a truncated form of Pseudomonas exotoxin (PE38) used to make immunotoxins for the treatment of cancer patients., J. Immunol. 177 (2006) 8822–34. doi:10.4049/JIMMUNOL.177.12.8822.
[106] M. Li, Z.-S. Liu, X.-L. Liu, Q. Hui, S.-Y. Lu, L.-L. Qu, Y.-S. Li, Y. Zhou, H.-L. Ren, P. Hu, Clinical targeting recombinant immunotoxins for cancer therapy., Onco. Targets. Ther. 10 (2017) 3645–3665. doi:10.2147/OTT.S134584.
[107] Z. Cao, X. Wu, L. Yen, C. Sweeney, K.L. Carraway, Neuregulin-induced ErbB3 downregulation is mediated by a protein stability cascade involving the E3 ubiquitin ligase Nrdp1., Mol. Cell. Biol. 27 (2007) 2180–8. doi:10.1128/MCB.01245-06.
[108] A. Sorkin, L.K. Goh, Endocytosis and intracellular trafficking of ErbBs, Exp. Cell Res. 315 (2009) 683–696. doi:10.1016/J.YEXCR.2008.07.029.